DOCTORAL THESIS

Enabling Technologies for the Construction and Ring-Opening of Three-Membered Cycles

Anastasiya Krech

Enabling Technologies for the Construction and Ring-Opening of Three-Membered Cycles

ANASTASIYA KRECH

**TAL
TECH** PRESS

TALLINN UNIVERSITY OF TECHNOLOGY
School of Science
Department of Chemistry and Biotechnology
This dissertation was accepted for the defense of the degree of Doctor of Philosophy in Chemistry on 13/11/2025

Supervisor:

Assist. Prof. Maksim Ošeka
School of Science
Tallinn University of Technology
Tallinn, Estonia

Reviewed by:

Dr. Mikk Kaasik and Dr. Aleksandra Murre
School of Science
Tallinn University of Technology
Tallinn, Estonia

Opponents:

Prof. Edgars Suna
Organic Chemistry Department
University of Latvia
Riga, Latvia

Assist. Prof. Luca Capaldo
University of Parma
Parma, Italy

Defense of the thesis: 12/12/2025, Tallinn

Declaration:
Hereby I declare that this doctoral thesis, my original investigation and achievement, submitted for the doctoral degree at Tallinn University of Technology has not been submitted for doctoral or equivalent academic degree.

Anastasiya Krech

----
signature

European Union
European Regional
Development Fund

Investing
in your future

Krech, A. (2025). *Enabling Technologies for the Construction and Ring-Opening of Three-Membered Cycles* [TalTech Press]. https://doi.org/10.23658/taltech.94/2025

Sünteesitehnoloogiad kolmeliikmeliste tsüklite saamiseks ja avamiseks

ANASTASIYA KRECH

Contents

List of publications

The list of author's publications, on the basis of which the thesis has been prepared:

I Krech, A.; Laktsevich-Iskryk, M.; Deil, N.; Fokin, M.; Kimm, M.; Ošeka, M. Asymmetric Cyclopropanation *via* an Electro-Organocatalytic Cascade. *Chemical Communications*, **2024**, *60* (95), 14026–14029.

II Krech, A.; Yakimchyk, V.; Jarg, T.; Kananovich, D.; Ošeka, M. Ring-Opening Coupling Reaction of Cyclopropanols with Electrophilic Alkenes Enabled by Decatungstate as Photoredox Catalyst. *Advanced Synthesis & Catalysis*, **2024**, *366* (1), 91–100.

III Laktsevich-Iskryk, M.; Krech, A.; Fokin, M.; Kimm, M.; Jarg, T.; Noël, T.; Ošeka, M. Telescoped Synthesis of Vicinal Diamines *via* Ring-Opening of Electrochemically Generated Aziridines in Flow. *Journal of Flow Chemistry*, **2024**, *14* (1), 139–147.

Author's contribution to the publications

Contribution to the papers in this thesis are:

I   The author had a significant role in the designing of the experiments and in the synthesis and characterization of compounds used in the study. The author had a major role in the preparation of the manuscript and a minor role in the compilation of the supporting information.

II   The author had a major role in the designing of the experiments and in the synthesis and characterization of compounds used in the study. The author had a major role in the preparation of the manuscript and in the compilation of the supporting information.

III   The author had a significant role in the synthesis and characterization of compounds used in the study. The author had a minor role in the preparation of the manuscript.

Introduction

For centuries, chemical synthesis was conducted primarily in round-bottom flasks using mechanical or magnetic stirring, heating, and complex, fragile glassware. Only in recent decades have chemists begun to harness electrons and photons as alternatives to traditional chemical reagents, and to employ microreactors instead of flasks to perform synthesis more efficiently. These so-called enabling technologies represent a modern approach to conducting chemical reactions and include flow chemistry, photochemistry, electrochemistry, mechanochemistry, microwave-assisted synthesis, asymmetric organocatalysis, and machine learning/artificial intelligence-enabled chemistry.[1–3]

Photochemistry and electrochemistry, which utilize photons and electrons respectively, enable novel transformations and precise control of reactive intermediates, offering new sustainable reaction pathways under mild conditions without the use of stoichiometric redox reagents.[4, 5] Furthermore, conducting photo- or electrochemical transformations in flow allows reactions to be scaled up to gram quantities and beyond. Thus, enabling technologies help bridge the gap between academia and industry, which have traditionally employed vastly different synthetic approaches.

Three-membered rings represent another important focus in organic chemistry.[6, 7] Their presence in natural products, combined with their biological activities, makes them attractive targets for the pharmaceutical industry. The high ring strain of three-membered rings also makes them useful precursors for synthesizing complex molecules. The main three-membered ring systems include cyclopropanes (all-carbon), aziridines (containing one nitrogen atom), and epoxides (containing one oxygen atom).
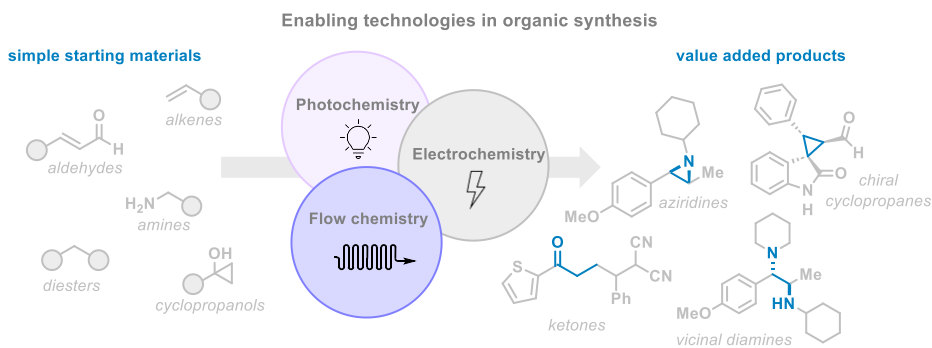
Figure 1. Enabling technologies allows organic chemists to achieve complex synthetic goals.

This thesis describes the application of enabling technologies for the construction and ring-opening of cyclopropanes and aziridines (Figure 1). In the first chapter, the merger of asymmetric organocatalysis with electrocatalysis enabled efficient and sustainable synthesis of enantioenriched cyclopropanes (**Publication I**). In the second chapter, photochemistry was employed for the deconstruction of cyclopropanols to access distantly functionalized ketones, and flow chemistry facilitated gram-scale synthesis (**Publication II**). In the third chapter, a telescoped flow setup combined electrochemical aziridine formation with subsequent ring-opening for the synthesis of valuable vicinal diamines (**Publication III**). This work advances both the fundamental understanding of novel reactions and the development of practical scale-up strategies, connecting academic discovery with industrial application.

Abbreviations

APE	alternating polarity electrolysis
BDE	bond dissociation energy
BET	back electron transfer
BHT	dibutylhydroxytoluene
Bn	benzyl
Boc	*tert*-butyloxycarbonyl
bpy	2,2'-bipyridine
bpz	2,2'-bipyrazine
C	graphite electrode
CCE	constant current electrolysis
CPA	chiral phosphate acid
CPE	constant potential electrolysis
CV	cyclic voltammetry
DCE	1,2-dichloroethane
DIPEA	*N,N*-diisopropylethylamine
DMSO	dimethyl sulfoxide
DMU	1,3-dimethylurea
d.r.	diastereomeric ratio
EDA	electron donor-acceptor complex
ET	electron transfer
EWG	electron-withdrawing group
Fc	ferrocene
GCE	glassy carbon electrode
GC-MS	gas chromatography–mass spectrometry
GSW	galvanized steel wire
HAT	hydrogen atom transfer
HER	hydrogen evolution reaction
HFIP	hexafluoro-2-propanol
HRMS	high-resolution mass spectrometry
ISC	intersystem crossing
ITU	isothiourea
IUPAC	International Union of Pure and Applied Chemistry
KIE	kinetic isotope effect
LEDs	light-emitting diodes
Mes-Acr	9-mesityl-10-methylacridinium
Ms	mesyl = methanesulfonyl
MTBE	methyl *tert*-butyl ether
NBS	*N*-bromosuccinimide
NCS	*N*-chlorosuccinimide
NFSI	*N*-fluorobenzenesulfonimide

NHCs	*N*-heterocyclic carbenes
NHE	normal hydrogen electrode
NIS	*N*-iodosuccinimide
NMR	nuclear magnetic resonance
Ns	nosyl = nitrobenzenesulfonyl
OER	oxygen evolution reaction
PC	photocatalyst
PCET	proton-coupled electron transfer
PG	protecting group
phen	1,10-phenanthroline
POMs	polyoxometalates
ppy	2-phenylpyridine
PT	proton transfer
PTC	phase-transfer catalyst
RE	reference electrode
RVC	reticulated vitreous carbon
SCE	saturated calomel electrode
SET	single-electron transfer
SOMO	singly occupied molecular orbital
SS	stainless steel
TBADT	tetrabutylammonium decatungstate
TBS	*tert*-butyl(dimethyl)silyl
TEMPO	2,2,6,6-tetramethylpiperidine-*N*-oxyl
TFA	trifluoroacetic acid
TMS	trimethylsilyl group
TPPA	phosphoric acid tripyrrolidide
Ts	tosyl = toluenesulfonyl
UV	ultraviolet
UV-Vis	ultraviolet-visible spectroscopy

1 Asymmetric cyclopropanation *via* an electro-organocatalytic cascade (Publication I)

Using electrons directly to perform the reaction has long been a focus of chemists, but only recently has it finally received deserved recognition among organic chemists. Moreover, electrochemistry itself is a green and powerful synthetic platform, serving as an enabling technology that unlocks new reactivity pathways previously inaccessible through conventional methods of organic synthesis.[8–10]

Perhaps one of the most famous electricity-driven reactions featured in every organic chemistry textbook is the Kolbe electrolysis, developed in 1840s (Figure 2).[11] This process employs anodic oxidation of carboxylic acids to provide convenient access to alkyl radicals. The Tafel reduction, developed in 1910s, was one of the first examples of cathodic reduction and enabled the preparation of hydrocarbons from carbonyl compounds. Shono oxidation, introduced in the 1970s, demonstrated the utility of anodic oxidation for the α-functionalization of amines and has since become a widely used method in organic synthesis.
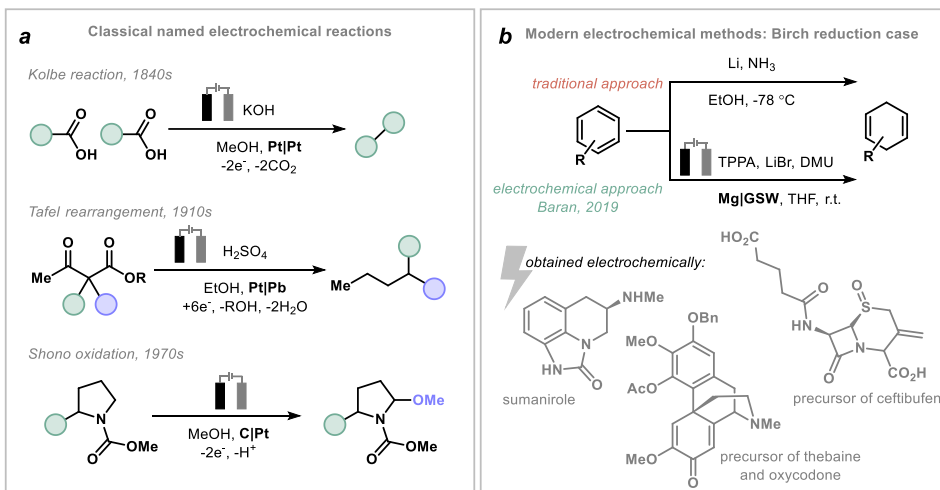
Figure 2. a) Classical electrochemical transformations in organic synthesis. b) Electrochemistry can improve traditional synthetic methods, such as Birch reduction, and be used as a key step in the synthesis of complex structures. TPPA – phosphoric acid tripyrrolidide, DMU – 1,3-dimethylurea, GSW – galvanized steel wire.

Modern electrochemistry has emerged as a powerful tool for both developing novel transformations and optimizing established synthetic methods.[12] A notable example is the electrochemical Birch reduction developed by the Baran group, which operates under ambient conditions rather than requiring the hazardous and anhydrous conditions of the classical protocol (Figure 2, b).[13] Electrosynthesis can be used in the industrial scale through flow chemistry setups.[14] Furthermore, the electrochemical approach can also be applied for complex synthetic challenges, including the preparation or late-stage functionalization of pharmaceuticals and biological molecules.[15] Additionally, asymmetric electrosynthesis has garnered growing interest for the synthesis of chiral compounds.[16]

Nevertheless, the slow adoption of electrosynthesis in organic chemistry can be attributed to its significant difference from conventional reaction setups, requiring

researchers to adopt new concepts and techniques when conducting electrolysis for the first time. To make electrochemistry more accessible to organic chemists, numerous tutorial articles have been published that introduce the fundamental principles and common operational modes.[17–20]

In this regard, the literature review of this chapter includes the basics of electrochemical setups and the physical principles governing electrolysis, discussion on electrocatalytic strategies including redox mediators, and recent advances in asymmetric electrochemical catalysis.

1.1 Literature review

1.1.1 Electrochemical setup

To perform electrochemical reactions a special setup is used: a power source is connected to a reaction mixture through two electrodes: a *working electrode*, where electron transfer with the substrate molecule occurs, and a *counter electrode*, needed to complete the circuit and performs conjoin reaction. The power source pushes electrons from the anode to the cathode, resulting in a reductive environment at the cathode and an oxidative environment at the anode (Figure 3, a). Depending on where reaction with the substrate takes place, either an anode or cathode can be the working electrode (paired electrolysis being an exception). Accordingly, the electrochemical reaction consists of two half-reactions (Figure 3, b). If there is a need to control the potential on the working electrode, reference electrode (RE) – an electrode with a constant and known potential – is used as a third electrode in the setup.
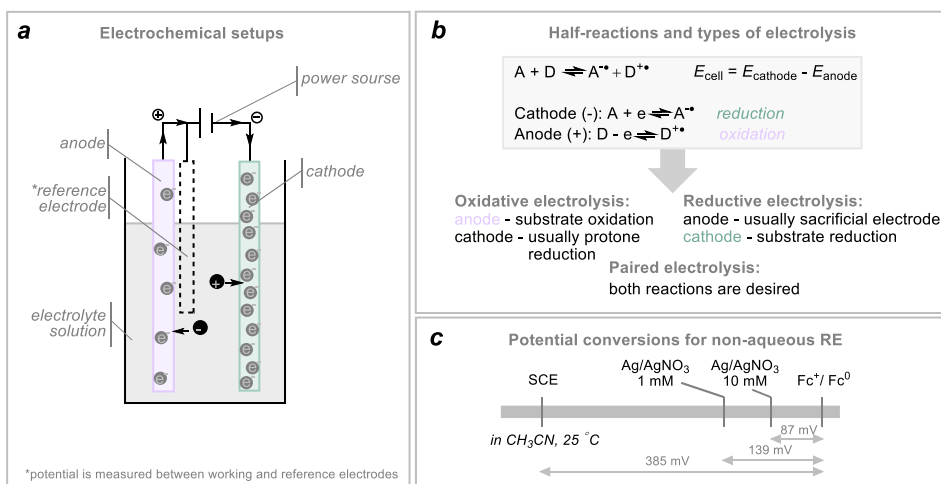
Figure 3. a) Electrochemical cell structure. b) Half-reactions and types of electrolysis. c) Potential conversions for non-aqueous reference electrodes.

When aqueous and protic solvents are used as electrolytic solvents, a saturated calomel electrode (SCE) and a silver-silver chloride (Ag/AgCl) electrode are typically used as a reference electrode. The situation is much more complex in non-aqueous solvents, as common aqueous reference electrodes are often unstable in such environments. Typically, an Ag/Ag^+ electrode is used for non-aqueous solutions, consisting of a silver wire immersed in the electrolyte solution with defined concentration of $AgNO_3$ in organic

solvent. However, its potential cannot be accurately predicted for each system. To overcome this problem, the measured potential should be referenced to a redox couple with a reproducible formal potential, which defines the zero of the potential scale. An IUPAC recommendation is the use of the ferrocene/ferrocenium (Fc/Fc$^+$; Figure 3, c) redox couple.[21, 22]

The reaction can be carried out in either *undivided* or *divided cells*, depending on whether separation of anodic and cathodic processes is required. In an undivided cell, both electrodes share the same electrolyte without a barrier, while in a divided cell, a membrane or frit separates the compartments to prevent mixing of compounds. A brief description of these setups is provided in Table 1 below.

Table 1. Comparison of undivided and divided cells.

Undivided cell	Divided cell
Working and counter electrodes are located in the same vessel	Anodic and cathodic chambers are separated by a partially permeable membrane
☑ Easy to assemble and use	☑ Prevents side reactions by separating anodic and cathodic processes
☑ Standardized setups available (e.g., IKA ElectraSyn) for reproducibility	☒ More complex setup
☒ Possible side reactions at the counter electrode involving intermediates or products from the working electrode	☒ Membranes can add cost and may reduce efficiency through contamination or ion selectivity

In electrochemical systems, the applied potential, or voltage, (U, in volts, V) constitutes the thermodynamic driving force that controls which redox reactions are energetically accessible. Current (I, in amperes, A), in contrast, serves as a kinetic parameter quantifying the rate of electron transfer at the electrode-solution interface. These parameters are interrelated through Ohm's law ($U = IR$), where R represents the resistance (in ohms, Ω) within the electrochemical cell.

Therefore, electrolytic reactions can be controlled by how current or potential is applied, which strongly influences selectivity and efficiency. The three main modes are constant current, constant potential, and alternating current electrolysis, each offering distinct advantages depending on the reaction (Table 2).[19, 23] In *galvanostatic electrolysis* (also called constant current electrolysis, CCE), the applied current is kept constant, and the electrode potential shifts as the reaction proceeds. In *potentiostatic electrolysis* (also called constant potential electrolysis, CPE), the electrode potential is held fixed, and the current varies according to the consumption of reactants. In *alternating polarity electrolysis* (APE), exposing both electrodes alternately to oxidative and reductive conditions.[24]

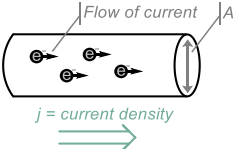*Table 2. Comparison of different electrolysis modes.*

Galvanostatic Electrolysis	Potentiostatic Electrolysis	Alternating Polarity Electrolysis
I = constant	*U* = constant	Square wave in current or potential
☑ Easy setup ☑ Control over equivalents of electrons ☒ Voltage range not controlled	☑ Control over potential improves selectivity ☒ Requires reference electrode ☒ Equivalents of electrons not controlled	☑ Can enable unique reactivity ☑ Helps to suppress electrode contamination ☒ Special power supply required

Typical variables to consider when conducting an electrochemical reaction seem to be endless, from normal chemical parameters such as solvent and temperature, to factors unique to electrochemistry such as electrode material or electrolyte selection.[17, 18] Additionally, stirring has an extreme importance for ensuring efficient mass transport to and from the electrodes. Some of the parameter choices are outlined in Table 3.

Table 3. Electrochemical variables in the reaction.

Electrodes	Solvents
Electrode choice is critical for controlling the reaction selectivity **Choice of electrodes:** ◊ Electrode material ◊ Electrode surface ◊ Geometry and surface condition ◊ Cost and availability ◊ Overpotential value **Typical electrodes:** Stainless steel (SS), graphite (C), glassy carbon (GCE), reticulated vitreous carbon (RVC), Pt, Ni foam	The choice of solvent impacts solubility of reactants, products, and supporting electrolytes. Oxidation of solvent should be considered with its *potential windows*.[25] **Typical solvents:** ◊ Polar aprotic (commonly employed) ◊ Polar protic (when sacrificial reduction is desired during anodic oxidation)

Potentials windows for typical solvents

dichloromethane
acetonitrile
tetrahydrofuran
water

-3 V   -2 V   -1 V   0 V   1 V   2 V

E / V vs SCE

Table 3 (continued).

Electrolytes	Current density, *j*	Faraday's law
Electrolytes are necessary to maintain the charge neutrality of the cell. May have a dual role as a reagent.[26]	Current density represents the local reaction rate of an electrochemical reaction independent of the size of the entire electrolysis cell	To find the total amount of electricity required for complete electrolysis of a compound
Typical electrolytes: ◊ Cations: ammonium and alkali metal-based salts, ◊ Anions: ClO_4^-, PF_6^-, BF_4^-, halides	$j = I/A$, [mA cm^{-2}] where *I* is the cell current, *A* is a geometrical electrode area	$Q = It = znF$ where *Q* - total charge [C], *I* – total current passed [A], *t* – electrolysis time [s], *F* is Faraday's constant (96485 C mol^{-1}), *n* – amount of substrate [mol], *z* – the number of electrons transferred per mole of substrate.
	Flow of current |A *j = current density*	Faradaic efficiency, *n* [%][17] $n = Q_{exp}/Q_{theo}$ Q_{theo}: theoretical charge [C], Q_{exp}: experimental passed charge [C]

1.1.2 Physical aspects of electrolysis

In electrochemistry, the addition or removal of electrons happens through the direct application of an electrical potential and therefore is a raw redox reaction. Electron transfer is a *heterogeneous process* occurring from the electrode surface to the molecule, and therefore the *electron transfer rate* from electrode to solution and *the rate of mass transport* of the substrate from the bulk solution to the electrode surface play central role in the reaction.[27] The reaction only takes place at the interface between the electrode and the solution.

Electrodes are polarized in an electrolyte solution, and the rearrangement of charge species takes place to counterbalance charge difference. The electrically charged electrode surface (negatively charged for cathode, positively – for anode) generates a very strong electrical field that tends to attract oppositely charged ions from the solution (Figure 4, a).[28] Therefore, an electrode-solution interface behaves as a capacitor and an *electrical double-layer* is formed close to the electrode surface. It creates a large potential drop and an intense electrical field (10^6 V cm^{-1}). This is the driving force for the electrochemical reaction at electrode interface. After the electron transfer occurs, new ions are transferred to the electrode interface, and this movement propagates current.[27]

The electrode reaction rate is governed by several processes: (1) *mass transfer* of reactants from bulk solution to the electrode surface, (2) *electron transfer* at the electrode surface, (3) *chemical reactions* preceding or following electron transfer, including homogeneous processes (protonation, dimerization) or heterogeneous ones (catalytic decomposition on the electrode surface), and (4) *surface reactions* such as adsorption, desorption, or crystallization (Figure 4, b).[29] These processes can be disrupted by the *absorption* or *grafting* of chemicals on the surface and may cause decrease in the electrode surface and in the electron transfer rate,[28] and leads to passivating film formation. Several strategies exist to prevent or reverse electrode passivation, including

selecting fouling-resistant electrode materials, alternating polarity, employing pulsed electrolysis, adding protective additives, or using mediated electron transfer. Additionally, proper *electrode treatment and cleaning* through polishing, rinsing, or electrochemical pre-conditioning is essential to ensure reproducibility and avoid contamination from adsorbed species.
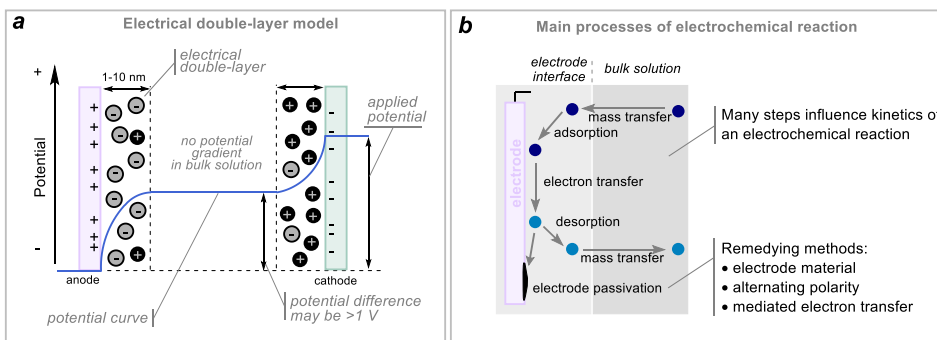

Figure 4. a) Simplified structure of electrical double-layer model of electrochemical process and potential gradient. b) Processes on the electrode surface and in the reaction media, preventing methods of electrode contamination.

1.1.3 Electrochemical electron transfer

In the electrochemical electron transfer, Gibbs free energy (ΔG_{ET}) determines whether the process is thermodynamically feasible. The relationship between the ΔG and the thermodynamically required cell potential (E_{cell}), is $\Delta G_{ET} = -nFE_{cell}$, where F is Faraday's constant and n is number of electrons transferred. When $\Delta G_{ET} < 0$, the reaction is spontaneous, however kinetics play a huge role in the actual feasibility of the process.

Since electrodes are commonly made of metals, their electronic structure provides important insight into electrochemical electron transfer to molecules.[27] Metals are composed of closely packed atoms with overlapping orbitals, forming a continuum of electron energy levels that are progressively filled from the lowest energies upward. The *Fermi level* (E_F) corresponds to the energy of the highest occupied states, analogous to the HOMO in molecular systems, and it determines the availability of electrons for transfer. E_F in a metal is not fixed and can be shifted by applying electrical energy. In electrochemistry, this is achieved by applying a voltage to the electrode (Figure 5, a). Depending on the relative position of the Fermi level to the orbital energies (HOMO and LUMO) of a substrate molecule in solution, it may be thermodynamically feasible to either reduce or oxidize the molecule.

This tunability of the electrode potential represents a *fundamental distinction between electrochemical and photochemical redox processes*: in electrochemistry, the driving force for electron transfer can be adjusted by changing the applied potential, whereas in photochemistry, the driving force is dictated by the intrinsic properties of the photocatalyst (Figure 5, b).[30] As a result, photochemical systems often require the design or synthesis of new catalysts with appropriate redox potentials or may be limited if no suitable catalyst exists.
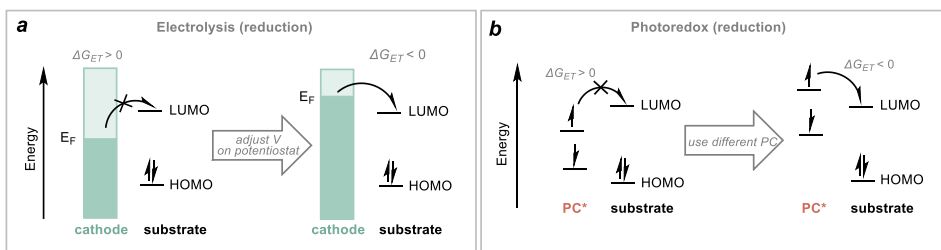
Figure 5. Comparison of electron transfer in a) electrochemistry and b) photoredox chemistry for a reduction reaction. PC – photocatalyst, HOMO – highest occupied molecular orbital, LUMO – lowest unoccupied molecular orbital.

1.1.4 Overpotential and cyclic voltammetry

At the equilibrium potential *E*, by definition, no cell current is flowing. The *standard potential E_0* is defined for the reference reaction at standard conditions (NHE – normal hydrogen electrode):

$$H_2 \rightleftharpoons 2H^+ + 2e^-$$

$$E_0 = 0 \text{ V } vs \text{ NHE}$$
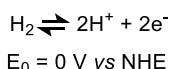
The Nernst equation (Equation 1) enables to calculate the equilibrium potential *E* at real conditions:

$$E = E^0 + \frac{RT}{nF} ln \left(\frac{a_{Ox}}{a_{Red}} \right) \qquad \text{Equation 1}$$

where Ox and Red are the oxidized and reduced forms of the substrate undergoing a reduction event. (R – gas constant, 8.314 J K^{-1} mol^{-1}, T – absolute temperature, a_{Ox}, a_{Red} – activities of the oxidized and reduced species of the reactants; at low concentrations, in place of activities approximately concentrations can be used).[28]

However, experimentally applied potential under the specified reaction conditions (E_{app}) is different from the equilibrium potential *E*. The additional potential required to drive the reaction is called *overpotential*, η (Figure 6, a).
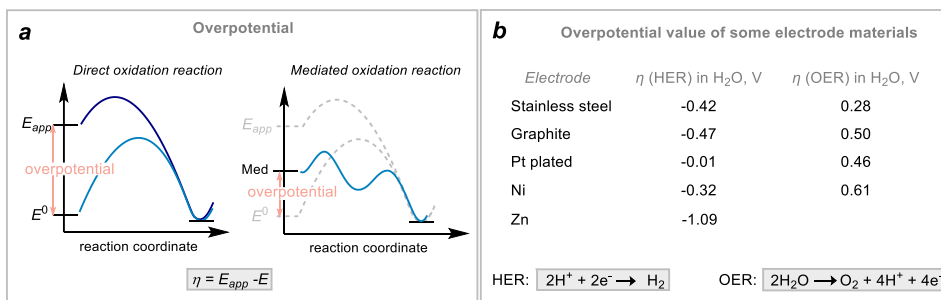
Figure 6. a) Illustration of the concept of overpotential for direct and mediated oxidation reactions. b) Overpotential values for some commonly used electrodes in organic synthesis.

Generally, overpotentials control the kinetics of electrochemical reactions and overall electrolysis performance. However, large overpotentials can limit synthetic applications, since many organic molecules contain functional groups prone to decomposition or side reactions, a challenge often referred to as the "overpotential problem."

Electrode materials significantly influence reaction overpotentials and critical sacrificial processes such as hydrogen evolution reaction (HER) and oxygen evolution reaction (OER) (Figure 6, b).[30, 31] Both HER and OER can act as nonproductive counter-electrode reactions during organic electrosynthesis. When these reactions are desired, low-overpotential electrode materials are selected; when undesirable, high-overpotential materials are preferred. Electrocatalysis can also play role in reducing overpotential.

Cyclic voltammetry (CV) is an analytical tool used to determine redox potentials for electrochemical transformations and can aid in the elucidation of reaction mechanisms. In CV, the electrode potential is swept linearly while the resulting current is measured, and characteristic oxidation and reduction peaks appear. If the reaction is reversible, for example in the ferrocene/ferrocenium couple, a characteristic "duck-shaped" voltammogram is observed. For such reversible reactions, $E_{1/2}$ (half-wave potential, the midpoint between anodic and cathodic peak potentials) can be calculated and is described by the Nernst equation. For irreversible reactions, E_p (peak potential, the potential at maximum current) is reported.

1.1.5 Electrocatalysis using redox mediators

The simplest and most common form of electrolysis is *direct electrolysis*, which relies on the direct transfer of electrons between the substrate molecule and the electrode.[19] However, this process can be kinetically hindered, leading to high overpotentials at the electrode surface, adsorption of organic species, and the formation of a polymeric film.[31]

To address these challenges, *indirect electrolysis* can be employed, using a *redox catalyst* or *mediator* (Figure 7, a).[32] In this approach, the mediator undergoes heterogeneous electron transfer at the electrode surface and subsequently acts as a homogeneous redox reagent in solution. As a result, electrolysis can be carried out at significantly lower redox potentials compared to direct electrolysis.
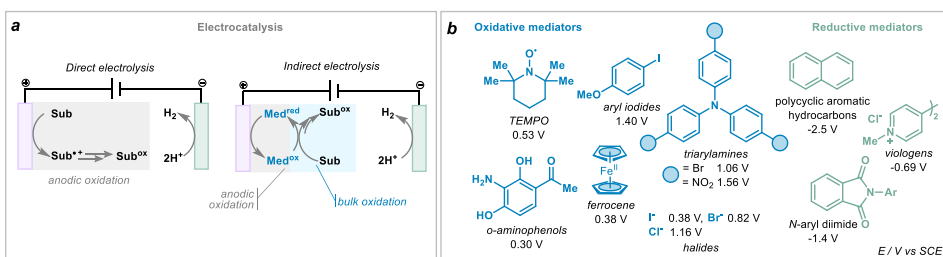
Figure 7. a) Representation of electrocatalysis for anodic oxidation reaction. b) Examples of common redox mediators with their redox potentials. Med – mediator, Sub – substrate, TEMPO – 2,2,6,6-tetramethylpiperidine-1-oxyl.

There are two main types of redox mediators: *oxidative* and *reductive* (Figure 7, b).[28] *Oxidative mediators* are typically activated through anodic oxidation, after which the resulting intermediates act as secondary oxidants. They also play an important role in preventing product overoxidation. Representative examples include triarylamines,

2,2,6,6-tetramethylpiperidine-1-oxyl (TEMPO), halide ions, and iodoarenes. *Reductive mediators*, in contrast, undergo cathodic reduction to generate species that function as subsequent reductants. Their application, however, has been more limited compared to oxidative mediators. The scope of both oxidative and reductive mediators can be further expanded by means of *electrophotocatalysis*.[20]

1.1.6 Halogen-mediated electrosynthesis

Halide salts are among the simplest and most commonly used halogen-based mediators in electrochemistry.[33–37] Halides generate on the anode reactive halogen species (e.g., Hal_2, $Hal\cdot$, Hal_3^-), which can subsequently react with water to generate hypohalites. Halide salts can also function as supporting electrolytes, thus playing a dual role in electrocatalytic reactions.[26] While they are often employed in catalytic amounts, in some cases stoichiometric quantities are used to ensure high reaction yields. Their low cost and low toxicity further enhance their appeal as mediators. In many cases, electricity is used instead chemical oxidants, such as peroxides or hypervalent iodine reagents,[35, 37] or it replaces the use of electrophilic halogens compounds, such as *N*-halosuccinimides.[38, 39]

A *typical mechanism* can be described as follows: anodic oxidation of halide ions first produces *polyhalogen anions*, which upon further oxidation at the anode yield *molecular halogen* (see Scheme 1, a). This sequence of two anodic oxidation steps is commonly observed for iodide and bromide, which are more prone to form polyhalogen anions.[40] In contrast, chloride generally exhibits only a single oxidation peak in cyclic voltammetry.[41] Additionally, single-electron transfer (SET) at the anode can also occur, resulting in halogen atom formation. In the presence of water, the situation becomes more complex due to the formation of various reactive hypohalite species (e.g., BrO^-, ClO^-, IO_4^-).[42] The presence of these intermediates makes it challenging to unambiguously identify and follow the exact reactive species generated at the anode. After the generation of active halogen species, halogenation of the substrate typically occurs, usually followed by nucleophilic substitution of halogen and product formation. Often, halide-mediated anodic reactions are accompanied by *base generation at the cathode* through the hydrogen evolution reaction in protic solvents such as MeOH or EtOH,[43–45] which may facilitate halogenation of the substrate.

Although halogen-mediated electrosynthesis has been extensively studied, several representative reaction types can be outlined, including (Scheme 1, b):

- Anodic α-functionalization of ketones;[46–48]
- Ring constructions:[49] cyclopropanation (see the section below), constructions of cyclobutanes,[45] indoles,[50] indolines,[51, 50] dihydropyrano[4,3-*b*]indoles,[52] sulphonated indenones,[53] oxoindoles,[54] 3-azido-indolines,[55] carbazoles,[56] lactams,[57] and azetidines;[58]
- Amide coupling,[59] cyanation,[60] C–H amination,[44, 61, 62] C–C bond construction,[43, 57] [4+2] annulation,[63] aziridination[64] and even electroreductive arylation of alkenes;[65]
- More exotic reactions, such as bromide-mediated silane oxidation[66] and synthesis of *N*-sulfonyl iminophosphoranes.[67]

It is worth noticing, that the reaction involving heteroatoms, often proceeds first through the formation of heteroatom-iodine covalent bond or a distinct compound (P–I,[59] S–I,[53] N–I,[64, 44] N–Br,[57]), which further react with the substrate.
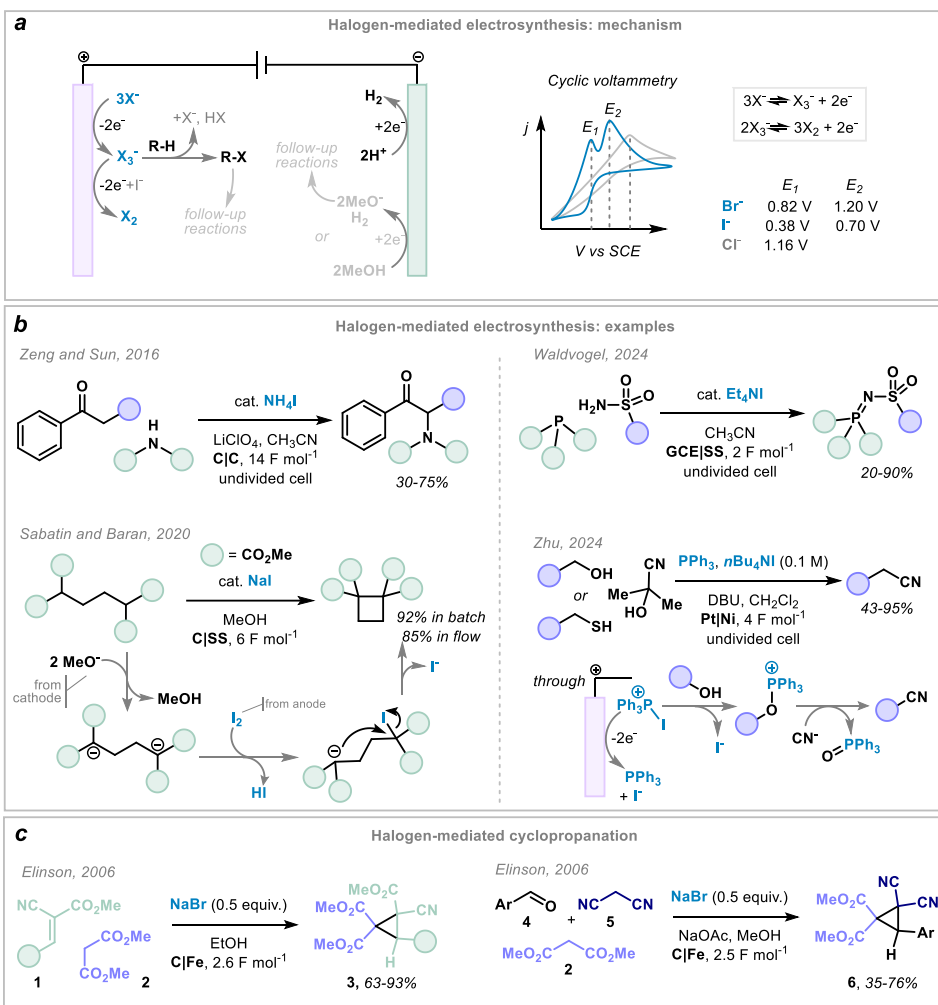
Scheme 1. a) Typical mechanism of halogen-mediated electrosynthesis and redox potentials of halide anions. b) Examples of electrochemical transformations with halides as mediators. c) Electrochemical halogen-mediated synthesis of cyclopropanes. GCE – glassy carbon electrode.

1.1.7 Electrochemical halogen-mediated cyclopropanation

Cyclopropane is a privileged motif in natural products and bioactive compounds.[68] Although many methods for its synthesis exist, the development of new approaches remains an active area of research.[69, 70] Classical cyclopropanations methods include Simmons-Smith, Kulinkovich, and Corey-Chaykovsky reactions, which mostly rely on toxic or dangerous reagents, while diazo-based strategies involve explosive diazo compounds and often utilize transition-metal catalysts such as Rh, Ru, Ir, Cr, or Cu.[69] In contrast, electrochemistry employs electrons as clean "reagents", thereby reducing the need for hazardous stoichiometric redox agents.

Some electrochemical cyclopropanation methods include electrooxidative reactions with methylene pronucleophiles[71–74] and geminal dihaloalkanes and trihaloalkanes.[75–78] In the same time, halogen-mediated electrochemical cyclopropanation represents a particularly valuable transformation within electrocatalysis, as it generates electrophilic

halogen species in catalytic amounts, thereby eliminating the need for stoichiometric reagents and oxidants.[34]

Nikishin, Elinson, and co-workers have developed numerous electrochemical transformations of C–H acidic compounds using halide salt mediators since the 1990s. These reactions are typically conducted in alcoholic solutions and initiated by the cathodic generation of an alkoxide base, which deprotonates the C–H acid.[79] For example, Elinson reported the functionalization of aldehydes **4** *via* multicomponent cyclization with malononitrile **5** and malonate **2** (Scheme 1, c),[80] and a related transformation involving alkylidene cyanoacetates **1** and malonate **2**.[81] Although a wide range of such transformations have been reported, they continue to inspire new approaches in the field of electrochemical synthesis.

1.1.8 Asymmetric electrochemical catalysis

Chiral molecules are abundant in nature and play a crucial role in pharmaceuticals. In light of previous discussions on the benefits of electrochemistry in organic synthesis, it is clear that the development of asymmetric electrochemical transformations presents significant opportunities in synthetic chemistry. These transformations can be achieved through chiral catalysts or mediators, or by employing chiral mediators electrolytes, electrodes, or solvents.[16, 82–86]

Asymmetric electrochemical catalysis is an emerging and actively developing strategy in organic chemistry, offering an economical and sustainable approach to the synthesis of chiral molecules.[16] The main modes of asymmetric electrocatalysis include transition metal catalysis, enzymatic catalysis, and organocatalysis. Notably, recent developments in asymmetric electrocatalyzed transformations under flow conditions make this approach particularly attractive for industrial applications.[87, 88]

Transition metal electrocatalysis is currently the most developed strategy for asymmetric electrochemical transformations due to the facile oxidation or reduction of metal complexes at the cathode or anode, which allows precise control of electron transfer and reaction pathways.[85, 89] The ability of *metal complexes* to engage in single- or multi-electron transfers and to stabilize intermediates makes them powerful tools for constructing complex molecules. When paired with chiral ligands, they enable stereoselective and efficient synthesis of chiral products. Commonly used transition metals in asymmetric electrosynthesis include Ni, Co, Cu, and Rh. Another strategy for inducing enantioselectivity is *Lewis acid catalysis*, which also employs transition metal complexes as Lewis acids.[90] Unlike in transition metal redox catalysis, the metal centers themselves are not oxidized or reduced at the electrodes. Instead, complexes coordinate with a substrate, typically bearing a removable auxiliary group to facilitate chelation, forming a chiral Lewis acid-bound radical (commonly an enolate) that then undergoes an electron transfer at the electrode.

Small organic molecules offer significant advantages in asymmetric electrocatalysis due to their structural simplicity, lower cost, and lower toxicity compared with transition metal catalysts, which typically rely on precious metals and elaborate ligands. Therefore, *organo-electrocatalysis* represents a highly appealing approach for enabling novel enantioselective transformations in a more sustainable way. Mainly, chiral activation in organocatalysis proceeds through *covalent* and *non-covalent interactions* between the catalyst and the substrate (Figure 8). Covalent activation typically includes amino catalysis and *N*-heterocyclic carbenes (NHCs), while non-covalent activation involves hydrogen bonding, halogen bonding, ionic interactions and van der Waals forces, and

includes squaramide- or thiourea-based catalyst, chiral phosphoric acids (CPAs), and phase-transfer catalysts (PTCs). Another benefit of organocatalysis compared to metal-based catalysis is higher compatibility with flow chemistry setups through immobilization on a solid support.[91]
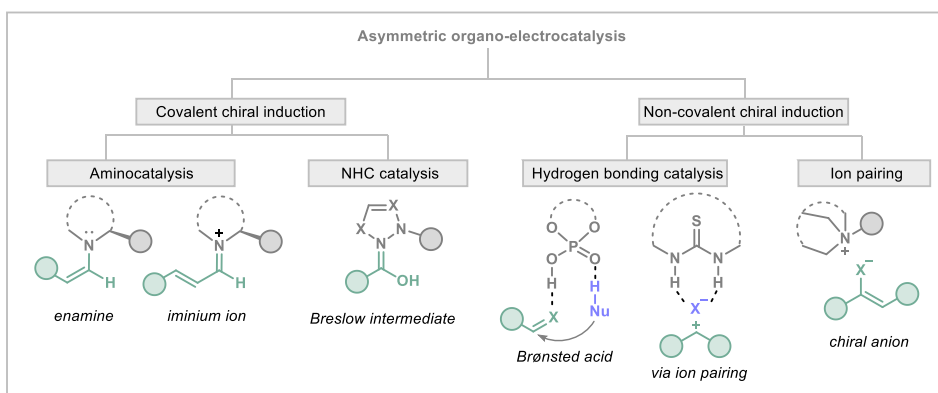

Figure 8. Schematic illustration of typical modes of asymmetric organocatalysis and representative examples.

Chiral induction via weak forces (such as hydrogen bonding) presents intrinsic challenges in electrochemical catalysis, since the highly polarized environment (electrolyte and polar solvents) of an electrochemical cell can disrupt the weak interactions. Nevertheless, recent advances have demonstrated that these reactions are feasible. In 2020, the Guo group reported an electrochemical alkylation of fluorinated *gem*-diols **7**, in which enantioinduction was achieved through a chiral hydrogen-bonding squaramide catalyst **11** (Scheme 2, left top).[92] The key reactive intermediate, *p*-quinone methide **10**, was generated by anodic oxidation of *p*-methylphenols **8** and subsequently reacted with the squaramide-bound fluorinated ketone.

Another breakthrough in the field was reported by Tan, Sun, and co-workers in 2023 (Scheme 2, right top).[93] The researchers developed aqueous/organic phase-transfer strategy for asymmetric bromocyclization of tryptamines **12**. In this transformation, anodically generated Br_2 in aqueous phase was shuttled into the organic phase by a phase-transfer catalyst **15** (PTC). There, it formed an organic-soluble ion pair (CPA-PTC-Br_2) with a chiral phosphate anion (**14-anion**, CPA⁻). The chiral phosphoric acid **14** was crucial for enantioinduction in this electricity-driven process, while $NaHCO_3$ suppressed the decomposition of Br_2. Notably, in the absence of the PTC **15**, the reaction proceeded with significantly reduced yields and enantioselectivity.

In 2024, Ling and co-workers developed an asymmetric counterion-directed electrocatalytic approach, where substrates **16** and **17** underwent direct electrochemical electron transfer for radical generation (Scheme 2, left bottom).[94] Chirality was induced by CPA anion (**19-anion**) through hydrogen-bonding interactions with both radicals **20** and **21**. This method was successfully applied to asymmetric indole-phenol [3+2] couplings as well as atroposelective C–H/N–H dehydrogenative couplings. The following year, Tan and Sun reported an electrocatalytic rearrangement of indoles **22** into spirooxindoles **23** catalyzed by CPA **24** in acidic aqueous media (Scheme 2, right bottom).[95] In this work, an CPA organocatalysis was combined with electrochemical halogen-mediated biphasic protocol, thereby eliminating the need for stoichiometric chemical oxidants (e.g., NBS).[96]
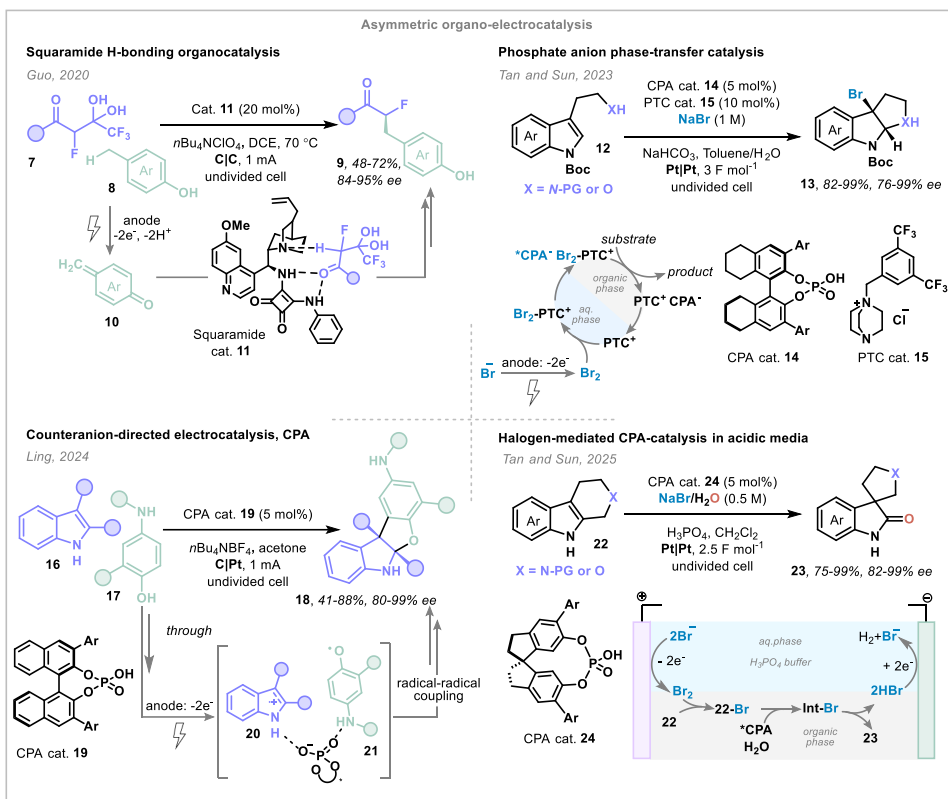
Scheme 2. Asymmetric electro-organocatalysis using chiral induction via weak forces. PG – protecting group.

Covalent chiral induction offers a versatile and effective strategy for achieving asymmetric electrosynthesis, particularly in the functionalization of carbonyl compounds. Within this context, aminocatalysis has been the most extensively investigated approach under electrochemical conditions.[97] Alternatively, *N*-heterocyclic carbenes (NHCs) and isothioureas have also been successfully employed in asymmetric electrochemical functionalization of aldehydes and esters.[85]

Reports on *non-aminocatalytic modes of activation* are scarce. Recently, the Zhu group reported an iodine-mediated electrocatalytic strategy employing NHC catalysis for the chiral activation of aldehydes **25** (Scheme 3, left).[98] This approach enabled a range of enantioselective transformations, including a formal [4 + 2] benzannulation *via* δ-activation of enals, a formal [3 + 3] cyclization *via* β-activation, and a formal [4 + 2] cyclization *via* γ-activation. Mechanistically, anodic single-electron oxidation of the Breslow intermediate **28** generated a radical cation species **29** that subsequently captured an iodine radical formed at the anode. Elimination of iodide from this adduct produced an acyl azolium intermediate **31**, which underwent further transformations. Importantly, careful control over the low concentration of iodine radical at the anode allowed to protect NHC catalyst **32** from iodine poisoning.

In 2025, Song and co-workers reported the use of covalent bonding interactions for chiral induction in electrochemical transformations, employing chiral isothiourea (ITU) catalysis as a Lewis base (Scheme 3, right).[99] This approach enabled the oxidative cross-coupling of esters **33** with silyl enol ethers **34**, with ferrocene serving as a redox

mediator. The reaction proceeds *via* formation of a chiral isothiourea-bound α-carbonyl radical species **38** derived from a C1-ammonium enolate **37**. The subsequent radical addition of the silyl enol ether **34** defines the stereochemical outcome, which is governed by an intramolecular 1,5-O···S chalcogen interaction between the carbonyl oxygen and the ITU sulfur atom. Despite recent advances, this area remains under active investigation.
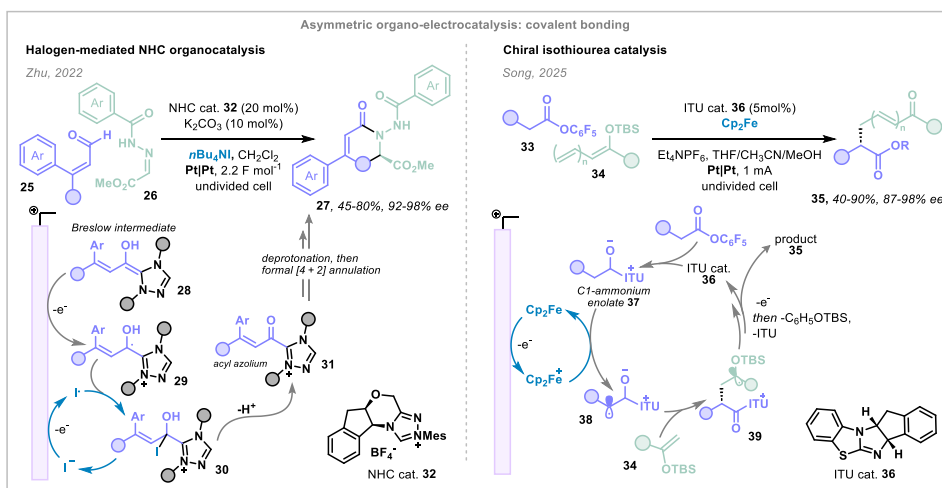
Scheme 3. Asymmetric electro-organocatalysis using covalent bonding: NHC and ITU cases.

Asymmetric electro-aminocatalysis has been in development for the last 15 years and still offers the possibility to carry out established enantioselective transformations in more sustainable way or enables the development of novel reactions (Figure 9). Mostly, electrochemical aminocatalysis has been demonstrated to proceed *via* enamine pathway, and operates through two distinct strategies:

(i) *electrochemical oxidation of the substrate* to generate the reactive electrophilic partner for subsequent reaction with the enamine, or

(ii) *anodic oxidation of the enamine itself* to afford a radical intermediate, enabling SOMO-type transformations (Figure 9).

The first strategy (i) requires that the oxidized substrate possesses the lowest oxidation potential within the system. While this imposes certain limitations on the scope of accessible reactivities, it likely protects the organocatalyst from overoxidation, since the substrate is present at the highest concentration. The second approach (ii) requires chiral enamine to possess a sufficiently low oxidation potential, enabling single-electron oxidation either directly at the anode or indirectly *via* a redox mediator in solution. This strategy broadens the scope of accessible transformations by allowing enantioselective radical-radical coupling reactions. However, it also introduces the risk of overoxidation of the organocatalyst, which is generally more susceptible to degradation under these conditions.[97]
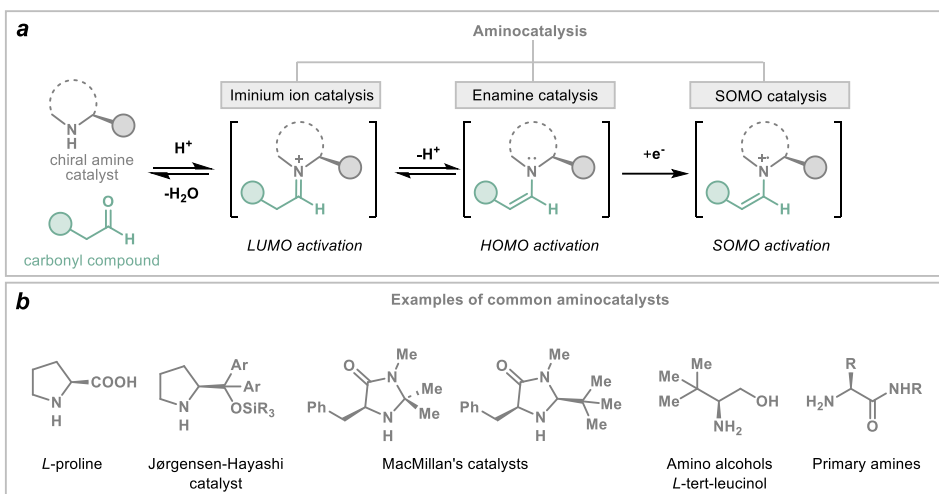
Figure 9. a) Activation modes in aminocatalysis. b) Typical aminocatalysts.

One of the earliest contributions to asymmetric electro-aminocatalysis *via* enamine formation and the first strategy (i) was reported by Jørgensen and co-workers in 2010, who described the synthesis of meta-substituted anilines **42** *via* the α-arylation of aldehydes **41** employing the Jørgensen-Hayashi catalyst **43** (Scheme 4, left).[100] In this transformation, anodic oxidation of the substituted aniline **40** generates an electrophilic intermediate **44**, which subsequently reacts with the enamine **45**, resulting in a Friedel-Crafts-type alkylation of anilines. In the same year, Jang and co-workers disclosed an enantioselective protocol for the α-alkylation of aldehydes **46** with xanthene **47** using MacMillan's catalyst **49** (Scheme 4, right top).[101] The authors proposed two possible mechanistic pathways: direct single-electron anodic oxidation of both the enamine and xanthene, followed by a radical-radical coupling, or two-electron oxidation of xanthene to generate a cationic intermediate, which then reacts with the enamine.
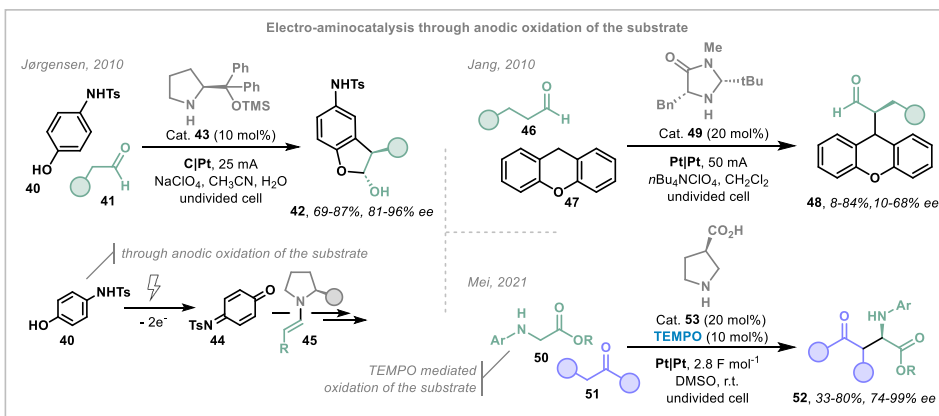
Scheme 4. Examples of asymmetric electro-aminocatalysis operating through anodic oxidation of the substrate, either directly or indirectly with redox mediator.

26

Redox mediators have further expanded the scope of asymmetric electro-aminocatalysis by enabling otherwise elusive transformations. For instance, in 2021, Mei and co-workers developed an asymmetric Shono-type oxidation of secondary acyclic amines **50**, employing an *N*-oxyl radical (TEMPO) as a redox mediator (Scheme 4, right bottom).[102] This mediator selectively oxidized the substrate **50** rather than the product, affording an imine intermediate that reacted with a ketone **51** derived enamine to furnish the product **52**. Notably, (*R*)-pyrrolidine-3-carboxylic acid **53** proved to be the most efficient organocatalyst for this transformation. Recently, the Xu group designed a bifunctional organocatalyst which combines a chiral aminocatalyst with a redox mediator.[103]

First report on enamine oxidation on the anode (strategy (ii)) was published by Jang in 2009, where they developed an enantioselective organocatalyzed α-oxyaminations of aldehydes with TEMPO.[104] In 2024, Mazzarella, Dell'Amico and co-workers successfully demonstrated this transformation *via* SOMO-activation of enamines for α-alkylation of aldehydes **54** employing a redox shuttle (Scheme 5, left).[105] The radical enamine intermediate **60** is produced at the anode and subsequently intercepted by silyl enol ether **55**, yielding radical cation. After a second anodic oxidation and hydrolysis, the desired product **56** is obtained. A biphenyl-based derivative **58** serves as the redox shuttle to prevent catalyst decomposition.

In a related recent investigation, the Luo group reported an efficient and stereoselective oxidative Suzuki-type coupling between β-keto-esters **61** and alkenyl trifluoroborates **62**, utilizing a chiral primary amine aminocatalyst **64** in combination with a redox mediator (Scheme 5, right).[106] Through systematic screening of suitable enamine redox mediators, dimethoxynaphthalene **65** emerged as an effective promoter for enamine SOMO-activation.
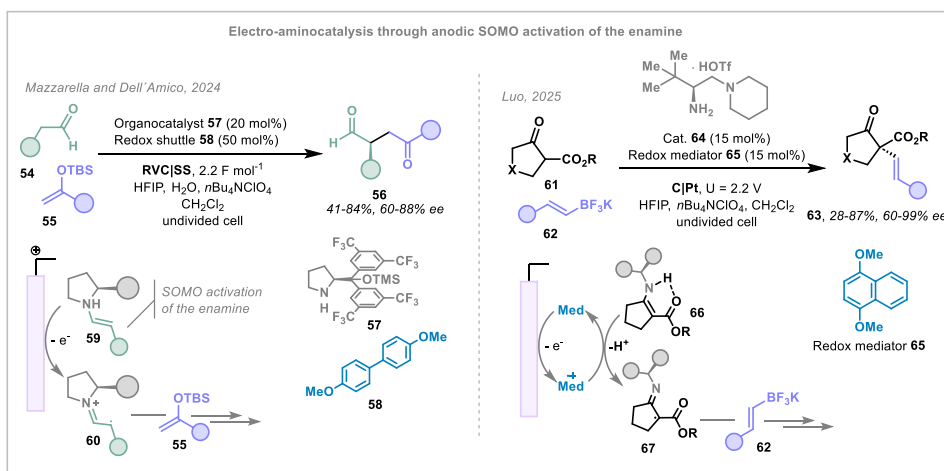
Scheme 5. Examples of asymmetric electro-aminocatalysis operating through anodic oxidation of the enamine intermediate, either directly or indirectly with redox mediator.

The reports on electrochemical aminocatalytic reactions proceeding *through iminium ion activation* are scarce; however, the area is undergoing active development. Our group developed an iminium ion-promoted asymmetric synthesis of cyclopropanes **70** *via* electrocatalytic, iodine-mediated ring closure (Scheme 6, left; see Results and Discussion for details).[107] Later, Albrecht reported asymmetric Diels-Alder cycloaddition

of hydroquinone **72** with α,β-unsaturated aldehydes **71**, where the dienophile **74** is generated electrochemically (Scheme 6, right).[108] These pioneering studies demonstrate the promising potential of combining electrochemistry with iminium catalysis to achieve novel stereoselective transformations.
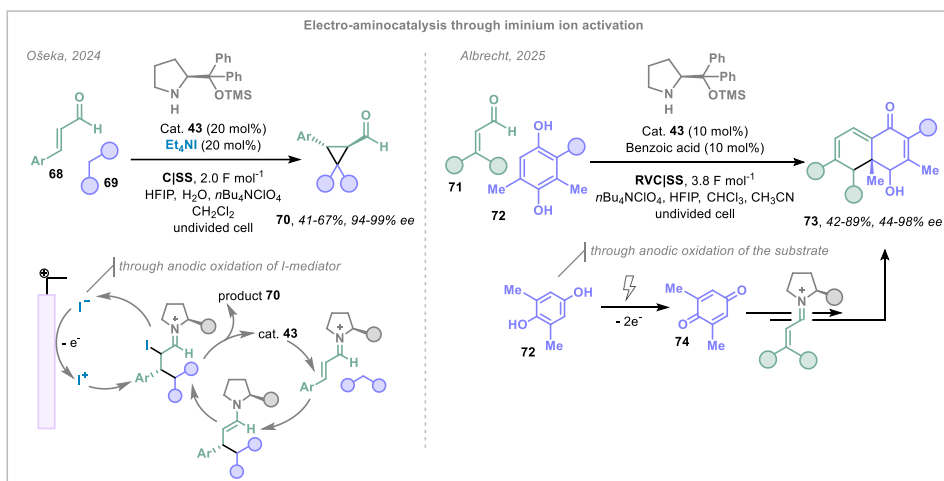
Scheme 6. Examples of asymmetric electro-aminocatalysis through iminium ion activation.

1.2 Motivation and aims of study

Electrocatalysis represents an attractive and sustainable approach for enabling novel enantioselective transformations. Developing new organocatalytic asymmetric transformations is a task of utmost importance in organic synthesis. Therefore, merging electrochemistry and organocatalysis motivated us to develop innovative reactions.

The specific aims of the study were:

- to develop an asymmetric organo-electrocatalytic cyclopropanation reaction;

- to discover the possibility of applying an electromediated approach using readily available halogen anions to promote the sustainability of the process;

- to demonstrate the robustness of the method through scope evaluation and perform mechanistic studies to elucidate the plausible mechanism of the transformation.

1.3 Results and discussions

The field of asymmetric electro-organocatalysis is currently under active investigation. Several landmark protocols reported over the last decade have opened new pathways to achieve greener and more efficient transformations driven by electricity. Recognizing existing gaps in this field, our group initiated the development of an asymmetric electrochemical reaction to demonstrate the proof-of-principle that electrochemistry is compatible with iminium ion organocatalysis.[107]

As a model reaction, we aimed to synthesize valuable chiral cyclopropanes. The traditional approach for cyclopropane synthesis involves Michael-initiated ring closure (MIRC) reactions, in which an iminium ion derived from an unsaturated aldehyde undergoes conjugate addition with a halogenated Michael donor, followed by intramolecular α-alkylation to form the cyclopropane ring.[109–112] Inspired by halogen-mediated electrochemical reactions for the efficient construction of cyclopropane rings, we designed a cascade process for cyclopropane formation using non-halogenated Michael donors and only catalytic amount of halide anion as a mediator (Figure 10, a).

The main challenge in related organo-electrocatalytic systems employing halogenated reagents, such as *N*-iodosuccinimide (NIS), is the undesired oxidative degradation of the organocatalyst, which frequently necessitates stoichiometric catalyst loading.[113] Our reaction design resolves this challenge: as the halide mediator serves as the most readily oxidizable species at the anode, the organocatalyst is effectively protected from destructive oxidation pathways.
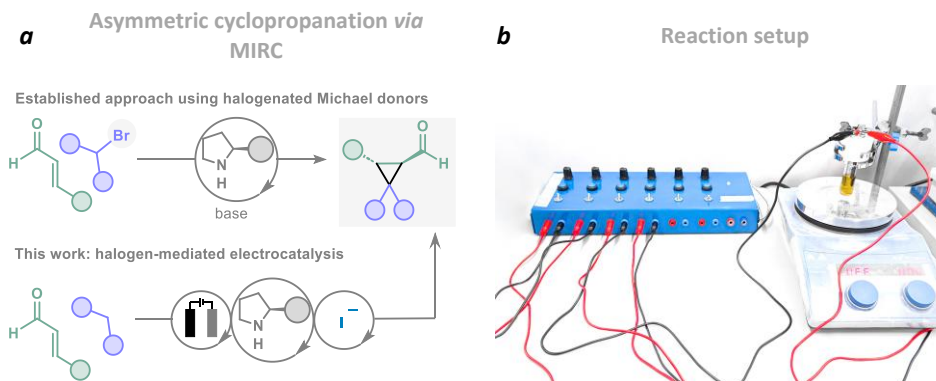
Figure 10. a) Previous reports on iminium ion promoted cyclopropanation utilizing halogenated substrates, and our report on electrochemical cyclopropanation. b) Electrochemical reaction setup featuring a custom-built power supply and cap, paired with an IKA ElectraSyn vial and electrodes.

1.3.1 Optimization

Initial investigations were performed with cinnamaldehyde **75** (1.5 equiv.) and dimethyl malonate **2** (1.0 equiv.), employing tetraethylammonium iodide (40 mol%) as the halogen source and organocatalyst **43** (20 mol%) in an undivided cell setup with a graphite (C) anode and stainless-steel (SS) cathode under galvanostatic conditions (1.0 mA, 2.0 F mol⁻¹). Initially, we conducted the reaction in EtOH, which served the dual role of solvent and electrochemically generated base, together with catalytic amounts of Et₄NI as the iodide source (Table 4, entry 2). A promising 37% yield of cyclopropane **76** was obtained with high enantio- and diastereoselectivity. Addition of acid (e.g., TFA or cinnamic acid) enhanced reaction productivity, affording 47–57% yield of the product. However, these

conditions exhibited high sensitivity to impurities in starting materials or catalyst, electrode contamination, and temperature fluctuations, resulting in poor reproducibility.

The reliability of the reaction was improved upon switching EtOH to CH_2Cl_2 as the solvent, with hexafluoro-2-propanol (HFIP) and H_2O as additives and nBu$_4$NClO$_4$ as electrolyte under the galvanostatic conditions (3.2 mA and 2.0 F mol^{-1}). HFIP can serve as proton source for cathodic reaction and was proven to stabilize iminium ions.[114] Under both EtOH and CH_2Cl_2 conditions, byproduct **78** formed (10–20% yield) *via* base-induced retro-Michael reaction of the enamine-cyclopropane intermediate, a pathway unrelated to the electrochemical conditions themselves. This side reaction represents a common challenge in previously reported aminocatalyzed syntheses of **76**,[110] and also diminished cyclopropane **76** yield in our system, with strong dependence on reaction time (correlating with electrochemical reaction rate and current density; see discussion below).

Table 4. Reaction condition optimization.^{a}

#	Deviation from reaction conditions	Yield, %			ee **76**, %^{b}
		76^c	**77**	**78**	
1	None	59	-	12	96
2	EtOH as solvent, no additives, 1.0 mA, 16 h	37	6	-	94
3	1.0 mA, 16 h	48	-	24	96
4	nBu$_4$NI instead of Et$_4$NI	47	4	7	97
5	I$_2$ or nBu$_4$NBr instead of Et$_4$NI	29/6	-/21	-	94
6	nBu$_4$NBF$_4$ or nBu$_4$NPF$_6$ as electrolytes	55	-	14-18	96
7	Pt or C as cathode	9	29-32	-	n.d.
8	CH$_3$CN as solvent	30	9	-	94
9	No halogen source	-	33	-	-
10	No organocatalyst	-	-	-	-
11	No electricity	-	49	-	-

^{a}Yields were determined by ^{1}H NMR analysis of the crude reaction mixture using trimethoxybenzene as an internal standard. ^{b} Enantiomeric excess of **76** was determined by chiral HPLC analysis. ^{c} Diastereomeric ratio of **76** was determined by ^{1}H NMR analysis of the crude reaction mixture and was for all entries <20 : 1. n.d.: not determined. Optimization of the reaction was performed together with Marharyta Laktsevich-Iskryk.

The optimal reaction time was determined to be 5 hours (Table 4, entry 1), whereas prolonging the reaction to 16 hours decreased product **76** yield while increasing byproduct **78** formation (entry 3). Changing the iodide source cation reduced cyclopropane **76** yield (entry 4), and substituting the halide with bromide or molecular iodine suppressed reaction conversion (entry 5). Alternative electrolytes slightly diminished cyclopropane **76** yield (entry 6). Substitution of the cathode material with graphite or platinum considerably suppressed cyclopropane formation (entry 7), and performing the reaction in acetonitrile reduced product **76** yield to 30% (entry 8). Importantly, no cyclopropane **76** was formed in the absence of halogen source, organocatalyst, or electricity (entries 9–11).

Aware that catalyst decomposition can occur through oxidation,[105, 115] and having observed degradation of catalyst **43** at the end of the reaction, we investigated alternative chiral aminocatalysts **79**–**86** with potentially greater stability. However, all tested organocatalysts proved susceptible to decomposition (as monitored by GC-MS and NMR analysis of the crude reaction mixture), and none of them improved yields or enantioselectivities of product **76** (Figure 11). We hypothesized that catalyst degradation proceeds through one or more pathways: reaction with electrophilic iodine species *via* Grob-type fragmentation,[114, 116] or electrochemical degradation through a Shono-type oxidation/elimination mechanism.[117]
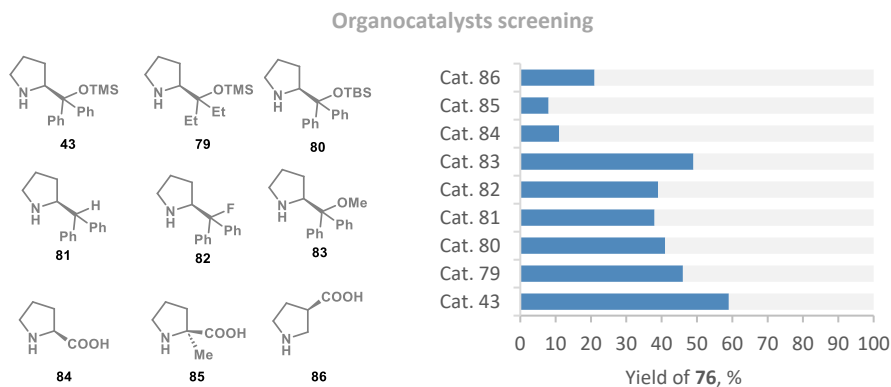
Figure 11. Results of organocatalysts screening. Reactions were performed under standard conditions (as in Table 4, entry 1), yields of 76 were determined by ^{1}H NMR analysis of the crude reaction mixture using trimethoxybenzene as an internal standard. TMS – Trimethylsilyl group, TBS – tert-butyl(dimethyl)silyl.

1.3.2 Mechanistic studies

To obtain initial insights into the reaction mechanism and side product formation pathways, we conducted kinetic studies on the model reaction between cinnamic aldehyde **75** and dimethyl malonate **2** under standard conditions (2.7 mA over 7 hours, Figure 12, left). Prior to applying current, intermediate **77** formed in 20% NMR yield. Upon passing 0.2 F mol^{-1} of charge, **77** increased to 30% while product **76** began to appear. As the reaction progressed, **77** was consumed completely by 1.7 F mol^{-1}, while the continued formation of both **76** and byproduct **78** was observed. Beyond 2.0 F mol^{-1}, cyclopropane **76** stopped forming and instead underwent degradation to **78**. Thus, limiting the charge to 2.0 F mol^{-1} is critical to prevent degradation of the product and minimize byproduct **78** formation.

We next used pre-synthesized **77** as the starting material, given its formation prior to electrolysis (Figure 12, right). After 1 h, **77** underwent partial conversion back to malonate **2** and aldehyde **75**, while cyclopropane **76** and byproduct **78** formed concurrently. This demonstrates reversibility of the Michael addition and complex reaction kinetics. Complete electrolysis (2 F mol^{-1}) provided **76** (43%) and **78** (17%).

*Figure 12. Kinetic studies of the model reaction and the reaction starting from **77**. Experiments were performed under standard conditions unless specified in the scheme.*

Control experiments with I_2 or NIS under non-electrochemical conditions resulted in decomposition of organocatalyst **43** without any product formation. This highlights the essential role of electrochemistry in generating the reactive electrophilic iodine species (F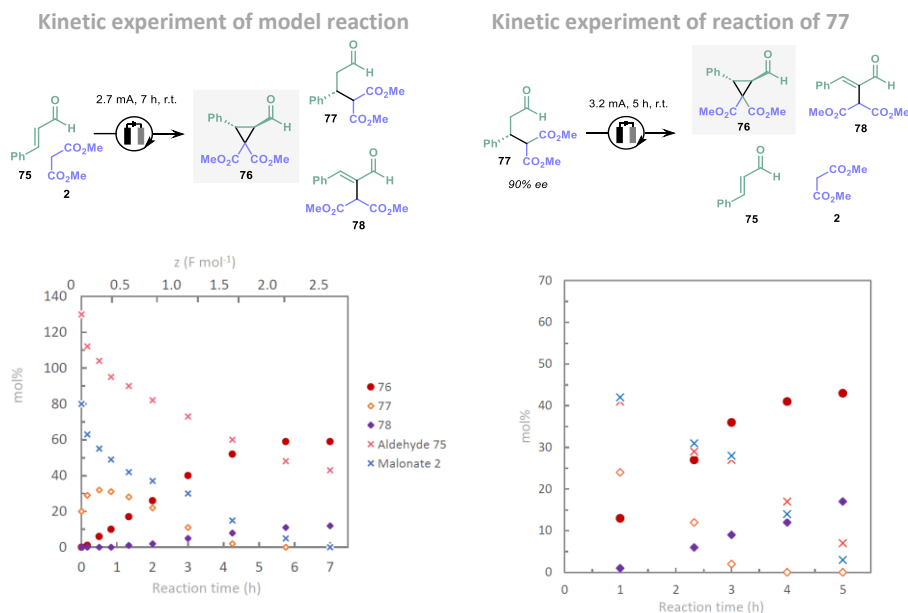igure 13, a, (i)). Then, we questioned whether the reaction proceeds through a polar or radical pathway. When the control experiment with *radical scavenger* dibutylhydroxytoluene (BHT) was performed, we still observed the formation of cyclopropane **76** (38% NMR yield) and traces of **77** (4% NMR yield) in the crude NMR (Figure 13, a, (ii)). This result indicates that no quenching of the potential enamine radical cation occurred. *Without aminocatalyst*, product **76** was formed from **77** in only 23% yield and lower diastereomeric ratio (2.5:1) (Figure 13, a, (iii)). Therefore, we propose that the reaction proceeds through a predominantly polar pathway.

To gain further understanding of the reaction mechanism, we also performed *cyclic voltammetry studies* for Et_4NI, catalyst **43**, aldehyde **75**, intermediate **77** and the mixtures of aminocatalyst **43** with aldehydes **75** and **77** (Figure 13, b). Iodide has two distinct peaks of oxidation at +0.19 V and +0.38 V, and the first oxidation has the lowest oxidation potential in the system. However, enamine formed from **77** (**77**+ cat. **43**) has an oxidation peak at +0.27 V, lower than the second oxidation peak of iodide, and might undergo SET oxidation in the reaction conditions. The other components of the reaction have higher oxidation potentials than iodide and should not undergo anodic oxidation.

Based on previous studies and control experiments, we propose a reaction mechanism involving two interconnected catalytic cycles (Scheme 7). The organocatalytic cycle begins with condensation of α,β-unsaturated aldehyde **75** and catalyst **43** to form iminium ion **A**. Malonate **2** then undergoes Michael addition to **A**, generating enamine intermediate **B**. This intermediate captures an electrophilic iodine species [I^+] produced in the electrocatalytic cycle *via* anodic oxidation of iodide. The resulting intermediate **C** undergoes intramolecular alkylation, forming iminium-cyclopropane **D** while releasing an

iodide anion. Hydrolysis of **D** regenerates the catalyst and yields the desired product **76**. Simultaneously, the cathodic counter reaction produces hydrogen gas.
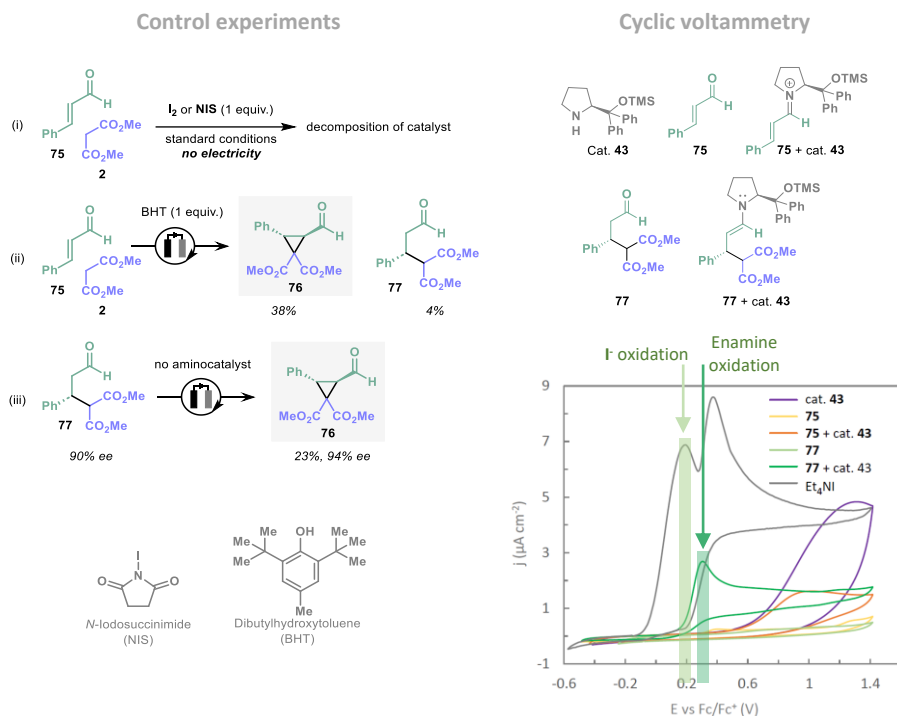
Figure 13. a) Control experiments. Experiments were performed under standard conditions unless specified on the scheme. b) Cyclic voltammetry experiments. Cyclic voltammetry measurements. Voltammograms recorded in 0.1 M nBu₄NPF₆ CH₃CN solution with Ag/Ag⁺ reference electrode and realigned with respect to Fc/Fc⁺ couple. Arrows indicate the direction of the potential scan. Experiment with BHT and cyclic voltammetry studies were performed by Marharyta Laktsevich-Iskryk.
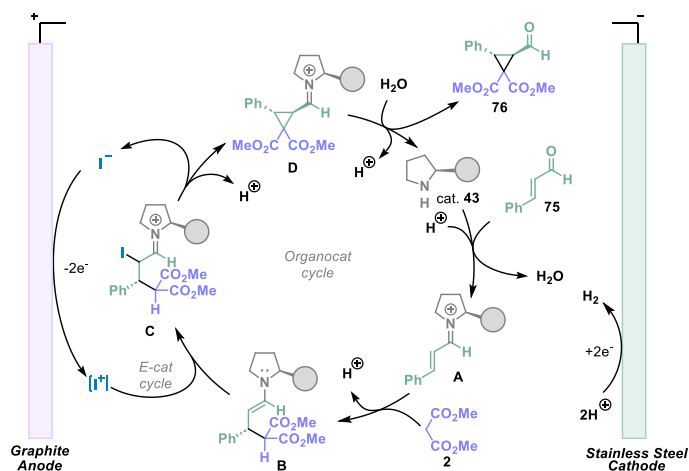
Scheme 7. Proposed reaction mechanism.

1.3.3 Scope

We then investigated the substrate scope of this transformation. Aromatic α,β-unsaturated aldehydes undergo the cascade transformation with consistently excellent stereoselectivity, achieving 94–98% *ee* and (>20:1 *d.r.*) across the substrate scope. A range of electron-withdrawing and -donating groups in the aromatic ring of aldehyde, including redox-sensitive nitro and methoxy substituents, are well-tolerated (**77**–**85**). Bearing heterocyclic rings α,β-unsaturated aldehydes (furylacrolein and tiophenyl acrolein) formed corresponding cyclopropanes in poor yields, and alkyl aldehydes completely decomposed under the electrochemical reaction. Ketoester nucleophile was also efficient in this transformation (product **87**), and we were pleased to observe that both unprotected and Bn-protected oxindoles delivered spirocyclopropanes **88** and **89** in good yields and *d.r.*, providing access to spirooxindole scaffolds.
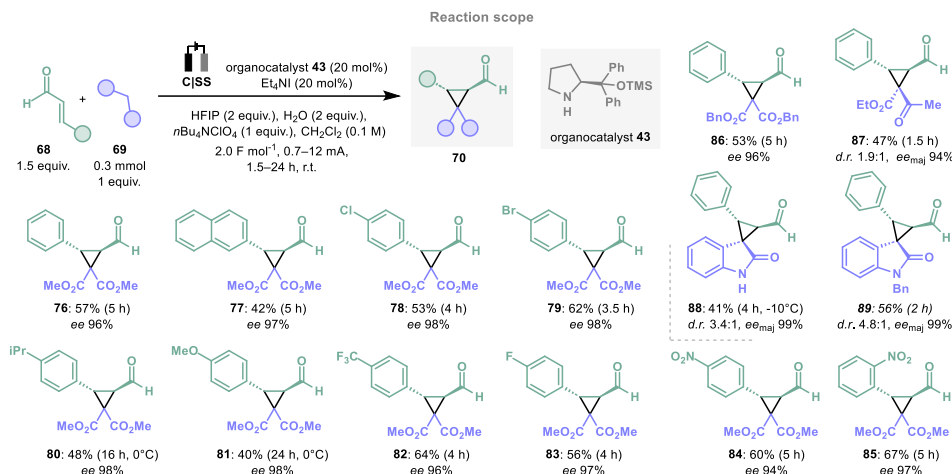
*Scheme 8. Substrate scope of the electro-organocatalytic cyclopropanation. Yields and enantiomeric excess refer to isolated products. Yields, d.r. and ee of products **88** and **89** correspond to the isolated products after in situ reduction to the corresponding alcohols with sodium borohydride. The scope of the reaction was prepared together with Marharyta Laktsevich-Iskryk in equal parts.*

During scope investigation, we noticed that achieving good yields of cyclopropanes **76** requires balancing the rates of the organocatalytic and electrocatalytic halogen-mediated steps while minimizing byproduct **78** formation. Reaction time, which controls the rate of electron transfer and consequently [I⁺] generation, and temperature, which controls the organocatalytic step, appeared to be critical parameters, improving yields from traces amounts to good yields for challenging substrates.

As an example, we performed a thorough *investigation of temperature and reaction time* effects using 4-methoxycinnamaldehyde as the substrate. We observed rapid formation of a retro-Michael byproduct when the reaction was conducted at room temperature (Figure 14). Under these conditions, maximum yield was achieved at 2 hours (34% cyclopropane **81**, 19% **byproduct-81**, 89% conversion of dimethyl malonate **2**). To suppress byproduct formation, the reaction was conducted at 0 °C. Although the reaction time increased significantly, we obtained higher yield of cyclopropane **81** over 24 hours (40% product **81**, 15% **byproduct-81**, 91% conversion of malonate **2**).
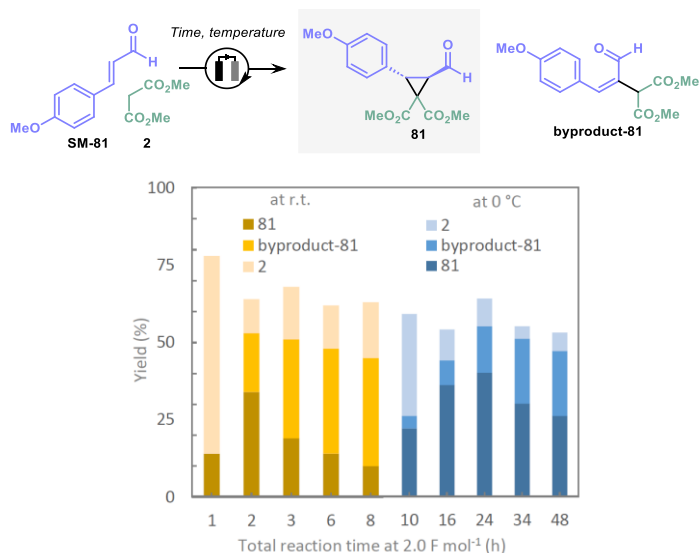
*Figure 14 The outcome of the reaction between **1i** and **2a** at varying temperatures and reaction times. Separate reactions with 2.0 F mol^{-1}. This study was performed together with Marharyta Laktsevich-Iskryk.*

1.4 Conclusions to Chapter 1

- We successfully developed the first asymmetric electrochemical cyclopropanation combining electrochemistry with iminium ion organocatalysis. Fourteen examples of cyclopropanes were obtained in 41–67% yields with excellent stereoselectivity (94–98% *ee*).

- Mechanistic investigations confirm the transformation proceeds through a polar pathway involving iminium formation, Michael addition, and intramolecular alkylation, with the electrochemically generated electrophilic iodine species serving as the key ring-closing mediator.

- While the method shows good scope for aromatic aldehydes and diverse nucleophiles, heterocyclic and alkyl aldehydes remain challenging.

2 Photoredox- and EDA complex-enabled ring-opening reaction of cyclopropanols

Photochemistry can be encountered everywhere in our everyday life: photosynthesis in plants, formation of vitamin D in human skin, eye vision, and photodegradation of plastics.[118] In science, photochemistry studies chemical interactions between photons and matter. The first general principle of photochemistry was established in 1817 by Theodor von Grotthuss and in 1841 by John W. Draper and stated that "only the light absorbed is effective in producing photochemical change". Later, Johannes Stark in 1908 and Albert Einstein in 1913 independently formulated *the photoequivalence law*: "there should be a 1:1 equivalence between the number of molecules decomposed and the number of photons absorbed".

Because photochemical reactions are often complex and absorption of a photon can be followed by other processes (for example, photophysical processes that eventually restore the reactant in the ground state) the efficiency of a specific photochemical process is expressed by its *quantum yield* (Φ, Equation 2):[119]

$$\Phi\,(\lambda)\ =\ \frac{amount\ of\ reactant\ consumed\ or\ product\ formed}{amount\ of\ photons\ absorbed} \qquad \textit{Equation 2}$$

However, sometimes one photon can produce a greater number of molecules (Φ > 1), which can be explained by chain mechanism.

In the wave model, light is electromagnetic radiation defined by its wavelength (λ), frequency (ν), and speed (*c*), related by $\lambda\nu = c$ (Figure 15). In the quantum model, light is viewed as a stream of photons, each with energy E = hν, where h is Planck's constant.[120] Therefore, quantum theory serves as the foundation of photochemistry, providing the quantitative background for understanding apply light-matter interactions.
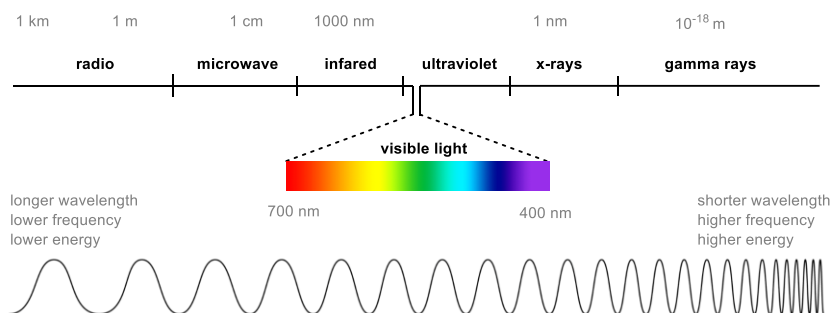
Figure 15. Electromagnetic spectrum.

2.1 Literature review

2.1.1 Excited state and reactions under direct excitation

When a molecule absorbs a photon of the right wavelength, it can be promoted to the *electronically exited state*. In this state, the molecule possesses more energy than in its ground state and tends to dissipate this excess energy through different pathways (Figure 16, a). The molecule can relax back to the ground state, mostly through *photophysical processes*, or it can undergo *photochemical processes* that change its structure. Such photochemical transformations can occur through unimolecular or bimolecular routes. The main unimolecular pathways include isomerization, fragmentation, and structural rearrangements, while bimolecular options encompass electron transfer, energy transfer, proton transfer, and photoaddition reactions (Figure 16, b).
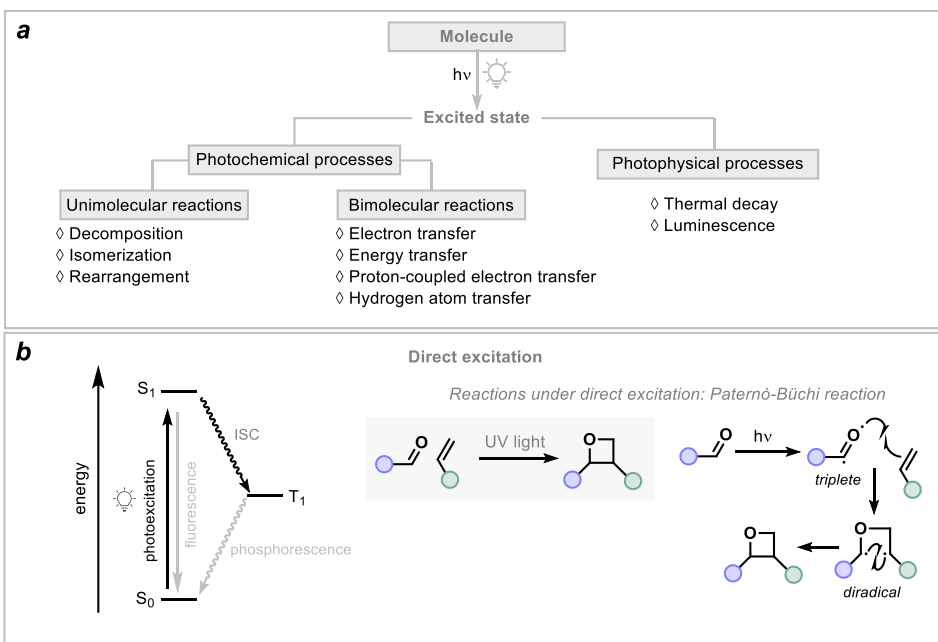
Figure 16. a) Processes initiated by the light absorbtion of the molecules. b) Direct photoexcitation and a reaction induced by direct excitation: an example of [2+2]-cycloadditon. ISC − intersystem crossing.

First photochemical synthetic transformations were performed in the 19th century by pioneers such as Stanislao Cannizzaro, Emanuele Paternó, and Giacomo Ciamician, using direct excitation of organic molecules by sunlight.[121] Though many reactions have been developed using this approach, including cycloaddition, isomerization, and cleavage, it has a major limitation. Most organic molecules absorb only high-energy light (such as UV) and have very short excited-state lifetimes. However, organic dyes and certain transition metal complexes are able to absorb light across a range of frequencies, including visible light, and then transfer their excited-state energy to another molecule. This process forms the basis of a field known as photochemistry.[122]

The wider accessibility to energy efficient, durable and precise light sources, such as light-emitting diodes (LEDs) gave a boost to the development of synthetic photochemistry.

These technologies allowed finely control the wavelength and intensity of light, thereby improving the selectivity, reproducibility and reducing the costs of photochemical reactions.[123]

2.1.2 Main mechanisms of photocatalysis

Most photochemical reactions occur directly from an excited state precursor (**R**), which can be obtained either directly by absorption of light or indirectly by *photosensitization* (*via* energy transfer) (see Scheme 9, a). In the *energy transfer* the excited photocatalyst (**PC**) is transferring excessive energy to the neighboring organic substrates, which cannot directly absorb light. If a photosensitizer functions as an electron donor or acceptor and is regenerated through an associated electron transfer reaction elsewhere in the reaction cycle, it is referred to as a *photoredox catalyst*.
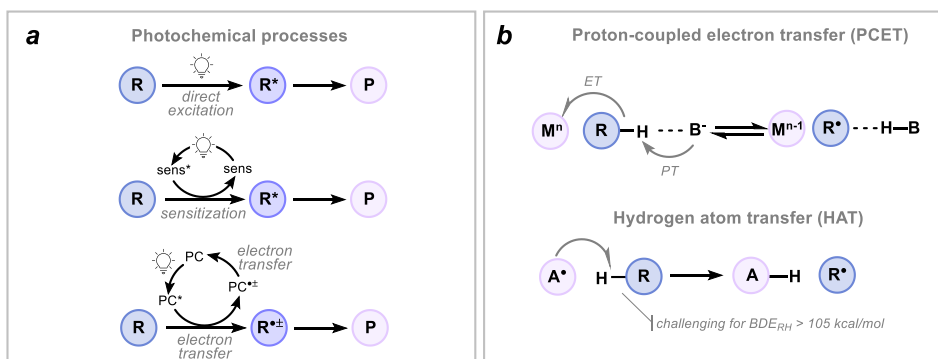
Scheme 9. a) Schematic representation of main photochemical pathways. b) Photochemical atom transfer reactions. BDE – bond dissociation energy. PC – photocatalyst, sens – photosensititizor, ET – electron transfer, PT – proton transfer, R – precursor, P – product, B – Brønsted base, M – metal center, A – hydrogen atom abstractor.

Another important mechanism of photochemical activation is *concerted proton-coupled electron transfer (PCET,* Scheme 9, b*)*. In PCET, the proton transfer (PT) from the precursor to a Brønsted base and electron transfer (ET) from the precursor to photocatalyst occur simultaneously in a single elementary step.[124, 125] Experimentally, in the concerted PCET reaction a kinetic isotope effect (KIE) is observed. Importantly, PCET can also be promoted by the reaction medium, expanding the scope and versatility of photoredox chemistry.

Hydrogen atom transfer (HAT) may be viewed as a special case of concerted PCET (Scheme 9, b). In HAT, the electron and proton transfer between the same donor and acceptor.[125, 126] HAT reactions play a central role in chemical synthesis and in the activity of biological antioxidants. The bond dissociation energy (BDE), which reflects bond strength, often governs the feasibility of hydrogen atom transfer (HAT) processes.[127, 128] Consequently, HAT is generally limited to the activation of relatively weak X–H bonds, even when very strong hydrogen-atom acceptors are employed. Activation of stronger bonds, such as O–H or N–H, is therefore much more challenging. In this context, PCET emerges as a complementary approach to HAT, capable of activating a broader variety of bonds.[129, 130]

2.1.3 Overview of Photoredox Catalysis

Mainly, photoredox catalysts operate through a single-electron transfer (SET) pathway, in which the excited photocatalyst donates or accepts an electron from an organic substrate, thereby generating reactive radical intermediates under mild conditions.[131] The pioneering studies on visible-light photoredox catalysis date back to the 1980s, with the contributions of Deronzier,[132] Kellnogg,[133] and others. However, the modern era of photoredox catalysis began in 2008–2009 with these innovative reports (Scheme 10, a): MacMillan's group demonstrated the merger of SOMO organocatalysis with photoredox catalysis (for mechanism, see Scheme 10, b),[134] Yoon's group applied photoredox catalysis to the intramolecular [2+2] cycloaddition of dienones,[135] and Stephenson's group developed photocatalyzed reductive dehalogenation reaction.[136]

Transition metal catalysts, such as iridium and ruthenium complexes, possess excellent photochemical properties and are widely used as photocatalysts, but their high cost and toxicity can hinder large-scale applications. Organic dyes offer an attractive alternative: they are cheaper, less toxic, and easy to handle. Therefore, organic photoredox catalysis has attracted significant attention (see their excided state potentials in Figure 17, b).[137] Nowadays, photoredox catalysis has become an essential part of modern synthetic organic chemistry offering a mild and versatile approach to the generation of reactive intermediates and valuable products.
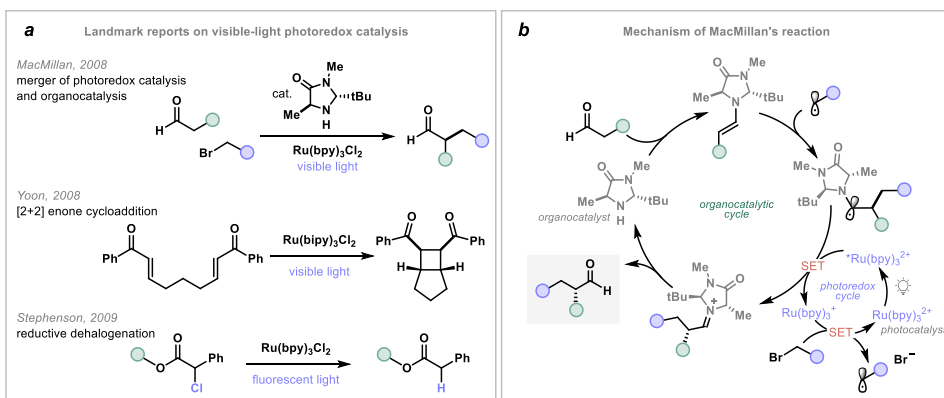
Scheme 10. a) Key works in photoredox catalysis signaled the revival of the field. b) Mechanism of MacMillan's SOMO organo- photoredox catalysis.

The most widely used photoredox catalysts are transition metal complexes, where the metal center is coordinated by organic ligands.[138] In their excited state, transition metal photocatalysts exhibit a dual character, functioning as both oxidants and reductants. This allows them to participate in redox reactions through two pathways: *oxidative* and *reductive quenching* (Figure 17, a). In the oxidative cycle, ***PC** acts as a reductant, donating an electron to an acceptor (**A**) to form **A$^{\bullet-}$** and **PC$^+$**. The latter is a strong oxidant that can be reduced back to **PC** by an electron donor (**D**), thereby closing the catalytic cycle. In the reductive cycle, ***PC** instead acts as an oxidant, accepting an electron from **D** to give **PC$^-$**, a strong reductant that can subsequently transfer an electron to **A** and regenerate the ground-state catalyst. The redox properties of these complexes can be finely tuned by ligand substitution: electron-donating groups increase reducing properties, while electron-withdrawing groups increase oxidizing properties. Beyond simple oxidative and reductive quenching, photocatalysts can also promote *redox-neutral reactions,*

in which substrates undergo both single-electron oxidation and single-electron reduction at different points in the mechanism. In such cases, the overall oxidation state of the system remains unchanged, and no stoichiometric external reagents are required to sustain the photocatalytic cycle.[131, 139, 140]

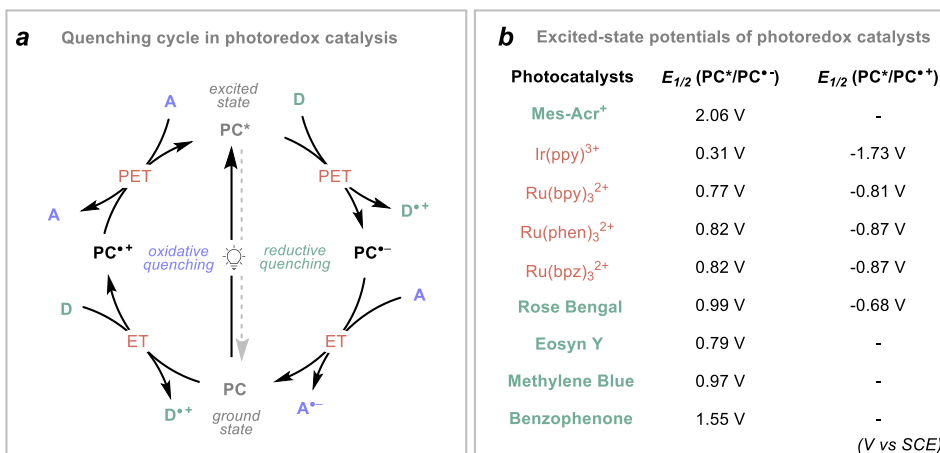| *a* Quenching cycle in photoredox catalysis	*b* Excited-state potentials of photoredox catalysts		
	Photocatalysts	$E_{1/2}$ (PC*/PC$^{\bullet-}$)	$E_{1/2}$ (PC*/PC$^{\bullet+}$)
	Mes-Acr$^+$	2.06 V	-
	Ir(ppy)$_3^{3+}$	0.31 V	-1.73 V
	Ru(bpy)$_3^{2+}$	0.77 V	-0.81 V
	Ru(phen)$_3^{2+}$	0.82 V	-0.87 V
	Ru(bpz)$_3^{2+}$	0.82 V	-0.87 V
	Rose Bengal	0.99 V	-0.68 V
	Eosyn Y	0.79 V	-
	Methylene Blue	0.97 V	-
	Benzophenone	1.55 V	-
			(V vs SCE)

Figure 17. a) Oxidative and reductive quenching cycles in photoredox catalysis. b) Excited-state potentials of common photocatalysts. E is given in V vs SCE. PET – photoinduced electron transfer, ET – electron transfer, A – acceptor, D – donor; ppy – 2-phenylpyridine, bpy – 2,2'-bipyridine, phen – 1,10-phenanthroline, bpz – 2,2'-bipyrazine, Mes-Acr – 9-mesityl-10-methylacridinium.

2.1.4 Chemistry of TBADT

Among transition metal photocatalysts, polyoxometalates (POMs) stand out as transition metal-oxygen clusters, usually based on W or Mo.[141] Their versatile properties, and lower cost compared to Ru- or Ir-based complexes make them valuable for photochemical catalysis. Particular interest attracts *tetrabutylammonium decatungstate* (nBu$_4$N)$_4$W$_{10}$O$_{32}$ (TBADT), known by its ability to absorb light at 310–400 nm and to cleave strong C–H bonds, even of the light hydrocarbons (Figure 18, a).[142] TBADT has enabled a number of synthetically useful C(sp^3)–H functionalizations,[143, 144] including oxidations,[145, 146] dehydrogenations,[147] fluorinations,[148] trifluoromethylation,[149] arylations,[150] and many others.

The absorption spectrum of the decatungstate anion shows a broad band centered at 324 nm, while almost all of its reduced derivatives involved in photocatalytic reactions are deep blue, with strong absorption bands in the 600–800 nm region.[151–153, 143] Upon excitation, the singlet excited state (S$_1$) is initially formed with a lifetime on the order of picoseconds, after which it rapidly decays to the relaxed triplet excited state (**wO**), the actual reactive species (see Figure 18, b). **wO** can react with organic molecules either by hydrogen atom transfer mechanism, or by SET mechanism ($E_{1/2}$ *[W$_{10}$O$_{32}$]$^{4-}$ / [W$_{10}$O$_{32}$]$^{5-}$ = +2.4 V *vs* SCE),[154] depending on the structural and redox properties of the substrate, leading to the monoreduced forms of decatungstate, H[W$_{10}$O$_{32}$]$^{5-}$ or [W$_{10}$O$_{32}$]$^{5-}$. [W$_{10}$O$_{32}$]$^{5-}$ might spontaneously disproportionate, giving the reduced [W$_{10}$O$_{32}$]$^{6-}$, a good reductant ($E^{red}_{1/2}$([W$_{10}$O$_{32}$]$^{5-}$/[W$_{10}$O$_{32}$]$^{6-}$) = −1.48 V *vs* SCE), and the oxidized [W$_{10}$O$_{32}$]$^{4-}$.[150] The HAT domain is the most prevalent for TBADT and enables site-selective functionalization of alkanes, alcohols, ethers, ketones, amides,

esters, nitriles, and pyridylalkanes, with selectivity governed by both polar and steric effects (Figure 18, c).[154]

Even though the decatungstate anion is a strong one-electron oxidant in its photoexcited state, the SET reactivity of decatungstate remain underdeveloped.[155] To the best of our knowledge, SET oxidation of aromatic hydrocarbons have been developed[156] along with the benzylation of electrophilic alkenes.[157, 158] In the second approach, Fagnoni and Ravelli developed TBADT-photocatalyzed reaction of benzylsilanes and arylacetic acids *via* the generation of benzylic radicals. Recently, the Fagnoni group demonstrated that substrates bearing redox-active esters (e.g., *N*-hydroxyphthalimide esters) can be reduced by $[W_{10}O_{32}]^{6-}$ acting as a single-electron reductant, thereby unveiling new opportunities within the photocatalytic cycle of TBADT (Figure 18, c).[159]
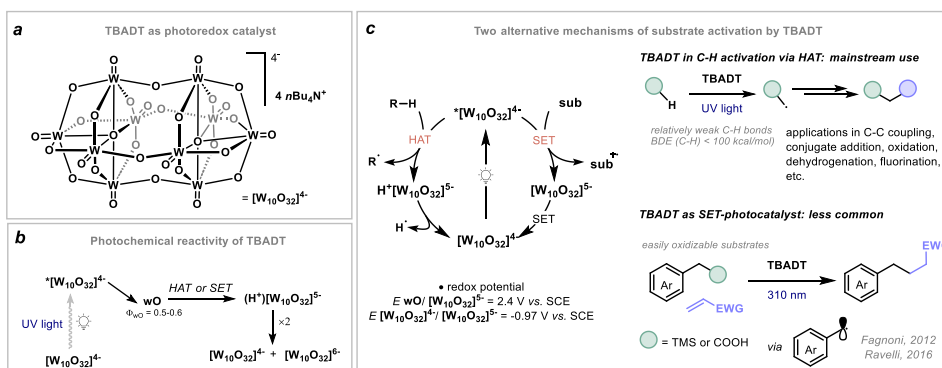
Figure 18. a) Structure of TBADT. b) Formation of reactive species of TBADT upon excitation. c) Mechanisms of TBADT operation: HAT and SET.

2.1.5 Light induced single-electron transfer *via* EDA complexes

Nowadays, the use of a photoredox catalyst is the most common and well-established strategy. Nevertheless, light induced single-electron transfer might be performed without any external photocatalyst between a pair of specific substrates which can form a complex. This photoactive *electron donor-acceptor (EDA) complex* is a ground-state association of an electron-rich substrate with an electron-accepting molecule, which has different physical properties from those of the separated substrates (Figure 19).[160–163] An EDA complex is a ground-state association characterized by the appearance of a new absorption band, the charge-transfer (CT) band, associated with a single-electron transfer (SET) from the donor to the acceptor, which often has maximum absorption in the visible region. The formation of EDA complexes is characterized by *association constant* (K_{EDA}), which characterizes the equilibrium between free donor and acceptor and the complex and describes the strength of the EDA complex.
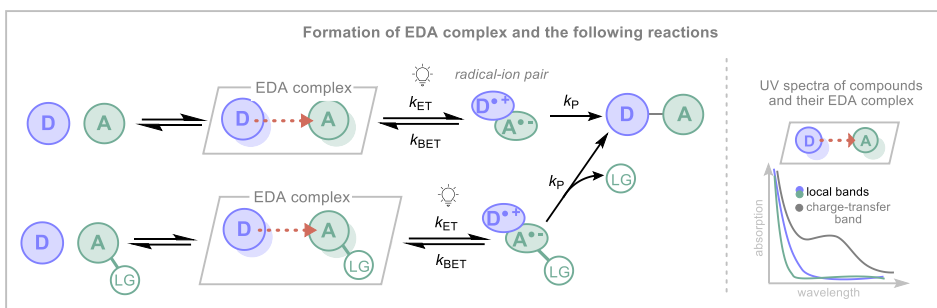
Figure 19. Formation and excitation of EDA complex via stoichiometric approach and leaving-group approach and the absorption spectra of compounds alone and of their EDA complex, with bathochromic shift.

Electron donor-acceptor (EDA) complexes have been investigated since the 1950s,[164, 161, 160] but their relevance to synthetic chemistry was revitalized in 2013 through studies by the Chatani and Melchiorre groups.[165, 166] In their pioneering report, the Melchiorre group demonstrated that catalytically formed chiral enamine-based EDA complexes, upon light irradiation, undergo ET to generate chiral contact radical ion pairs (Scheme 11). The key driving force for subsequent transformation was the presence of a suitable leaving group in the radical anion partner, which promoted fragmentation at a rate faster than back electron transfer (BET). This strategy enabled an α-alkylation of aldehydes **1** with electron-deficient alkyl bromides **2** through simple visible-light irradiation of the reaction mixture, without the need for an external photocatalyst.
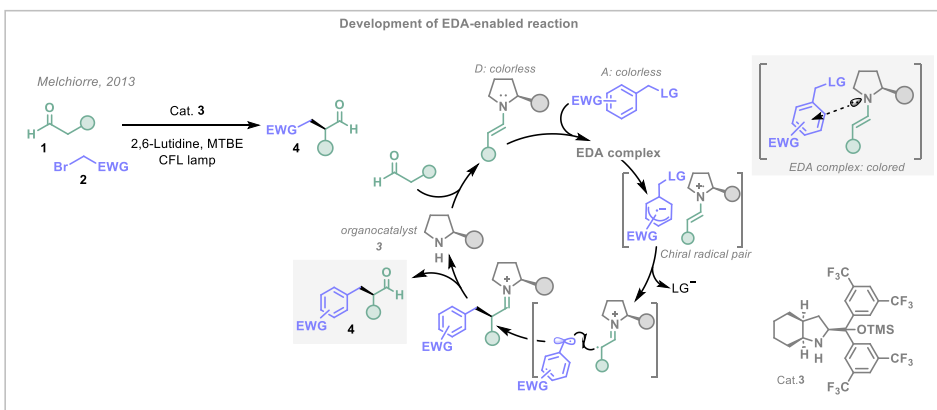
Scheme 11. The pioneering report on synthetic applications of EDA complexes by Mechiorre group.

Since then, research on EDA complexes has expanded rapidly, enabling novel C–C, C–N, and C–O bond formations with broad functional group tolerance and stereocontrol.[167, 168] Recent advances in *general catalytic systems* for EDA photoactivation now allow the generation of photoactive complexes from a wide range of radical precursors.[169] Ongoing efforts focus on the catalytic design of both EDA donors[170–172] and acceptors,[173, 174] demonstrating the continued evolution of this field.

2.1.6 Photochemical reactions of strained rings systems and cyclopropanols

Cyclopropanols are valuable building blocks in organic synthesis due to their straightforward preparation by Kulinkovich or Simmons-Smith reactions and high reactivity enabled by cyclopropane ring strain (Figure 20).
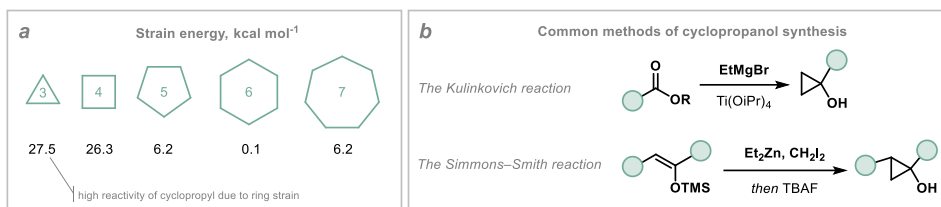
Figure 20. a) Ring strain values for the range of carbocycles. b) The main strategies towards cyclopropanol synthesis.

Most commonly, tertiary cyclopropanols undergo ring-opening through *heterolytic* (homoenolate-mediated) or *homolytic* (affording β-keto radical) cleavage of C1–C2 bonds (Scheme 12, a). These processes have found already multiple synthetic applications but remain inexhaustible source for further innovations.[175–177]

In particular, the generation of β-keto radicals could proceed *via* two distinct transient species: *alkoxy radical* **I** or *radical-cation* **II** (Scheme 12, a). The generation of *alkoxy radical* **I** through the homolytic cleavage of O−H bond is challenging in view of rather high bond dissociation energy (BDE) of O−H bonds in alcohols (typical BDE values 103–105 kcal mol^{-1}).[178, 179] Recently, photoredox catalysis provided facile access to alkoxy radicals from cyclopropanols by means of proton-coupled electron transfer (PCET) catalyzed by transition metal-containing photocatalysts or organophotocatalysts.[180–187] Alternatively, alkoxy radicals can be generated by photoinduced ligand-to-metal charge transfer in the presence of iron or cerium compounds.[188–192] The alternative strategy *via radical-cation* **II** relies on photocatalytic single-electron transfer (SET) oxidation of cyclopropanols and usually requires a stoichiometric oxidant.[193–195] Traditionally, in non-photochemical reactions, transition metal compounds (Ag (I)[196, 197], Fe (III)[198–200], or Mn(III)[201, 202]) are applied as SET oxidants, often in combination with additional oxidative reagents and under harsh reaction conditions (Scheme 12, b). Light-induced transformations frequently merge photochemical reactivity with transition metal catalysis, a synergistic strategy that has enabled a wide range of efficient and versatile reactions.[203]
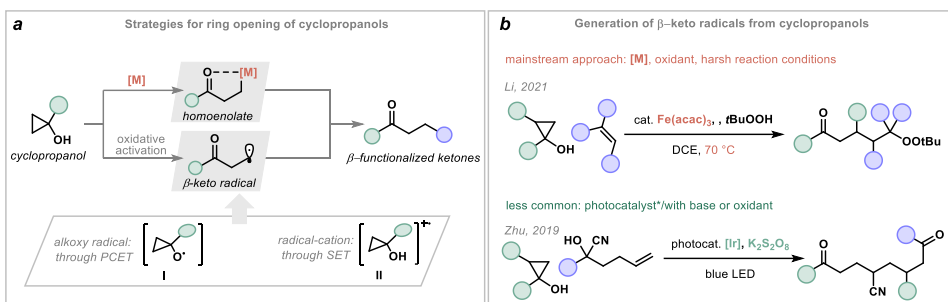
Scheme 12. a) Main strategies of cyclopropanol ring-opening. b) Examples of mainstream, transition metal catalysed approach, and photocatalyzed strategy.

Although β-keto radical generation from cyclopropanols has been extensively studied, their *photocatalytic reactions with electron-deficient alkenes* remain largely unexplored. (Scheme 13, a).

The group of Yamamoto used PCET strategy for the intramolecular reaction of cyclopropanols and electro-deficient alkenes **5** leading to the ring expansion.[184] Organic photocatalyst 4CzIPN was used along with nBu$_4$P$^+$(PhO)$_2$POO$^-$ as a base and blue LEDs as the light source to afford 1-tetralone **6** and 1-benzosuberone derivatives **7**.

In 2022, Hu and co-workers developed chlorine radical-induced reaction of alcohols **8**, including cyclopropanols, and alkenes **9** catalyzed by iron salts under blue LED irradiation.[204] Mechanistically, an excited iron chloride complex generates chlorine radicals that, with base assistance, abstract hydrogen from the OH group of cycloalkanols to form an alkoxy radical, which then undergoes β-scission to yield an alkyl radical.

Another interesting example was reported by Melchiorre and co-workers in 2018. The researchers developed an enantioselective photochemical cascade reaction of cyclopropanols **12** and α,β-unsaturated aldehydes **11**, which combined the excited-state and ground-state reactivity of chiral organocatalytic intermediates.[205] The excited iminium ion served as a strong SET oxidant, which could oxidize cyclopropanols to β-keto radical cation. Then, this radical reacts with an iminium ion to form enamine, with subsequent cyclization to form cyclopentanols **13** with excellent enantiomeric excess.

Recently, electron-rich cyclopropanols were found to form EDA complexes with electron-deficient alkenes, undergoing photoinduced ring-opening followed by the addition to the double bond (Scheme 13, b). Our group first described this phenomenon specifically for cyclopropanols **15** (n = 1),[206] and shortly thereafter Alemán and Marzo expanded the scope of the transformation through a PCET activation strategy to both strained and unstrained cycloalkanols **15** (n = 1–10).[207]
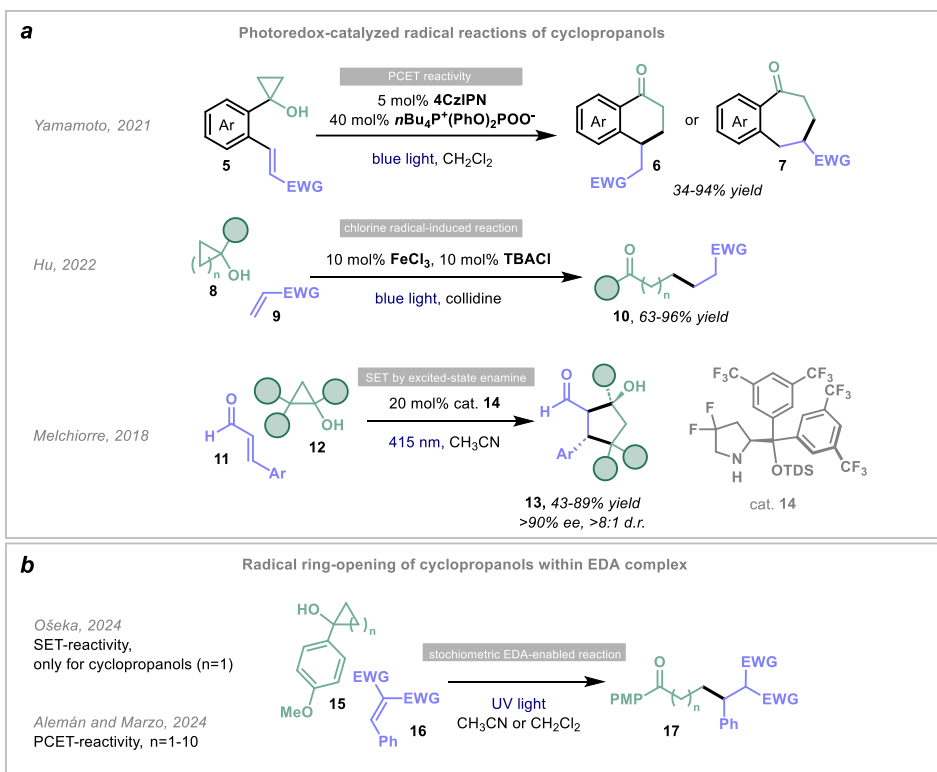
Scheme 13. a) Photocatalytic reactions of cyclopropanols with electron-deficient alkenes. b) Photoinduced cyclopropanol ring-opening through EDA complex formation.

2.2 Motivation and aims of study

Photochemistry offers a mild and versatile approach to the generation of reactive intermediates and valuable products. We aimed to develop a photocatalytic protocol for β-keto radical generation from cyclopropanols and their reactivity towards electron-deficient alkenes.

The specific aims of the study were:

- to develop a photocatalytic ring-opening cross-coupling of cyclopropanols with electron-deficient alkenes was established using TBADT;

- to explore the substrate scope and limitations of the developed transformation;

- to perform mechanistic studies to elucidate plausible mechanism of the transformation.
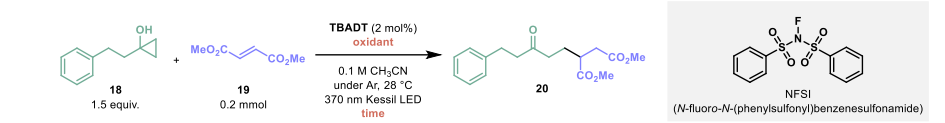
2.3 Results and discussions

The development of new strategies for generating β-keto radicals from cyclopropanols remains an attractive area of research. To address existing limitations, we sought to establish a simple and cost-effective photochemical protocol for efficient cyclopropanol ring-opening, followed by the addition of the resulting radical to electron-deficient alkenes. This approach provides access to a variety of β-functionalized ketones – valuable synthetic intermediates and building blocks in organic chemistry[206].

2.3.1 Optimization

Our investigation began with the reaction of 1-phenylethylcyclopropanol **18** and dimethyl fumarate **19**, employing 2 mol% TBADT as the photocatalyst in acetonitrile under an inert atmosphere and ambient temperature (Table 5). Irradiation with UV light (Kessil lamp, 370 nm) for 3 h afforded traces of the desired product **20** (entry 1). Interestingly, the addition of an external oxidant significantly influenced the outcome: the use of oxygen or potassium persulfate ($K_2S_2O_8$) as oxidants gave modest yields (30–36%, entries 2 and 3), whereas *N*-fluorobenzenesulfonimide (NFSI) proved more effective, especially when the cyclopropanol loading was increased to 3 equivalents (entry 5). Lowering the NFSI loading to 0.5 equivalents did not significantly affect efficiency (entry 6), suggesting that catalytic amounts are sufficient. Control experiments confirmed that no product was obtained in the absence of the photocatalyst, even under irradiation (entry 7). Furthermore, changing the solvent to dichloromethane and lowering the TBADT loading improved the yield of **20** to 63% (entry 8).

Table 5. Optimization of the reaction of 1-phenethylcyclopropanol with dimethyl fumarate.[a]
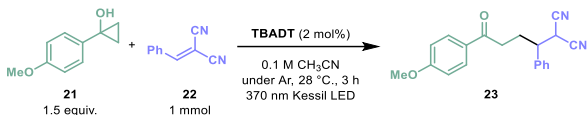
Entry	Oxidant	Time, h	Yield, %[b]
1	none	16	5
2	O₂ (air)	16	30
3	$K_2S_2O_8$ (0.5 equiv.)	6	36
4	NFSI (1.0 equiv.)	3	39
5[c]	NFSI (1.0 equiv.)	3	57
6[c]	NFSI (0.5 equiv.)	3	55
7[d]	NFSI (1 equiv.)	3	0
8[e]	NFSI (0.5 equiv.)	3	63

[a] *Oxidative reaction conditions: Alkene **19** (0.2 mmol), cyclopropanol **18** (1.5 equiv.), TBADT (2 mol%), CH₃CN (0.1 M), 43 W 370 nm Kessil LED, under Ar, 28 °C, 3 h.* [b] *Yields were determined by ¹H NMR analysis of the crude reaction mixture against triphenylmethane as an internal standard.* [c] *3 equiv. of cyclopropanol **18**.* [d] *No TBADT.* [e] *3 equiv. of cyclopropanol **18**, TBADT (1 mol%), CH₂Cl₂ (0.2 M).*

Based on these findings, we hypothesized that electron-rich aryl cyclopropanols, having lower oxidation potentials compared to the alkyl cyclopropanols, could undergo efficient TBADT-mediated oxidation without the need for an external oxidant, thereby enabling a redox-neutral process. Indeed, irradiation of *p*-methoxyphenyl cyclopropanol **21** and benzylidene malononitrile **22** in the presence of TBADT provided β-functionalized ketone **23** in 84% yield after 3 h, even in the absence of an oxidant (Table 6, entry 1).

Table 6. Optimization of the reaction conditions.[a]

Entry	Deviations	Yield, %[b]
1	none	84
2	without photocatalyst	25
3	no light	0
4	10 mol% benzophenone instead of TBADT	44
5	1 h	75
6	1 mol% TBADT, 1 h	57
7	50% light intensity, 1 h	65
8	1 mol% TBADT, CH$_2$Cl$_2$ as solvent, 1 h	90

[a] *Neutral reaction conditions: Alkene* **22** *(0.2 mmol), cyclopropanol* **21** *(1.5 equiv.), TBADT (2 mol%), CH$_3$CN (0.1 M), 43 W 370 nm Kessil LED, under Ar, 28 °C, 3 h.* [b] *Yields were determined by* ^{1}*H NMR analysis of the crude reaction mixture against triphenylmethane as an internal standard.*

Notably, the reaction proceeded, though less efficiently, without TBADT, affording 25% yield of **23** (entry 2), suggesting a slower pathway *via* an electron donor-acceptor (EDA) complex (see discussion below). No desired product was formed in the absence of UV irradiation (entry 3), confirming the photochemical nature of the transformation. Alternative photocatalysts proved less effective: 10 mol% benzophenone afforded **23** in only 44% yield (entry 4).[208] Reducing reaction time or catalyst loading did not improve the outcome (entries 5 and 6). The reaction was also sensitive to light intensity, with reduced yields observed at lower lamp power (entry 7). Remarkably, changing the solvent to dichloromethane (CH$_2$Cl$_2$) significantly enhanced efficiency, affording the product **23** in 90% yield within 1 h at only 1 mol% TBADT loading, despite limited solubility of TBADT in CH$_2$Cl$_2$ (entry 8).

2.3.2 Scope

With the optimized conditions established, we next investigated the scope of the transformation (Scheme 14). A broad range of *aryl cyclopropanols*, bearing both electron-donating and electron-withdrawing substituents on the aromatic ring, proved compatible with the photochemical protocol. Notably, heteroaryl substituents such as pyrrolyl and thiophenyl groups were well tolerated, affording the corresponding products (**32** and **33**). Interestingly, for a disubstituted cyclopropanol **34**, ring-opening occurred exclusively at the most substituted C$_1$–C$_2$ bond of the cyclopropane ring, giving

35 in 75% yield. The reaction also was effective toward *electrophilic alkenes*, including fumarates, sulfones, and *N*-phenylmaleimides (**44**, **45**, and **51** respectively). Remarkably, alkylidene oxindoles underwent smooth conversion, delivering the desired products in good yields (**62** and **63**).

However, *alkyl cyclopropanols* proved less efficient under optimized conditions, affording the corresponding products **36**–**40** in 40–61% yield. Oxidative optimized conditions were subsequently adopted as General Conditions C (Scheme 14). Although the precise role of the oxidant remains unclear, it may function as a radical initiator or serve as a terminal oxidant in the TBADT photocatalytic cycle.[209–211] Notably, the addition of oxidant enabled reactions of otherwise unreactive substrates, affording products **41**, **42**, and **20** in satisfactory 40–58% yields.
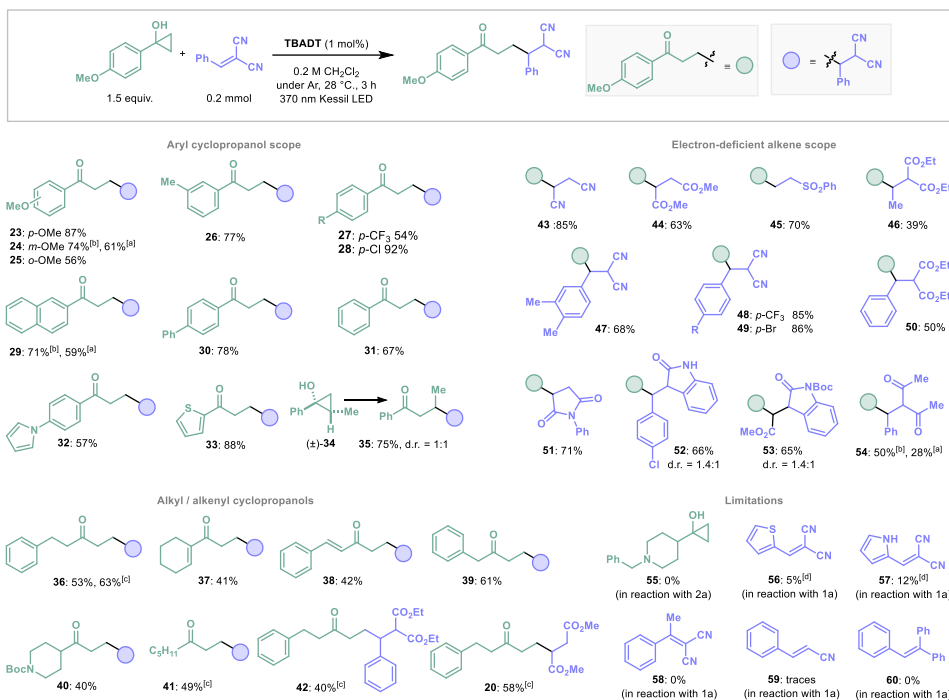
Scheme 14. [a] *Scope of the TBADT-photocatalyzed reaction of cyclopropanols with electron-deficient alkenes and limitations. Yields correspond to isolated products.* [a]*General procedure A: alkene (0.2 mmol), cyclopropanol (1.5 equiv.), TBADT (1 mol%), CH₂Cl₂ (0.2 M), 43 W 370 nm Kessil LED, under argon, 28 °C, 1–48 h.* [b]*General procedure B: alkene (0.2 mmol), cyclopropanol (1.5 equiv.), TBADT (2 mol%), CH₃CN/H₂O (9:1, 0.2 M substrate 2a), 43 W 370 nm Kessil LED, under argon, 28 °C, 3–24 h.* [c]*General procedure C: alkene (0.2 mmol), cyclopropanol (3 equiv.), TBADT (1 mol%), NFSI (0.5 equiv.), CH₂Cl₂ (0.2 M), 43 W 370 nm Kessil LED, under argon, 28 °C, 3–24 h.* [d] *Yield determined by* ¹H *NMR analysis of the crude reaction mixture against triphenylmethane as an internal standard.*

Despite the broad substrate scope, the reaction exhibited some limitations with certain alkenes under both the standard conditions and in the presence of NFSI. Heteroarylidene malononitriles **56** and **57**, as well as the mononitrile substrate **59**, afforded only trace amounts of the desired adducts (up to 12%) along with complex mixtures of byproducts. Likewise, the methyl-substituted benzylidene malononitrile **58** proved unreactive, presumably due to steric hindrance from the methyl substituent. Additionally, electron-rich triphenylethylene **60** also failed to deliver the target product.

2.3.3 Reaction scale-up under continuous flow mode and derivatization

As photochemical reactions are driven by the absorption of photons, their overall efficiency is directly dependent on the extent of light absorption within the reaction medium. In batch setups, however, light penetration is often restricted by reactor geometry and optical path length, as described by the Lambert-Beer law ($A = \varepsilon cl$), where A is absorption, ε is the molar extinction coefficient, c is concentration, and l is path length. Consequently, as the reactor radius increases, the effective absorption of light decreases markedly, making the scale-up of photochemical reactions inherently problematic.[212, 213] In contrast, continuous flow reactors overcome these limitations by conducting reactions within microchannels (typically with internal diameters <1 mm). This geometry enables efficient and uniform irradiation, maximizes photon flux, facilitates heat exchange, and ensures reproducibility and reliability of scale-up. Flow chemistry defines reaction time through the residence time, the period reagents spend in the irradiated zone of the reactor. The residence time (t_R) is determined by the ratio of the reactor volume (V) to the overall flow rate (q): $t_R = V/q$.[213]

We performed the scale-up of our photochemical reaction cyclopropanols **21** and **18** with benzylidene malononitrile **22** in continuous flow (Figure 21). Because of the limited solubility of TBADT in dichloromethane, acetonitrile was employed as the solvent under continuous flow conditions. After a brief optimization, we were able to prepare compounds **23** and **36** in good 74–75% yields and gram amounts with 20–30 min of residence time. The flow experiments used a custom setup with a syringe pump, 2 m FEP tubing loop (ϕ 0.8 × 1.6 mm, 1 mL volume) in a metal tube containing a 370 nm LED strip (2 m, 36 W, 25 mm LED-to-loop distance), cooling fan, and collection vessel.
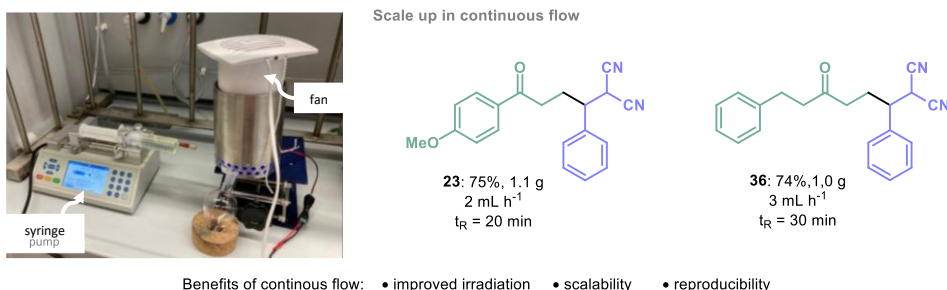
Figure 21. Translation to continuous flow conditions and scale-up. Reaction conditions for **23**: alkene (1.0 equiv.), cyclopropanol (1.2 equiv.), TBADT (2 mol%), CH₃CN (0.1 M), 370 nm LED strip, under Ar, t_R = 20 min, flow rate = 2 mL min⁻¹. Reaction conditions for **36**: alkene (4.5 mmol), cyclopropanol (3 equiv.), TBADT (2 mol%), NFSI (0.5 equiv.), CH₃CN (0.1 M), 370 nm LED strip, under Ar, t_R = 30 min, flow rate = 3 mL min⁻¹. Yields of isolated products are given.

2.3.4 The discovery of EDA complex formation

Next, we explored the plausible formation of an electron donor-acceptor (EDA) complex between cyclopropanol **21**, bearing an electron-rich arene moiety, and benzylidene malononitrile **22**, a strong electron acceptor and one-electron oxidant.[214] Upon excitation with 370 nm light, formation of the product **23** was observed, albeit less efficiently than in the presence of the TBADT (Scheme 15). In acetonitrile, irradiation of a mixture of **21** and **22** with UV light afforded **23** in 25% yield after 3 h and 77% yield after 24 h. In contrast, phenyl cyclopropanol **61**, possessing a less electron-donating aryl substituent,

reacted with **22** more slowly, providing **31** in only 13% yield after 3 h. Similarly, reaction of **21** with the less electron-deficient dimethyl fumarate **19** afforded product **31** in only 16% yield after 19 h.
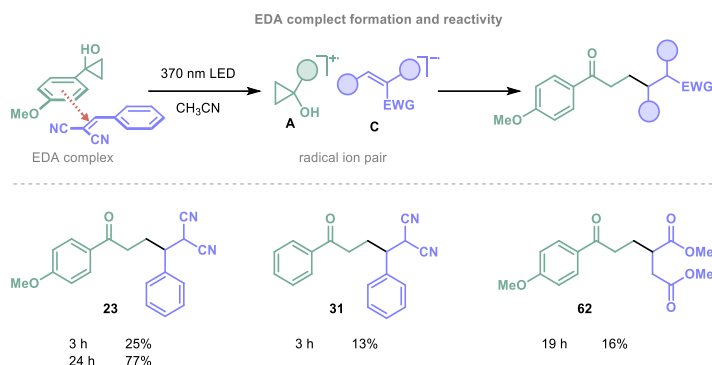
Scheme 15. EDA complex-mediated cross-coupling of aryl cyclopropanols with electrophilic alkenes. Reaction conditions: Alkene (0.2 mmol), cyclopropanol (1.5 equiv.), CH₃CN (0.2 M), 370 nm Kessil LED, under Ar, r.t. Yields were determined by ^{1}H NMR analysis of the crude reaction mixture against triphenylmethane as an internal standard.

The formation of an EDA association was investigated using both UV-Vis spectroscopy and ^{1}H NMR titration. UV-Vis analysis revealed a new bathochromically shifted absorption band for the mixture of **21** and **22** (purple line, Figure 22, a). The excessive absorption in the 370–400 nm range became evident after subtracting the spectrum of **21** from that of the mixture (blue line). Complementary ^{1}H NMR titration experiments provided additional evidence for complex formation and enabled estimation of the association constant (Figure 22, b). Upon gradual addition of **21** (1–95 equivalents), clear upfield shifts were observed for the two diagnostic protons H_a and H_b of **22**. Fitting the experimental titration data with BindFit yielded an association constant of $K_a = 0.16$ M^{-1}, indicating a weakly associated EDA complex.[215]

2.3.5 Proposed mechanism

EDA interaction is relatively weak and slow, whereas the TBADT-photocatalyzed reaction proceeds efficiently and proves to be more synthetically valuable. The main mechanism is proposed as follows:

Irradiation promotes TBADT into its excited state, followed by intersystem crossing to yield the triplet excited species *[W$_{10}$O$_{32}$]$^{4-}$. The photoexcited W(VI) species oxidizes cyclopropanol, generating cation radical **A**. Concurrently, disproportionation of the resulting [W$_{10}$O$_{32}$]$^{5-}$ regenerates the ground-state photocatalyst [W$_{10}$O$_{32}$]$^{4-}$ and produces [W$_{10}$O$_{32}$]$^{6-}$, a stronger reductant than the initially formed [W$_{10}$O$_{32}$]$^{5-}$. The electron-deficient alkene undergoes one-electron reduction to afford the radical anion **C**, which subsequently recombines with the β-ketoalkyl radical **B** (derived from ring-opening of the cyclopropanol radical cation **A**) to furnish anionic intermediate **D**. This step is proposed considering the remarkable influence of an alkene structure on the reaction efficiency and supporting CV measurements (Figure 23, b). Protonation of **D** then delivers the final product. Photoinduced charge transfer within the EDA complex is considered as a complementary mechanistic pathway, which may operate in cases involving electron-rich cyclopropanols and highly electron-deficient olefins.
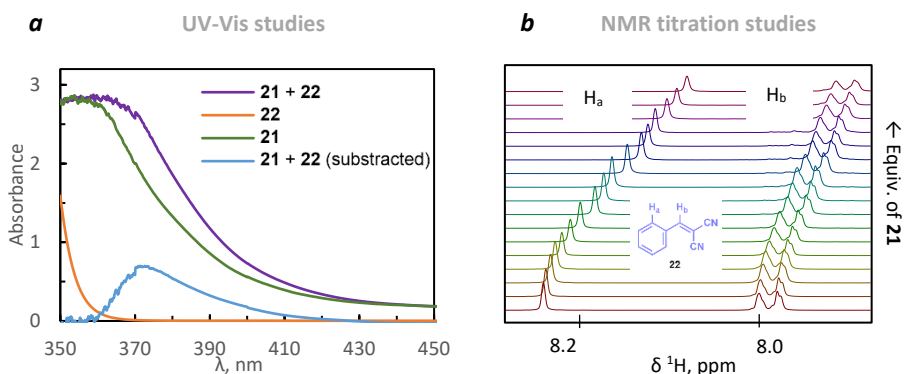
*Figure 22. a) UV-Vis studies of EDA complex formation. UV-Vis spectra of cyclopropanol **21** (1.5 M, green line), alkene **22** (0.01 M, orange line), and their mixture (150:1 ratio, 0.01 M for **22**, purple line) in methanol. The blue line is the result of subtraction of a spectrum of pure **21** (green line) from the mixture of **21** and **22** (purple line). b) ^{1}H NMR titration studies of EDA complex formation in CD$_3$OD.*

The proposed mechanism is further supported by control experiments (Figure 23, a):

(i) *Radical trapping experiment:* The formation of radical **B** was confirmed by performing the reaction in the presence of TEMPO (2,2,6,6-tetramethylpiperidine-*N*-oxyl) as a radical scavenger. In this case, formation of **23** was completely suppressed and the TEMPO-trapped adduct **62** was obtained instead in 83% ^{1}H NMR yield.

(ii) *Deuterium-labeling experiment:* The reaction of benzylidene malononitrile **22** with deuterium-labeled cyclopropanol **21-*d*** (87% D) in dry dichloromethane gave **23-*d*** with 69% D incorporation at the δ-position, indicating that the hydroxyl group of **21** serves as the source of the δ-hydrogen. Primary KIE was also observed: the reaction of deuterated cyclopropanol proceeded significantly slower than that of the non-deuterated substrate, demonstrating that cleavage of the O–H bond is the rate-limiting step of the overall process.

(iii) *Hydrogen atom transfer (HAT) control:* When ketone **63** was subjected to reaction with benzylidene malononitrile **22** under standard conditions, HAT from the methoxy group occurred, affording product **64** in 13% yield after 16 h (confirmed by ^{1}H NMR and HRMS analysis). This result suggests that HAT processes are slow under the standard conditions, even for relatively weak C–H bonds. Furthermore, no notable C–H activation at sensitive benzylic positions was observed during substrate scope studies, confirming that TBADT does not promote competitive side reactions of this type.

(iv) *CV measurements*: Oxidation and reduction potentials of substrates correlate with reactivity, supporting our mechanism (Figure 23, b). Electron-rich cyclopropanols oxidize more easily and react faster (**21** > **61** > **18**). Similarly, alkenes with lower reduction potentials react faster (**22** > **19** > **65**), supporting the intermediacy of radical anion **C**. Notably, radicals from the Giese reaction are much stronger oxidants (–0.3 to –0.1 V *vs* Fc/Fc$^+$) and should show less alkene-dependent reactivity.[216]
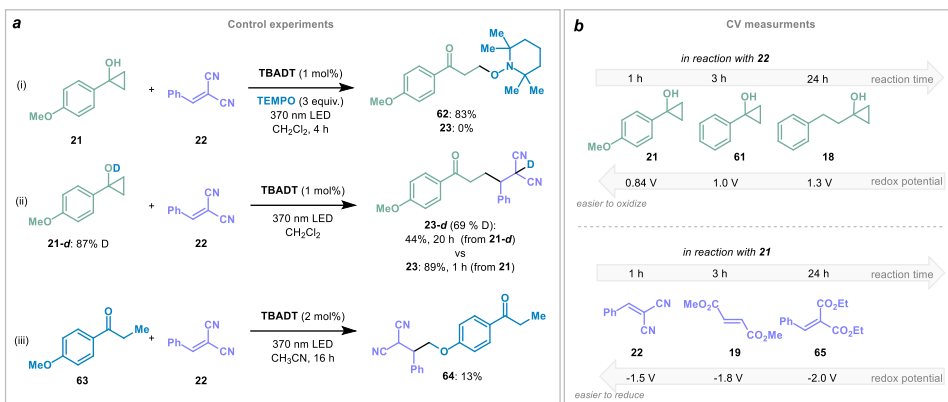
Figure 23. a) Selected control experiments. b) CV measurements of the peak potentials for the selected alkenes and cyclopropanols and their reaction times. $E_{1/2}$ *$[W_{10}O_{32}]^{4-}$/$[W_{10}O_{32}]^{5-}$ are reported by Ravelli et al.[155] and realigned with respect to Fc/Fc+ couple.

However, an alternative SET pathway cannot be fully excluded. In this scenario, nucleophilic radical **B** undergoes a Giese-type radical addition to the electrophilic alkene, affording radical intermediate **E**. This species can then be reduced by either $[W_{10}O_{32}]^{5-}$ or $[W_{10}O_{32}]^{6-}$, leading to product formation (see the intermediate structure on Scheme 16). Nevertheless, based on CV measurements, we propose the direct SET alkene reduction pathway as the predominant mechanism.
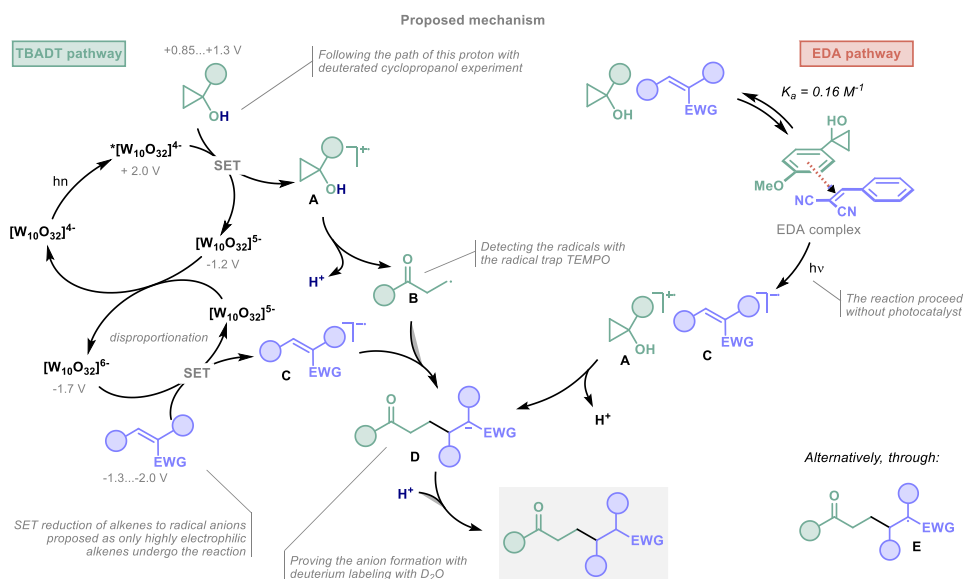
Scheme 16. Proposed mechanism. The numbers in gray color represent measured oxidation and reduction potentials for the species involved (reported in V vs Fc/Fc+).

2.4 Conclusions to Chapter 2

- A redox-neutral ring-opening cross-coupling of cyclopropanols with electron-deficient alkenes was established using TBADT as photoredox catalyst under UV light irradiation. This approach delivered distally functionalized ketones with moderate to excellent yields (40–92%) across 31 diverse examples, demonstrating broad substrate scope. However, limitations were observed for more electron-rich alkenes.

- Photoactive electron donor-acceptor (EDA) complexes formation between electron-rich cyclopropanols and electron-deficient olefins was described, leading to the generation of β-keto radical and the desired products under UV light irradiation.

- Mechanism was proposed based on comprehensive mechanistic studies. Unusual SET-reduction of electron-deficient alkenes by reduced TBADT species is thought to be the main mechanistic pathway.

- Scalability and synthetic utility of the reaction was demonstrated. The methodology was successfully translated to continuous flow conditions for gram-scale synthesis, and product derivatization showcased diverse reactivity through cyclization, oxidation, hydrolysis, and reduction transformations.

3 Telescoped synthesis of vicinal diamines in flow

Vicinal diamines are a privileged structural motif in organic chemistry due to their occurrence in pharmaceuticals, natural products, and catalysts for asymmetric synthesis. The introduction of 1,2-diamine functionalities is highly important in synthetic methodology development.

The most straightforward approach to vicinal diamine synthesis is based on metal-catalyzed diamination of alkenes. Transition metal catalysts can be problematic in pharmaceutical synthesis due to their toxicity, high cost, and possible metal contamination. Moreover, the substrate scope is often limited to symmetrical diamine products. Although aziridine ring-opening offers better structural diversity and access to non-symmetrical diamines, this strategy requires the synthesis and isolation of unstable aziridine intermediates. Additionally, batch protocols are typically time-consuming and raise safety concerns when handling reactive intermediates and hazardous reagents.

In this chapter, we describe the development of a telescoped continuous flow methodology that combines electrochemical aziridination with their *in situ* ring-opening towards the synthesis of various amines. This approach eliminates aziridine isolation and provides direct access to symmetrical and non-symmetrical vicinal diamines, as well as amino azides, amino ethers, and amino alcohols from readily available alkene and amine starting materials.

3.1 Literature review

3.1.1 Vicinal diamines: importance and synthesis

1,2-Diamines are frequently found in bioactive natural products, therapeutic agents, molecular catalysts and in ligands for asymmetric metal-catalysis and organocatalysts (Figure 24).[217, 218] These ligands enable a wide range of enantioselective transformations, including oxidations, reductions, oxirane ring-openings, and carbon-carbon bond formations.[219, 220]
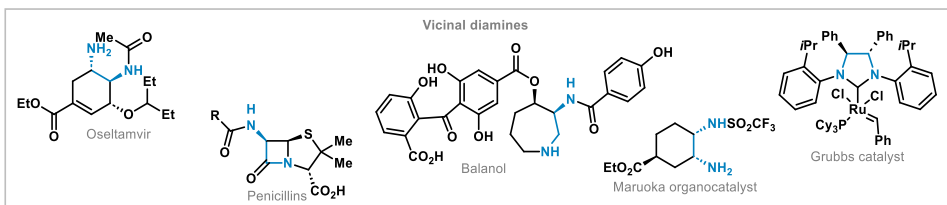
Figure 24. Pharmaceuticals, catalysts and ligands containing vicinal diamine moiety. Cy – cyclohexyl.

Vicinal diamines can be synthesized through several methods, but this review focuses on the two most important: alkene amination and aziridine ring-opening (Scheme 17). *Alkene amination* is the more commonly studied approach and typically relies on *metal catalysis* (iron,[221] copper,[222] rhodium,[223] palladium,[224] and others).[225, 226] However, this strategy presents significant limitations for pharmaceutical applications. Transition metal catalysts suffer from practical drawbacks: precious metals like rhodium and palladium are expensive and scarce, metal salts and complexes are often toxic, and residual metal contamination in active pharmaceutical ingredients is difficult to remove.[227] These concerns have motivated interest in developing *non-metal-catalyzed alternatives* (for example through iodine or hypervalent iodine catalysis).[228–230]

Additionally, conventional metal-catalyzed diamination frequently produces only symmetrical diamines with identical amine substituents, limiting structural diversity. Another important amination strategy involves *azidation* followed by reduction of the azide to an amino group, providing access to primary amine motifs.[231, 232] Additionally, *electrochemical* methods have also emerged as selective and sustainable approaches for amination reactions.[231, 233] In contrast, *aziridine ring-opening* provides a more flexible route to 1,2-diamines, particularly for synthesizing non-symmetrical diamine structures that bear different substituents on each amine.[234, 235] An even more advantageous strategy combines these two approaches: alkenes undergo aziridination followed by ring-opening to afford the desired diamines. This sequence exploits readily available alkenes to access diverse non-symmetrical diamine structures, benefiting from the unique reactivity of aziridines. Ruffoni and Leonori demonstrated this strategy through the selective synthesis of vicinal 1,2-diamines **4** from readily available olefins **1**. Their approach involved forming tetra-alkyl aziridinium ions **3** followed by regioselective ring-opening with primary or secondary amines.[236]
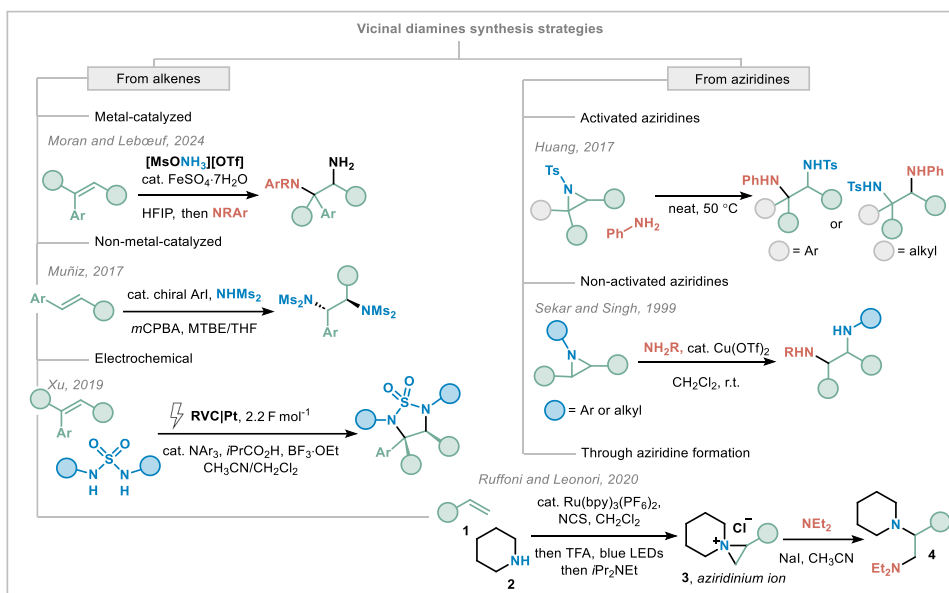
Scheme 17. Two important strategies for the synthesis of vicinal diamines: direct amination of alkenes and aziridine ring-opening. HFIP – hexafluoro-2-propanol, NCS – N-chlorosuccinimide, TFA – trifluoroacetic acid.

3.1.2 Ring-opening reactions of aziridines to access vicinal diamines

Aziridines are three-membered nitrogen-heterocycle, which combines high ring strain (around 112 kJ mol^{-1})[237] with electronegativity of the heteroatom, leading to facile ring-cleavage of aziridines under relatively mild conditions.[238]

Aziridines can be classified as *activated* and *non-activated*, depending on the substituent on the N-atom (Figure 25).[239]

- *Activated aziridines* (*N*-carbonyl, *N*-sulfonyl): electron-withdrawing groups stabilize negative charge at nitrogen, enabling direct nucleophilic ring-opening.
- *Non-activated aziridines (N-alkyl, N-H):* the basic nitrogen requires activation *via* protonation, quaternization, or Lewis acid coordination prior to ring-opening.
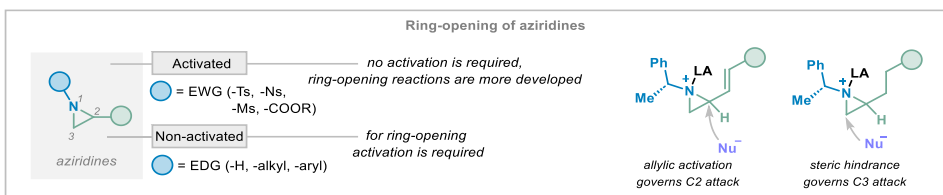
Figure 25. Reactivity of aziridines in ring-opening reactions. EWG – electron-withdrawing group, EDG – electron-donating group , Ts – tosyl, Ns – nosyl, Ms – mesyl.

The nucleophilic ring-opening reaction proceeds *via* an S_N2 mechanism with backside attack, typically yielding *anti*-products.[240] However, the regioselectivity depends on the structure of the carbon backbone, the substituent on nitrogen, the nature of the activator, and even the type of nucleophile. However, mostly regioselectivity of non-activated aziridines rely on the substituents on the carbon backbone: allylic or aryl groups direct attack to C2 through electronic stabilization, while alkyl substituents allow the attack at the sterically less hindered position (Figure 25).

Ring-opening reactions of non-activated aziridines are less developed compared to activated ones and generally require external activation (Scheme 18). Conventional activators for such reactions include TMSN$_3$,[241, 242] Sc(OTf)$_3$,[243] Cu(OTf)$_2$,[234] FeCl$_3$,[244] Ti(O*i*Pr)$_4$,[245] AlCl$_3$,[246] and silicagel[247]. TMSN$_3$ serves a dual role: Lee and Ha demonstrated its use as both activator and azide source, enabling ring-opening of aziridine **11**. Following reduction with hydrogen yielded 1,2-diamine **12** (Scheme 18, right).[248] When NaN$_3$ is employed as the azide source instead, Lewis acids such as AlCl$_3$ are required for aziridine activation (for example, of aziridine **13**).[249]
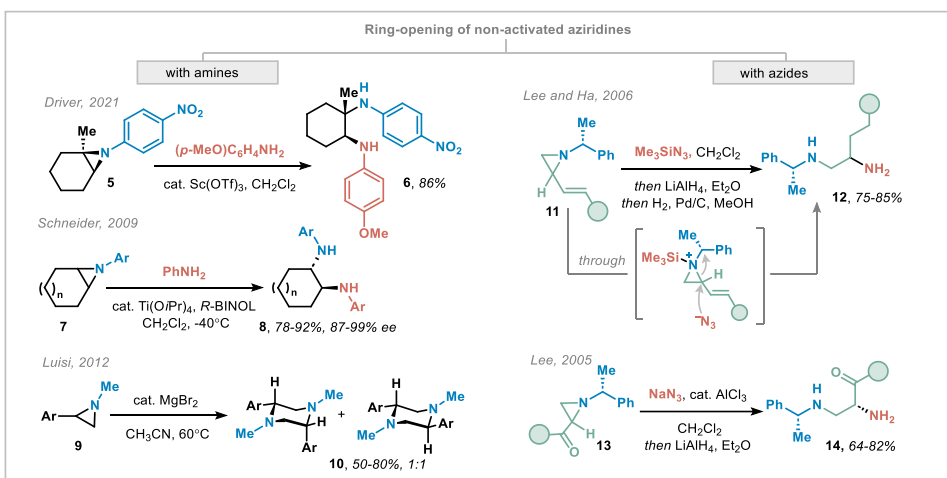
Scheme 18. Examples of ring-opening reactions of non-activated aziridines with amines and azides.

In the reaction with amines, Driver and co-workers used Sc(OTf)$_3$ for regioselective ring-opening of aryl-substituted aziridine **5** (Scheme 18, left).[243] Enantioselective approaches have also been developed. Schneider's group employed a chiral catalyst generated *in situ* from Ti(O*i*Pr)$_4$ and (*R*)-BINOL to promote highly enantioselective ring-opening of *meso*-aziridines **7** with anilines.[245] Interestingly, Luisu and coworkers

reported Lewis acid-catalyzed dimerization of non-activated aziridines **9** to afford piperazines **10**.[250] Given the synthetic value of vicinal diamines, continued development of efficient and practical synthetic routes remains an active area of research.

3.1.3 Continuous flow synthesis

Traditional laboratory synthesis relies on batch processing with standard glassware: round-bottom flasks, magnetic stirrers, and reflux condensers. In contrast, continuous flow setups offer a range of significant benefits compared to conventional synthesis methods:[251, 252]

- **Enhanced process control and efficiency**

Flow reactors improve mass and heat transfer, resulting in rapid reaction mixing and enabling precise control over reaction parameters. This increases overall process selectivity, efficiency, and safety. The small reaction volume allows for high-pressure and high-temperature reactions with quick and efficient heating and cooling, providing more precise process control and higher conversion rates.[253, 254]

- **Safety benefits**

Flow chemistry enables safer handling of hazardous chemicals. Highly exothermic and fast reactions can accumulate heat and form hot spots in batch mode, potentially resulting in uncontrollable side reactions or even runaway reactions. In microreactors, only a small portion of reagents are actively involved in a reaction zone at any given time. Therefore, flow chemistry facilitates safer reactions with diazocompounds, organometallics, azides, phosgene, and halogenating reagents.[255]

- **Multiphase reactions and catalyst recycling**

Flow chemistry enables more efficient reactions with gases by creating controlled and efficient gas-liquid mixing.[256] Similarly, solid-phase catalysis becomes more practical with using packed-bed reactors containing immobilized catalysts or supported reagents, which simplifies product purification and enables catalyst regeneration and recycling.[91, 257]

- **Compatibility with automation and machine learning**

Flow chemistry shows promise in developing automated synthesis platforms. Robotic flow setups have been under active development for achieving scalable, reproducible synthesis. When integrated with machine learning algorithms and high-throughput screening, these platforms accelerate the identification of optimal reaction conditions and discover novel transformations.[258–260]

- **Integration with enabling technologies**

Flow chemistry can enhance productivity and alter reactivity when combined with photo- or electrochemistry. In electro-flow chemistry, the short distance between electrodes reduces ohmic resistance, allowing supporting electrolyte to be omitted or used at low concentrations. Continuous removal of the reaction mixture minimizes overoxidation, a major problem in batch electrolysis.[261, 262] In photochemistry, the small dimensions of microreactors ensure excellent light irradiation throughout the reaction medium, resulting in increased radiation homogeneity, higher reaction selectivity, shorter reaction times, and lower catalyst loadings.[263–266]

- **Multistep synthesis and pharmaceutical applications**

Flow chemistry can benefit the manufacturing of active pharmaceutical ingredients through safer processes and multistep synthesis.[267, 268] Multistep synthesis allows conducting synthesis without intermediate isolation, reducing costs and improving overall process efficiency.[269]

- **Limitations**

Flow chemistry is not a universal solution. Certain reaction types are unsuitable for flow conditions, including those involving highly viscous materials, solid-forming reactions, and very slow reactions. The use of heterogeneous reagents or formation of solids is particularly problematic due to potential clogging of microreactors.

3.1.4 Typical flow setup

Continuous flow reactors require pumping systems (HPLC, syringe, or peristaltic pumps) to deliver reagents through tubing that function simultaneously as reaction vessel. Material selection is governed by thermal, mechanical, and chemical requirements. Perfluorinated polymers (PTFE, PFA, PEEK, FEP) exhibit sufficient chemical resistance and thermal stability for most laboratory-scale operations. Applications involving extreme conditions, high pressures, elevated temperatures, or highly corrosive media, necessitate stainless steel or specialized alloys.[256]

Modular flow reactors integrate different units of continuous flow systems with various reactor configurations to match a chemist's requirements (Figure 26).[270] The main benefit of modularity is that components can be integrated, reconfigured, or removed without redesigning the entire system. Common modules include packed-bed reactors with immobilized catalysts, quenching units, and degassing units. Real-time monitoring capabilities can be incorporated through spectroscopic techniques (NMR, IR, UV-Vis, or mass spectrometry), enabling continuous monitoring of reaction progress, yield, and selectivity without interrupting flow.
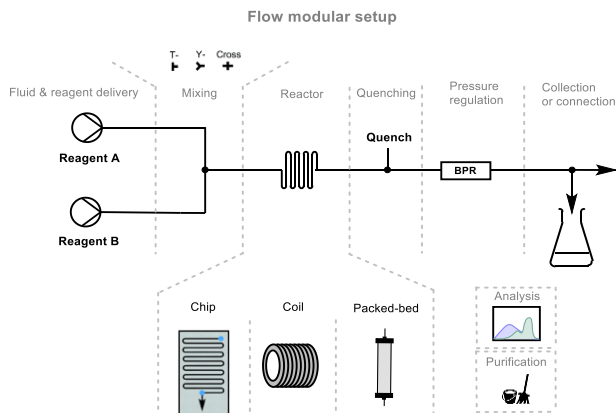
Figure 26. Components of flow chemical setup. The scheme was adopted from the article of Guidi et al.[270]

3.1.5 Telescoped Synthesis

Multi-step synthesis of complex molecules traditionally requires isolation and purification after each transformation, maximizing the efficacy of each step but consuming significant time and resources.[252] *Telescoped continuous flow synthesis* integrates sequential reactions into a single system, where crude products flow directly from one reactor to the next without intermediate isolation. The advantages: fewer purification steps, reduced solvent consumption, and shorter synthesis times, are significant. However, integrating sequential reactor modules may be technically demanding. The primary challenge in telescoped processes is the accumulation of byproducts after each step, which can

interfere with next steps. This can be controlled through inline purification and prior optimization of each step to minimize impurity formation. When successful, direct conversion of simple starting materials to valuable products can be achieved more economically and sustainably.[269, 271]

3.2 Motivation and aims of study

Given the abundance of 1,2-diamine motifs in various pharmaceuticals, catalysts, and ligands, new approaches for their synthesis are needed. Flow chemistry offers many possibilities to work with unstable intermediates without their isolation and to handle hazardous reagents. We applied telescoped continuous flow chemistry to efficiently synthesize vicinal diamines.

The specific aims of the study were:

- to develop a synthesis of vicinal diamines from readily available starting materials (alkenes and amines) under continuous flow conditions;

- to efficiently combine an electrochemical flow reactor and a subsequent heating module in one telescoped modular setup;

- to demonstrate the robustness of the method for obtaining various symmetrical and non-symmetrical vicinal diamines.

3.3 Results and discussion

In 2021, the Noël group reported a continuous flow method for the electrochemical aziridination of styrene-type alkenes **15** with primary amines **16** (Figure 27, a).[272] A range of valuable, non-activated aziridines **17** were synthesized from available starting materials. Some aziridines, especially very electron-rich aziridines and ones bearing small *N*-alkyl substituents, were unstable and underwent decomposition. In such cases, they were *in situ* converted to 1,2-amino thioethers **18** and isolated as functionalized products. Interestingly, hydrogen generated on the cathode was used for an inline formal hydroamination protocol. To obtain hydroaminated product **19**, a packed-bed reactor filled with Pd/C was connected to the electrochemical flow reactor, and the gas-liquid mixture from the first reactor was directly passed through the Pd/C bed.
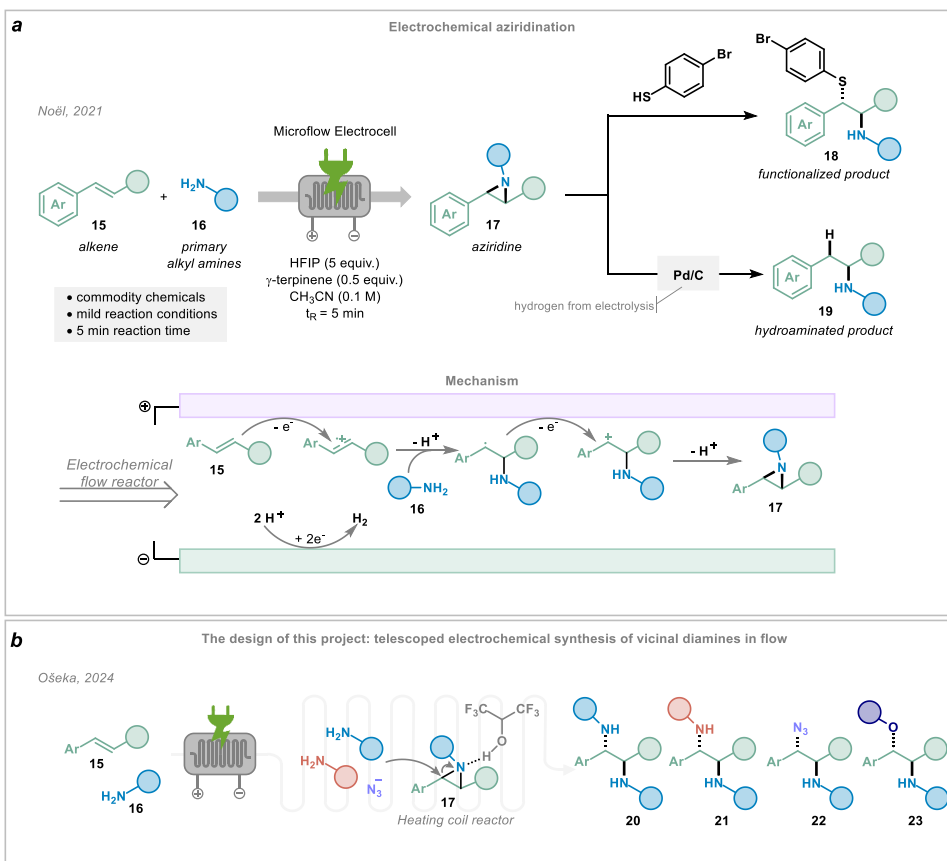
Figure 27. a) Electrochemical aziridination of internal alkenes with primary amines reported by the Noël's group and the mechanism of the reaction. b) Development of telescoped process for the synthesis of vicinal diamines from internal alkenes and primary amines.

Recognizing the potential to expand this continuous flow setup for telescoped synthesis of vicinal diamines, our group developed a two-step flow methodology for their synthesis from internal alkenes **15** and primary amines **16** *via* aziridine intermediates (Figure 27, b).[273]

3.3.1 Development of flow reaction setup and optimization of the reaction conditions

Noël's electrochemical methodology employed HFIP as both a radical stabilizer and a proton source for the cathodic counter reaction. Previous studies have demonstrated the critical role of HFIP in various transformations, including nucleophilic epoxide ring-opening.[274–276] We hypothesized that HFIP might serve as an effective activator for the ring-opening of non-activated aziridines. This hypothesis was validated when the crude reaction mixture from the flow electrochemical reactor, containing aziridine derived from anethole and cyclohexylamine, was heated at 60°C in batch overnight. Complete conversion of the aziridine was observed, resulting from its reaction with excess primary amine present in the crude mixture.

Next, we designed the modular flow system consisting of: syringe pump → electrochemical microreactor[277] → degassing vessel → HPLC pump → heated coil reactor → back pressure regulator (BPR) → collection flask (Figure 28).
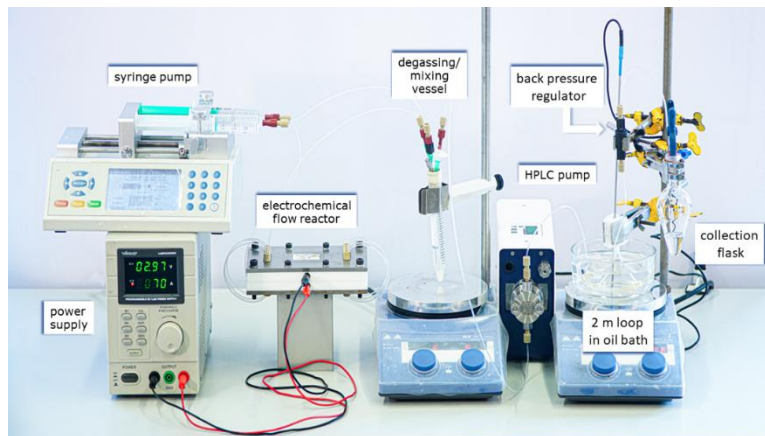
Figure 28. Reaction setup for telescoped synthesis of non-symmetrically substituted vicinal diamines.

A degassing vessel was incorporated to remove hydrogen gas generated during the electrochemical step. Additionally, since the electroreactor was limited to 2 bar and the pressures in the coil reactor were substantially higher, direct connection between these two units was not feasible. Importantly, the flow setup enabled reactions to be conducted at elevated temperatures (over the boiling point of solvents), potentially facilitating the ring-opening of aziridines. The back pressure regulator (BPR) was used to maintain elevated temperatures while preventing vaporization of the reaction components.

The following optimal parameters for flow were established (Scheme 19):

- coil was immersed in oil bath, temperature of 150 °C was optimal for ring-opening with amines, 100 °C – with *O*-nucleophiles, 70 °C – with azides;
- coil length of 2 meters (corresponding to 1 mL active volume);
- flow rate of 0.15 mL·min⁻¹ (residence time of 6.7 minutes).

Under these optimized conditions, the model diamine **24** was obtained in 56% yield based on the starting alkene. Electrochemical conditions were taken from prior work.[273] This flow approach enabled complete aziridine conversion within minutes, dramatically reducing the reaction time from the hours or overnight required in batch process.
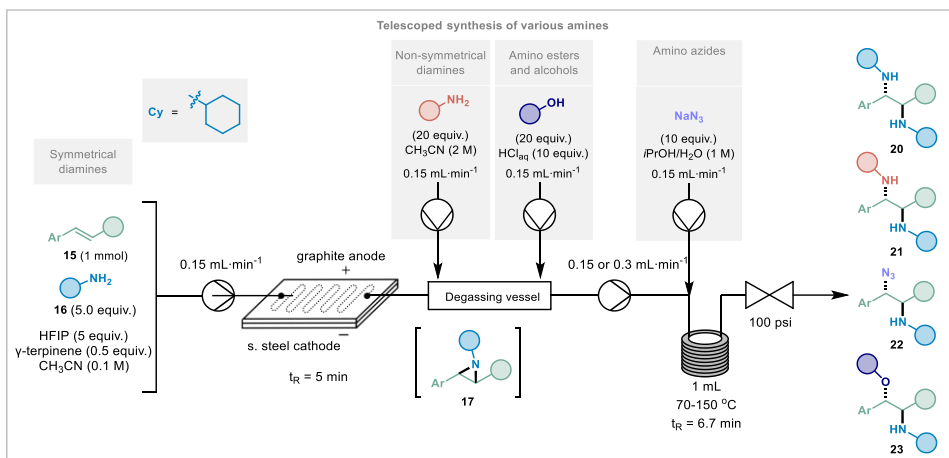
Scheme 19. Scheme of the continuous flow setup for the telescoped synthesis of vicinal diamines, amino azides and amino esters.

3.3.2 Scope of symmetrically substituted vicinal diamines

We applied this flow configuration to access symmetrical vicinal diamine products by ring-opening electrochemically prepared aziridine intermediates (Figure 29). The excess of primary amine served in the next step as a nucleophile for ring-opening. Our scope evaluation included both aziridine substrates reported by the Noël research group (compounds **24**–**26**) alongside not previously investigated examples (**27** and **28**).

The ring-opening reaction proceeded with complete stereoselectivity *via* S_N2 pathway, yielding diamines exclusively as *anti*-diastereomers (verified through NMR analysis of diastereomeric ratios). Various alkenes and amines proved compatible with this protocol, affording symmetrical 1,2-diamines **24**–**28** in 46–56% yields. Remarkably, the flow protocol overcame some limitations of ring-opening of sterically hindered aziridines: while the isopropyl-substituted aziridine required 48 hours for complete ring-opening under batch conditions, the corresponding diamine **27** was obtained within minutes using continuous flow. However, aziridines derived from stilbene and trisubstituted alkenes exhibited poor reactivity, providing only trace quantities of the desired products.

3.3.3 Scope of non-symmetrically substituted vicinal diamines

Subsequently, we investigated the synthesis of non-symmetrical 1,2-diamines. The setup sequence had one critical modification: introduction of a different amine, which was delivered with the second syringe pump (with the same flow rate as the first syringe pump) as the solution in acetonitrile to the degassing vessel (Scheme 19). To ensure continuous operation of modular flow setup, the HPLC pump flow rate was doubled. 20-fold excess of external amine was used to suppress the formation of symmetric byproduct; if the small amounts of byproduct were formed, they were successfully separated from the product with reverse-phase chromatography.

Four different external primary amines tested in this procedure, giving desired diamines **29**–**32** in 40–51% yields (Figure 29). Secondary amine nucleophiles possess enhanced nucleophilicity and the symmetric byproduct was completely suppressed,[278] and the corresponding products were isolated products **33**–**35** with 38–59% yields.
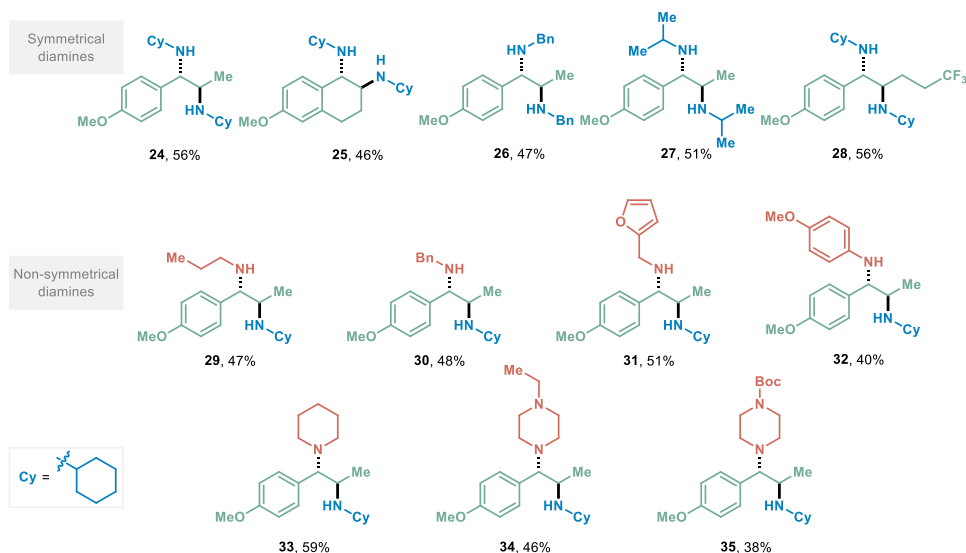
Figure 29. Scope of the telescoped synthesis of vicinal diamines in continuous flow.
Reaction conditions for the synthesis of symmetrically substituted vicinal diamines: alkene (1 mmol),
amine (5 mmol), HFIP (5 mmol), γ-terpinene (0.5 mmol), CH_3CN (10 mL), graphite anode/stainless
steel cathode, 2.3–3.1 mA cm^{-2}. Reaction conditions for the synthesis of non-symmetrically
substituted vicinal diamines: anethole (1 mmol), cyclohexyl amine (5 mmol), HFIP (5 mmol),
γ-terpinene (0.5 mmol), CH_3CN (10 mL), graphite anode/stainless steel cathode, 3.1 mA cm^{-2},
external amine (20 mmol in 10 mL of CH_3CN). Collection time 66.6 min. The yields correspond to
isolated products. Scope of symmetrical diamines was performed by Marharyta Laktsevich-Iskryk.
Scope of non-symmetrical diamines was performed by Marharyta Laktsevich-Iskryk and Mihhail Fokin.

3.3.4 Scope of vicinal amino esters and amino alcohols

Amino esters and amino alcohols were accessed by introducing *O*-centered nucleophiles
into the degassing vessel (Scheme 19). Hydrochloric acid (10 equivalents) was added to
protonate excess primary amine in the reaction mixture and suppress competitive
side reactions. Methanol, isopropanol, and water were successfully employed as
O-nucleophiles (Figure 30). Amino ethers were obtained as diastereomeric mixtures,
likely due to an S_N1 mechanism operating under acidic conditions, whereas the aqueous
ring-opening afforded a single diastereomer. These results demonstrate that the
methodology extends beyond *N*-nucleophiles to access amino ether **36**–**37** and amino
alcohol **38** products.

3.3.5 Scope of vicinal amino azides

Moreover, vicinal diamines are accessible *via* reduction of amino azides, making aziridine
ring-opening with azides synthetically valuable for the formation of non-symmetrical
diamines bearing a primary amino group as one substituent. Importantly, the explosive
nature of sodium azide necessitates careful handling. Flow chemistry diminishes this risk
by preventing azide accumulation in the system.

To maintain NaN_3 solubility and prevent tubing blockage, an isopropanol–water
mixture (1:1 v/v) was employed to ensure complete dissolution. The azide solution was
delivered *via* syringe pump through a Y-mixer positioned after the HPLC pump (Scheme
19). Excess of sodium azide (10 equivalents) was employed to suppress symmetrical
byproduct formation, with the optimal temperature determined to be 70 °C. This lower

temperature relative to amine ring-opening was probably due to higher reactivity and nucleophilicity of the azide anion compared to primary amines. Additionally, the compact size of azide can enable reactivity even with sterically hindered aziridines. A range of amino azides **39–43** was prepared with yields 40–71% (Figure 30).

To showcase the versatility of the azido group, post-synthetic derivatization was investigated. Hydrogenation over Pd/C yielded the primary amine, converting amino azide **41** to diamine **44** in 81% yield. Furthermore, CuI-catalyzed azide-alkyne cycloaddition with hexyne transformed amino azide **39** into triazole **45** in 88% yield, demonstrating the compatibility with click chemistry protocols (Figure 30).
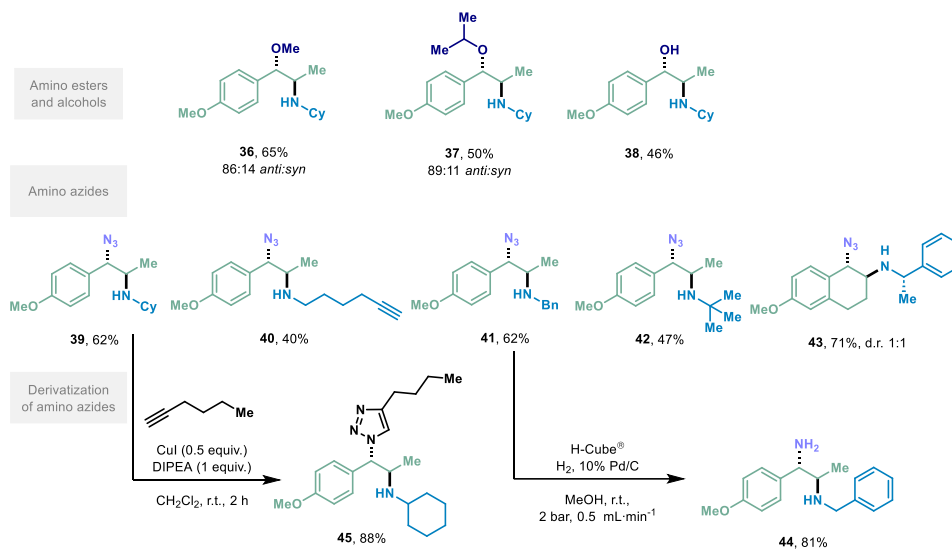
Figure 30. Scope of the telescoped synthesis of amino esters and amino azides in continuous flow and derivatization of amino azides. Reaction conditions for the synthesis of vicinal amino ethers and alcohols: anethole (1 mmol), cyclohexyl amine (5 mmol), HFIP (5 mmol), γ-terpinene (0.5 mmol), CH$_3$CN (10 mL), graphite anode/stainless steel cathode, 3.1 mA cm^{-2}, HCl$_{aq}$ (10 mmol in 10 mL of alcohol or in 10 mL of H$_2$O/THF 1:1). Reaction conditions for the synthesis of vicinal amino azides: alkene (1 mmol), amine (5 mmol), HFIP (5 mmol), γ-terpinene (0.5 mmol), CH$_3$CN (10 mL), graphite anode/stainless steel cathode, 1.9–3.3 mA cm^{-2}, sodium azide (10 mmol in 10 mL of iPrOH/H$_2$O 1:1). Scope of azides was prepared together with Marharyta Laktsevich-Iskryk. The derivatization was performed by Marharyta Laktsevich-Iskryk.

3.4 Conclusions to Chapter 3

- We developed a modular electrochemical aziridination and ring-opening platform in continuous flow for the synthesis of diverse 1,2-difunctionalized products, affording 20 examples in 38–71% yields.

- The telescoped protocol enabled direct conversion of alkenes and amines to valuable diamine derivatives without aziridine isolation.

- The methodology proved robust and operationally safe, affording vicinal symmetrical and non-symmetrical diamines, amino azides, amino ethers, and amino alcohols from satisfactory to good yields directly from available amines and alkenes.

- We merged two main strategies of vicinal diamines synthesis – reaction of amines with alkene and aziridine ring-opening, in an efficient continuous flow procedure.

References

[1]   Fitzpatrick, D. E.; Battilocchio, C.; Ley, S. V. Enabling Technologies for the Future of Chemical Synthesis. *ACS Cent. Sci.*, **2016**, *2* (3), 131–138. https://doi.org/10.1021/acscentsci.6b00015.

[2]   Oliver Kappe, C.; Mack, J.; Bolm, C. Enabling Techniques for Organic Synthesis. *J. Org. Chem.*, **2021**, *86* (21), 14242–14244. https://doi.org/10.1021/acs.joc.1c02326.

[3]   Han, B.; He, X.-H.; Liu, Y.-Q.; He, G.; Peng, C.; Li, J.-L. Asymmetric Organocatalysis: An Enabling Technology for Medicinal Chemistry. *Chem. Soc. Rev.*, **2021**, *50* (3), 1522–1586. https://doi.org/10.1039/D0CS00196A.

[4]   Wegner, J.; Ceylan, S.; Kirschning, A. Flow Chemistry – A Key Enabling Technology for (Multistep) Organic Synthesis. *Adv. Synth. Catal.*, **2012**, *354* (1), 17–57. https://doi.org/10.1002/adsc.201100584.

[5]   Bonciolini, S.; Pulcinella, A.; Noël, T. Tech-Enhanced Synthesis: Exploring the Synergy between Organic Chemistry and Technology. *J. Am. Chem. Soc.*, **2025**, *147* (32), 28523–28545. https://doi.org/10.1021/jacs.5c10303.

[6]   De Meijere, A.; Kozhushkov, S. I.; Schill, H. Three-Membered-Ring-Based Molecular Architectures. *Chem. Rev.*, **2006**, *106* (12), 4926–4996. https://doi.org/10.1021/cr0505369.

[7]   Han, X.; Zhang, N.; Li, Q.; Zhang, Y.; Das, S. The Efficient Synthesis of Three-Membered Rings *via* Photo- and Electrochemical Strategies. *Chem. Sci.*, **2024**, *15* (34), 13576–13604. https://doi.org/10.1039/D4SC02512A.

[8]   Yuan, Y.; Lei, A. Is Electrosynthesis Always Green and Advantageous Compared to Traditional Methods? *Nat Commun*, **2020**, *11* (1), 802. https://doi.org/10.1038/s41467-020-14322-z.

[9]   Meyer, T. H.; Choi, I.; Tian, C.; Ackermann, L. Powering the Future: How Can Electrochemistry Make a Difference in Organic Synthesis? *Chem*, **2020**, *6* (10), 2484–2496. https://doi.org/10.1016/j.chempr.2020.08.025.

[10]   Novaes, L. F. T.; Liu, J.; Shen, Y.; Lu, L.; Meinhardt, J. M.; Lin, S. Electrocatalysis as an Enabling Technology for Organic Synthesis. *Chem. Soc. Rev.*, **2021**, *50* (14), 7941–8002. https://doi.org/10.1039/D1CS00223F.

[11]   Yan, M.; Kawamata, Y.; Baran, P. S. Synthetic Organic Electrochemical Methods Since 2000: On the Verge of a Renaissance. *Chem. Rev.*, **2017**, *117* (21), 13230–13319. https://doi.org/10.1021/acs.chemrev.7b00397.

[12]   Pollok, D.; Waldvogel, S. R. Electro-Organic Synthesis – a 21st Century Technique. *Chem. Sci.*, **2020**, *11* (46), 12386–12400. https://doi.org/10.1039/D0SC01848A.

[13]   Peters, B. K.; Rodriguez, K. X.; Reisberg, S. H.; Beil, S. B.; Hickey, D. P.; Kawamata, Y.; Collins, M.; Starr, J.; Chen, L.; Udyavara, S.; et al. Scalable and Safe Synthetic Organic Electroreduction Inspired by Li-Ion Battery Chemistry. *Science*, **2019**, *363* (6429), 838–845. https://doi.org/10.1126/science.aav5606.

[14]   Noël, T.; Cao, Y.; Laudadio, G. The Fundamentals Behind the Use of Flow Reactors in Electrochemistry. *Acc. Chem. Res.*, **2019**, *52* (10), 2858–2869. https://doi.org/10.1021/acs.accounts.9b00412.

[15]   Cantillo, D. Synthesis of Active Pharmaceutical Ingredients Using Electrochemical Methods: Keys to Improve Sustainability. *Chem. Commun.*, **2022**, *58* (5), 619–628. https://doi.org/10.1039/D1CC06296D.

[16]   Jiao, K.-J.; Wang, Z.-H.; Ma, C.; Liu, H.-L.; Cheng, B.; Mei, T.-S. The Applications of Electrochemical Synthesis in Asymmetric Catalysis. *Chem Catalysis*, **2022**, *2* (11), 3019–3047. https://doi.org/10.1016/j.checat.2022.09.039.

[17]   Schotten, C.; Nicholls, T. P.; Bourne, R. A.; Kapur, N.; Nguyen, B. N.; Willans, C. E. Making Electrochemistry Easily Accessible to the Synthetic Chemist. *Green Chem.*, **2020**, *22* (11), 3358–3375. https://doi.org/10.1039/D0GC01247E.

[18]   Kingston, C.; Palkowitz, M. D.; Takahira, Y.; Vantourout, J. C.; Peters, B. K.; Kawamata, Y.; Baran, P. S. A Survival Guide for the "Electro-Curious." *Acc. Chem. Res.*, **2020**, *53* (1), 72–83. https://doi.org/10.1021/acs.accounts.9b00539.

[19]   Hilt, G. Basic Strategies and Types of Applications in Organic Electrochemistry. *ChemElectroChem*, **2020**, *7* (2), 395–405. https://doi.org/10.1002/celc.201901799.

[20]   Zhu, C.; Ang, N. W. J.; Meyer, T. H.; Qiu, Y.; Ackermann, L. Organic Electrochemistry: Molecular Syntheses with Potential. *ACS Cent. Sci.*, **2021**, *7* (3), 415–431. https://doi.org/10.1021/acscentsci.0c01532.

[21]   Pavlishchuk, V. V.; Addison, A. W. Conversion Constants for Redox Potentials Measured versus Different Reference Electrodes in Acetonitrile Solutions at 25°C. *Inorganica Chimica Acta*, **2000**, *298* (1), 97–102. https://doi.org/10.1016/S0020-1693(99)00407-7.

[22]   Elgrishi, N.; Rountree, K. J.; McCarthy, B. D.; Rountree, E. S.; Eisenhart, T. T.; Dempsey, J. L. A Practical Beginner's Guide to Cyclic Voltammetry. *J. Chem. Educ.*, **2018**, *95* (2), 197–206. https://doi.org/10.1021/acs.jchemed.7b00361.

[23]   Rafiee, M.; Mayer, M. N.; Punchihewa, B. T.; Mumau, M. R. Constant Potential and Constant Current Electrolysis: An Introduction and Comparison of Different Techniques for Organic Electrosynthesis. *J. Org. Chem.*, **2021**, *86* (22), 15866–15874. https://doi.org/10.1021/acs.joc.1c01391.

[24]   Kawamata, Y.; Hayashi, K.; Carlson, E.; Shaji, S.; Waldmann, D.; Simmons, B. J.; Edwards, J. T.; Zapf, C. W.; Saito, M.; Baran, P. S. Chemoselective Electrosynthesis Using Rapid Alternating Polarity. *J. Am. Chem. Soc.*, **2021**, *143* (40), 16580–16588. https://doi.org/10.1021/jacs.1c06572.

[25]   Roth, H.; Romero, N.; Nicewicz, D. Experimental and Calculated Electrochemical Potentials of Common Organic Molecules for Applications to Single-Electron Redox Chemistry. *Synlett*, **2015**, *27* (05), 714–723. https://doi.org/10.1055/s-0035-1561297.

[26]   Gombos, L. G.; Nikl, J.; Waldvogel, S. R. Dual Roles of Supporting Electrolytes in Organic Electrosynthesis. *ChemElectroChem*, **2024**, *11* (8), e202300730. https://doi.org/10.1002/celc.202300730.

[27]   Atobe, M.; Inagi, S.; Fuchigami, T. *Fundamentals and Applications of Organic Electrochemistry*; Synthesis, Materials, Devices; Wiley, 2015.

[28]   Speiser, B.; Hammerich, O. *Organic Electrochemistry Revised and Expanded*, 5th Edition.; CRC Press, 2015.

[29]   Bard, A.; Faulkner, L.; White, H. *Electrochemical Methods: Fundamentals and Applications*, 3rd edition.; John Wiley & Sons, Inc., 2022.

[30]   Tay, N. E. S.; Lehnherr, D.; Rovis, T. Photons or Electrons? A Critical Comparison of Electrochemistry and Photoredox Catalysis for Organic Synthesis. *Chem. Rev.*, **2022**, *122* (2), 2487–2649. https://doi.org/10.1021/acs.chemrev.1c00384.

[31]   Heard, D. M.; Lennox, A. J. J. Electrode Materials in Modern Organic Electrochemistry. *Angew. Chem. Int. Ed.*, **2020**, *59* (43), 18866–18884. https://doi.org/10.1002/anie.202005745.

[32] Francke, R.; Little, R. D. Redox Catalysis in Organic Electrosynthesis: Basic Principles and Recent Developments. *Chem. Soc. Rev.*, **2014**, *43* (8), 2492. https://doi.org/10.1039/c3cs60464k.

[33] Liu, K.; Song, C.; Lei, A. Recent Advances in Iodine Mediated Electrochemical Oxidative Cross-Coupling. *Org. Biomol. Chem.*, **2018**, *16* (14), 2375–2387. https://doi.org/10.1039/C8OB00063H.

[34] Tang, H.-T.; Jia, J.-S.; Pan, Y.-M. Halogen-Mediated Electrochemical Organic Synthesis. *Org. Biomol. Chem.*, **2020**, *18* (28), 5315–5333. https://doi.org/10.1039/D0OB01008A.

[35] Lian, F.; Xu, K.; Zeng, C. Indirect Electrosynthesis with Halogen Ions as Mediators. *The Chemical Record*, **2021**, *21* (9), 2290–2305. https://doi.org/10.1002/tcr.202100036.

[36] Novaes, L. F. T.; Liu, J.; Shen, Y.; Lu, L.; Meinhardt, J. M.; Lin, S. Electrocatalysis as an Enabling Technology for Organic Synthesis. *Chem. Soc. Rev.*, **2021**, *50* (14), 7941–8002. https://doi.org/10.1039/D1CS00223F.

[37] Yang, W.; Guo, J.; Hee, S.; Chen, Y. Recent Advances in Iodine-Mediated Radical Reactions. *Adv. Synth. Catal.*, **2025**, *367* (7), e202401486. https://doi.org/10.1002/adsc.202401486.

[38] Li, Y.-L.; Li, J.; Ma, A.-L.; Huang, Y.-N.; Deng, J. Metal-Free Synthesis of Indole *via* NIS-Mediated Cascade C–N Bond Formation/Aromatization. *J. Org. Chem.*, **2015**, *80* (8), 3841–3851. https://doi.org/10.1021/acs.joc.5b00090.

[39] Ye, Z.; Adhikari, S.; Xia, Y.; Dai, M. Expedient Syntheses of *N*-Heterocycles *via* Intermolecular Amphoteric Diamination of Allenes. *Nat Commun*, **2018**, *9* (1), 721. https://doi.org/10.1038/s41467-018-03085-3.

[40] Tariq, M. Electrochemistry of Br^- /Br_2 Redox Couple in Acetonitrile, Methanol and Mix Media of Acetonitrile–Methanol: An Insight into Redox Behavior of Bromide on Platinum (Pt) and Gold (Au) Electrode. *Zeitschrift für Physikalische Chemie*, **2020**, *234* (2), 295–312. https://doi.org/10.1515/zpch-2018-1321.

[41] Duan, Y.; Luo, S. Phase-Transfer Catalysis for Electrochemical Chlorination and Nitration of Arenes. *Angew. Chem. Int. Ed.*, **2024**, *63* (17), e202319206. https://doi.org/10.1002/anie.202319206.

[42] Steckhan, E. Indirect Electroorganic Syntheses—A Modern Chapter of Organic Electrochemistry [New Synthetic Methods (59)]. *Angew. Chem. Int. Ed.*, **1986**, *25* (8), 683–701. https://doi.org/10.1002/anie.198606831.

[43] Elinson, M. N.; Dorofeev, A. S.; Feducovich, S. K.; Belyakov, P. A.; Nikishin, G. I. Stereoselective Electrocatalytic Oxidative Coupling of Phenylacetonitriles: Facile and Convenient Way to *Trans* -α,β-Dicyanostilbenes. *Eur. J. Org. Chem.*, **2007**, *2007* (18), 3023–3027. https://doi.org/10.1002/ejoc.200601108.

[44] Wang, H.; Shi, J.; Tan, J.; Xu, W.; Zhang, S.; Xu, K. Electrochemical Synthesis of *Trans* -2,3-Disubstituted Aziridines *via* Oxidative Dehydrogenative Intramolecular C(Sp[3])–H Amination. *Org. Lett.*, **2019**, *21* (23), 9430–9433. https://doi.org/10.1021/acs.orglett.9b03641.

[45] Chen, L.; Barton, L. M.; Vantourout, J. C.; Xu, Y.; Chu, C.; Johnson, E. C.; Sabatini, J. J.; Baran, P. S. Electrochemical Cyclobutane Synthesis in Flow: Scale-Up of a Promising Melt-Castable Energetic Intermediate. *Org. Process Res. Dev.*, **2021**, *25* (12), 2639–2645. https://doi.org/10.1021/acs.oprd.0c00270.

[46] Gao, H.; Zha, Z.; Zhang, Z.; Ma, H.; Wang, Z. A Simple and Efficient Approach to Realize Difunctionalization of Arylketones with Malonate Esters *via* Electrochemical Oxidation. *Chem. Commun.*, **2014**, *50* (39), 5034–5036. https://doi.org/10.1039/C4CC01277A.

[47] Liang, S.; Zeng, C.-C.; Tian, H.-Y.; Sun, B.-G.; Luo, X.-G.; Ren, F. Electrochemically Oxidative α-C–H Functionalization of Ketones: A Cascade Synthesis of α-Amino Ketones Mediated by NH_4 I. *J. Org. Chem.*, **2016**, *81* (23), 11565–11573. https://doi.org/10.1021/acs.joc.6b01595.

[48] Yavari, I.; Shaabanzadeh, S. Electrochemical Synthesis of β-Ketosulfones from Switchable Starting Materials. *Org. Lett.*, **2020**, *22* (2), 464–467. https://doi.org/10.1021/acs.orglett.9b04221.

[49] Chicas-Baños, D. F.; Frontana-Uribe, B. A. Electrochemical Generation and Use in Organic Synthesis of *C* -, *O* -, and *N* -Centered Radicals. *The Chemical Record*, **2021**, *21* (9), 2538–2573. https://doi.org/10.1002/tcr.202100056.

[50] Hu, K.; Zhang, Y.; Zhou, Z.; Yang, Y.; Zha, Z.; Wang, Z. Iodine-Mediated Electrochemical $C(Sp^2)$–H Amination: Switchable Synthesis of Indolines and Indoles. *Org. Lett.*, **2020**, *22* (15), 5773–5777. https://doi.org/10.1021/acs.orglett.0c01821.

[51] Liang, S.; Zeng, C.-C.; Luo, X.-G.; Ren, F.; Tian, H.-Y.; Sun, B.-G.; Little, R. D. Electrochemically Catalyzed Amino-Oxygenation of Styrenes: N-Bu_4 NI Induced C–N Followed by a C–O Bond Formation Cascade for the Synthesis of Indolines. *Green Chem.*, **2016**, *18* (7), 2222–2230. https://doi.org/10.1039/C5GC02626A.

[52] Choi, S.; Park, J.; Yu, E.; Sim, J.; Park, C. Electrosynthesis of Dihydropyrano[4,3- *b*]Indoles Based on a Double Oxidative [3+3] Cycloaddition. *Angew. Chem. Int. Ed.*, **2020**, *59* (29), 11886–11891. https://doi.org/10.1002/anie.202003364.

[53] Wen, J.; Shi, W.; Zhang, F.; Liu, D.; Tang, S.; Wang, H.; Lin, X.-M.; Lei, A. Electrooxidative Tandem Cyclization of Activated Alkynes with Sulfinic Acids To Access Sulfonated Indenones. *Org. Lett.*, **2017**, *19* (12), 3131–3134. https://doi.org/10.1021/acs.orglett.7b01256.

[54] Jiang, Y.-Y.; Liang, S.; Zeng, C.-C.; Hu, L.-M.; Sun, B.-G. Electrochemically Initiated Formation of Sulfonyl Radicals: Synthesis of Oxindoles *via* Difunctionalization of Acrylamides Mediated by Bromide Ion. *Green Chem.*, **2016**, *18* (23), 6311–6319. https://doi.org/10.1039/C6GC01970F.

[55] Guo, S.; Liu, L.; Hu, K.; Sun, Q.; Zha, Z.; Yang, Y.; Wang, Z. Electrochemical Synthesis of 3-Azido-Indolines from Amino-Azidation of Alkenes. *Chinese Chemical Letters*, **2021**, *32* (3), 1033–1036. https://doi.org/10.1016/j.cclet.2020.09.041.

[56] Zhang, P.; Li, B.; Niu, L.; Wang, L.; Zhang, G.; Jia, X.; Zhang, G.; Liu, S.; Ma, L.; Gao, W.; et al. Scalable Electrochemical Transition-Metal-Free Dehydrogenative Cross-Coupling Amination Enabled Alkaloid Clausines Synthesis. *Adv. Synth. Catal.*, **2020**, *362* (12), 2342–2347. https://doi.org/10.1002/adsc.202000228.

[57] Zhang, S.; Li, L.; Xue, M.; Zhang, R.; Xu, K.; Zeng, C. Electrochemical Formation of *N* -Acyloxy Amidyl Radicals and Their Application: Regioselective Intramolecular Amination of Sp^2 and Sp^3 C–H Bonds. *Org. Lett.*, **2018**, *20* (12), 3443–3446. https://doi.org/10.1021/acs.orglett.8b00981.

[58] Minato, D.; Mizuta, S.; Kuriyama, M.; Matsumura, Y.; Onomura, O. Diastereoselective Construction of Azetidin-2-Ones by Electrochemical Intramolecular C–C Bond Forming Reaction. *Tetrahedron*, **2009**, *65* (47), 9742–9748. https://doi.org/10.1016/j.tet.2009.09.087.

[59] Großmann, L. M.; Beier, V.; Duttenhofer, L.; Lennartz, L.; Opatz, T. An Iodide-Mediated Anodic Amide Coupling. *Chem. Eur. J.*, **2022**, *28* (54), e202201768. https://doi.org/10.1002/chem.202201768.

[60] Guo, X.; Price, N. G.; Zhu, Q. Electrochemical Cyanation of Alcohols Enabled by an Iodide-Mediated Phosphine P(V/III) Redox Couple. *Org. Lett.*, **2024**, *26* (35), 7347–7351. https://doi.org/10.1021/acs.orglett.4c02550.

[61] Nikolaienko, P.; Jentsch, M.; Kale, A. P.; Cai, Y.; Rueping, M. Electrochemical and Scalable Dehydrogenative C(Sp[3])−H Amination *via* Remote Hydrogen Atom Transfer in Batch and Continuous Flow. *Chem. Eur. J.*, **2019**, *25* (29), 7177–7184. https://doi.org/10.1002/chem.201806092.

[62] Sun, C.; Lian, F.; Xu, K.; Zeng, C.; Sun, B. Electrochemical Synthesis of Allylamines *via* a Radical Trapping Sequence. *Adv. Synth. Catal.*, **2019**, *361* (17), 4041–4047. https://doi.org/10.1002/adsc.201900537.

[63] Liu, K.; Song, C.; Wu, J.; Deng, Y.; Tang, S.; Lei, A. Electrochemical Oxidation Synergizing with Brønsted-Acid Catalysis Leads to [4 + 2] Annulation for the Synthesis of Pyrazines. *Green Chem.*, **2019**, *21* (4), 765–769. https://doi.org/10.1039/C8GC03786H.

[64] Chen, J.; Yan, W.-Q.; Lam, C. M.; Zeng, C.-C.; Hu, L.-M.; Little, R. D. Electrocatalytic Aziridination of Alkenes Mediated by *n* -Bu₄ NI: A Radical Pathway. *Org. Lett.*, **2015**, *17* (4), 986–989. https://doi.org/10.1021/acs.orglett.5b00083.

[65] Li, X.; Zhou, J.; Deng, W.; Wang, Z.; Wen, Y.; Li, Z.; Qiu, Y.; Huang, Y. Electroreductive Deuteroarylation of Alkenes Enabled by an Organo-Mediator. *Chem. Sci.*, **2024**, *15* (29), 11418–11427. https://doi.org/10.1039/D4SC03049D.

[66] Avanthay, M. E.; Goodrich, O. H.; Tiemessen, D.; Alder, C. M.; George, M. W.; Lennox, A. J. J. Bromide-Mediated Silane Oxidation: A Practical Counter-Electrode Process for Nonaqueous Deep Reductive Electrosynthesis. *JACS Au*, **2024**, *4* (6), 2220–2227. https://doi.org/10.1021/jacsau.4c00186.

[67] Bieniek, J. C.; Nater, D. F.; Eberwein, S. L.; Schollmeyer, D.; Klein, M.; Waldvogel, S. R. Efficient and Sustainable Electrosynthesis of *N*-Sulfonyl Iminophosphoranes by the Dehydrogenative P–N Coupling Reaction. *JACS Au*, **2024**, *4* (6), 2188–2196. https://doi.org/10.1021/jacsau.4c00156.

[68] Talele, T. T. The "Cyclopropyl Fragment" Is a Versatile Player That Frequently Appears in Preclinical/Clinical Drug Molecules. *J. Med. Chem.*, **2016**, *59* (19), 8712–8756. https://doi.org/10.1021/acs.jmedchem.6b00472.

[69] Han, X.; Zhang, N.; Li, Q.; Zhang, Y.; Das, S. The Efficient Synthesis of Three-Membered Rings *via* Photo- and Electrochemical Strategies. *Chem. Sci.*, **2024**, *15* (34), 13576–13604. https://doi.org/10.1039/D4SC02512A.

[70] Liu, M.; Uyeda, C. Redox Approaches to Carbene Generation in Catalytic Cyclopropanation Reactions. *Angew. Chem. Int. Ed.*, **2024**, *63* (29), e202406218. https://doi.org/10.1002/anie.202406218.

[71] Jie, L.-H.; Guo, B.; Song, J.; Xu, H.-C. Organoelectrocatalysis Enables Direct Cyclopropanation of Methylene Compounds. *J. Am. Chem. Soc.*, **2022**, *144* (5), 2343–2350. https://doi.org/10.1021/jacs.1c12762.

[72] Kim, M. J.; Wang, D. J.; Targos, K.; Garcia, U. A.; Harris, A. F.; Guzei, I. A.; Wickens, Z. K. Diastereoselective Synthesis of Cyclopropanes from Carbon Pronucleophiles and Alkenes. *Angew. Chem. Int. Ed.*, **2023**, *62* (21), e202303032. https://doi.org/10.1002/anie.202303032.

[73] Yi, W.; Xu, P.-C.; He, T.; Shi, S.; Huang, S. Organoelectrocatalytic Cyclopropanation of Alkenyl Trifluoroborates with Methylene Compounds. *Nat Commun*, **2024**, *15* (1), 9645. https://doi.org/10.1038/s41467-024-54082-8.

[74] Liu, M.; Wang, Y.; Gao, C.; Jia, J.; Zhu, Z.; Qiu, Y. Electrochemical Cyclopropanation of Unactivated Alkenes with Methylene Compounds. *Angew. Chem. Int. Ed.*, **2025**, *64* (9), e202425634. https://doi.org/10.1002/anie.202425634.

[75] Durandetti, S.; Sibille, S.; Perichon, J. Electrochemical Cyclopropanation of Alkenes Using Dibromomethane and Zinc in Dichloromethane/DMF Mixture. *J. Org. Chem.*, **1991**, *56* (10), 3255–3258. https://doi.org/10.1021/jo00010a015.

[76] Njue, C. K.; Nuthakki, B.; Vaze, A.; Bobbitt, J. M.; Rusling, J. F. Vitamin B12-Mediated Electrochemical Cyclopropanation of Styrene. *Electrochemistry Communications*, **2001**, *3* (12), 733–736. https://doi.org/10.1016/S1388-2481(01)00255-7.

[77] Zhang, X.; Cheng, X. Electrochemical Reductive Functionalization of Alkenes with Deuterochloroform as a One-Carbon Deuteration Block. *Org. Lett.*, **2022**, *24* (47), 8645–8650. https://doi.org/10.1021/acs.orglett.2c03443.

[78] Regnier, M.; Vega, C.; Ioannou, D. I.; Zhang, Z.; Noël, T. Flow Electroreductive Nickel-Catalyzed Cyclopropanation of Alkenes Using *Gem*-Dichloroalkanes. *Angew. Chem. Int. Ed.*, **2025**, *64* (15), e202500203. https://doi.org/10.1002/anie.202500203.

[79] Ogibin, Y. N.; Elinson, M. N.; Nikishin, G. I. Mediator Oxidation Systems in Organic Electrosynthesis. *Russ. Chem. Rev.*, **2009**, *78* (2), 89–140. https://doi.org/10.1070/RC2009v078n02ABEH003886.

[80] Elinson, M. N.; Feducovich, S. K.; Vereshchagin, A. N.; Gorbunov, S. V.; Belyakov, P. A.; Nikishin, G. I. Electrocatalytic Multicomponent Cyclization of an Aldehyde, Malononitrile and a Malonate into 3-Substituted-2,2-Dicyanocyclopropane-1,1-Dicarboxylate—the First One-Pot Synthesis of a Cyclopropane Ring from Three Different Molecules. *Tetrahedron Letters*, **2006**, *47* (51), 9129–9133. https://doi.org/10.1016/j.tetlet.2006.10.075.

[81] Elinson, M. N.; Feducovich, S. K.; Starikova, Z. A.; Vereshchagin, A. N.; Belyakov, P. A.; Nikishin, G. I. Stereoselective Electrocatalytic Transformation of Malonate and Alkylidenecyanoacetates into (E)-3-Substituted 2-Cyanocyclopropane-1,1,2-Tricarboxylates. *Tetrahedron*, **2006**, *62* (17), 3989–3996. https://doi.org/10.1016/j.tet.2006.02.027.

[82] Lin, Q.; Li, L.; Luo, S. Asymmetric Electrochemical Catalysis. *Chem. Eur. J.*, **2019**, *25* (43), 10033–10044. https://doi.org/10.1002/chem.201901284.

[83] Chang, X.; Zhang, Q.; Guo, C. Asymmetric Electrochemical Transformations. *Angew. Chem. Int. Ed.*, **2020**, *59* (31), 12612–12622. https://doi.org/10.1002/anie.202000016.

[84] Rein, J.; Zacate, S. B.; Mao, K.; Lin, S. A Tutorial on Asymmetric Electrocatalysis. *Chem. Soc. Rev.*, **2023**, *52* (23), 8106–8125. https://doi.org/10.1039/D3CS00511A.

[85] Jiang, X.; Zou, C.; Zhuang, W.; Li, R.; Yang, Y.; Yang, C.; Xu, X.; Zhang, L.; He, X.; Yao, Y.; et al. Asymmetric Electrosynthesis: Emerging Catalytic Strategies and Mechanistic Insights. *Green Chem.*, **2025**, *27* (4), 915–945. https://doi.org/10.1039/D4GC05316H.

[86] Mao, K.; Liu, C.; Wang, Y.; Gu, C.; Putziger, J. M.; Cemalovic, N. I.; Muniz, C.; Qi, Y.; Lin, S. Dynamic Kinetic Resolution of Phosphines with Chiral Supporting Electrolytes. *Nature*, **2025**, *643* (8074), 1288–1296. https://doi.org/10.1038/s41586-025-09238-x.

[87] Chen, P.-Y.; Huang, C.; Jie, L.-H.; Guo, B.; Zhu, S.; Xu, H.-C. Unlocking the Potential of Oxidative Asymmetric Catalysis with Continuous Flow Electrochemistry. *J. Am. Chem. Soc.*, **2024**, *146* (11), 7178–7184. https://doi.org/10.1021/jacs.4c00878.

[88] Mazzarella, D. Asymmetric Electrochemical Synthesis in Flow. *J. Flow Chem.*, **2024**, *14* (1), 357–366. https://doi.org/10.1007/s41981-023-00293-x.

[89] Ma, C.; Guo, J.-F.; Xu, S.-S.; Mei, T.-S. Recent Advances in Asymmetric Organometallic Electrochemical Synthesis (AOES). *Acc. Chem. Res.*, **2025**, *58* (3), 399–414. https://doi.org/10.1021/acs.accounts.4c00656.

[90] Jiao, K.-J.; Wang, Z.-H.; Ma, C.; Liu, H.-L.; Cheng, B.; Mei, T.-S. The Applications of Electrochemical Synthesis in Asymmetric Catalysis. *Chem Catalysis*, **2022**, *2* (11), 3019–3047. https://doi.org/10.1016/j.checat.2022.09.039.

[91] De Risi, C.; Bortolini, O.; Brandolese, A.; Di Carmine, G.; Ragno, D.; Massi, A. Recent Advances in Continuous-Flow Organocatalysis for Process Intensification. *React. Chem. Eng.*, **2020**, *5* (6), 1017–1052. https://doi.org/10.1039/D0RE00076K.

[92] Chang, X.; Zhang, J.; Zhang, Q.; Guo, C. Merging Electrosynthesis and Bifunctional Squaramide Catalysis in the Asymmetric Detrifluoroacetylative Alkylation Reactions. *Angew. Chem. Int. Ed.*, **2020**, *59* (42), 18500–18504. https://doi.org/10.1002/anie.202006903.

[93] Tan, X.; Wang, Q.; Sun, J. Electricity-Driven Asymmetric Bromocyclization Enabled by Chiral Phosphate Anion Phase-Transfer Catalysis. *Nat Commun*, **2023**, *14* (1), 357. https://doi.org/10.1038/s41467-023-36000-6.

[94] Xu, Z.; Zheng, C.; Lin, J.; Huang, W.; Song, D.; Zhong, W.; Ling, F. Asymmetric Counteranion-Directed Electrocatalysis for Enantioselective Control of Radical Cation. *Angew. Chem. Int. Ed.*, **2025**, *64* (1), e202413601. https://doi.org/10.1002/anie.202413601.

[95] Tan, X.; Zhou, Z.; Shao, M.; Sun, J. Electrochemical Enantioselective Oxidation of Indoles *via* Chiral Phosphoric Acid Catalysis in Cooperation with H_3PO_4 in Aqueous Media. *Angew. Chem. Int. Ed.*, **2025**, *64* (33), e202510078. https://doi.org/10.1002/anie.202510078.

[96] Qian, C.; Li, P.; Sun, J. Catalytic Enantioselective Synthesis of Spirooxindoles by Oxidative Rearrangement of Indoles. *Angew. Chem. Int. Ed.*, **2021**, *60* (11), 5871–5875. https://doi.org/10.1002/anie.202015175.

[97] Ma, D.; Qiu, Y. Electrochemical Strategies for Advancing Enantioselective Enamine Catalysis. *Chinese Chemical Letters*, **2025**, 111892. https://doi.org/10.1016/j.cclet.2025.111892.

[98] Zhou, P.; Li, W.; Lan, J.; Zhu, T. Electroredox Carbene Organocatalysis with Iodide as Promoter. *Nat Commun*, **2022**, *13* (1), 3827. https://doi.org/10.1038/s41467-022-31453-7.

[99] Li, N.; Ye, X.; Liu, Y.; Song, J. Enantioselective Radical α-Enolation of Esters *via* Electrochemical Chiral Isothiourea Catalysis. *Nat Catal*, **2025**, *8* (9), 957–967. https://doi.org/10.1038/s41929-025-01408-4.

[100] Jensen, K. L.; Franke, P. T.; Nielsen, L. T.; Daasbjerg, K.; Jørgensen, K. A. Anodic Oxidation and Organocatalysis: Direct Regio- and Stereoselective Access to *Meta*-Substituted Anilines by α-Arylation of Aldehydes. *Angew. Chem. Int. Ed.*, **2010**, *49* (1), 129–133. https://doi.org/10.1002/anie.200904754.

[101]   Ho, X.; Mho, S.; Kang, H.; Jang, H. Electro-Organocatalysis: Enantioselective α-Alkylation of Aldehydes. *Eur. J. Org. Chem.*, **2010**, *2010* (23), 4436–4441. https://doi.org/10.1002/ejoc.201000453.

[102]   Wang, Z.-H.; Gao, P.-S.; Wang, X.; Gao, J.-Q.; Xu, X.-T.; He, Z.; Ma, C.; Mei, T.-S. TEMPO-Enabled Electrochemical Enantioselective Oxidative Coupling of Secondary Acyclic Amines with Ketones. *J. Am. Chem. Soc.*, **2021**, *143* (38), 15599–15605. https://doi.org/10.1021/jacs.1c08671.

[103]   He, J.-Y.; Zhu, C.; Duan, W.-X.; Kong, L.-X.; Wang, N.-N.; Wang, Y.-Z.; Fan, Z.-Y.; Qiao, X.-Y.; Xu, H. Bifunctional Chiral Electrocatalysts Enable Enantioselective α-Alkylation of Aldehydes. *Angew. Chem. Int. Ed.*, **2024**, e202401355. https://doi.org/10.1002/anie.202401355.

[104]   Bui, N.; Ho, X.; Mho, S.; Jang, H. Organocatalyzed α-Oxyamination of Aldehydes Using Anodic Oxidation. *Eur. J. Org. Chem.*, **2009**, *2009* (31), 5309–5312. https://doi.org/10.1002/ejoc.200900871.

[105]   Mazzarella, D.; Qi, C.; Vanzella, M.; Sartorel, A.; Pelosi, G.; Dell'Amico, L. Electrochemical Asymmetric Radical Functionalization of Aldehydes Enabled by a Redox Shuttle. *Angew. Chem. Int. Ed.*, **2024**, *63* (25), e202401361. https://doi.org/10.1002/anie.202401361.

[106]   Duan, Y.; Zhang, Y.; Chen, J.; Zeng, F.; Cheng, L.; Luo, S. Asymmetric Electrochemical Alkenylation by Synergistic Chiral Primary Amine and Naphthalene Catalysis. *Angew. Chem. Int. Ed.*, **2025**, *64* (26), e202505826. https://doi.org/10.1002/anie.202505826.

[107]   Krech, A.; Laktsevich-Iskryk, M.; Deil, N.; Fokin, M.; Kimm, M.; Ošeka, M. Asymmetric Cyclopropanation *via* an Electro-Organocatalytic Cascade. *Chem. Commun.*, **2024**, *60* (95), 14026–14029. https://doi.org/10.1039/D4CC05092D.

[108]   Pomikło, D.; Romaniuk, K.; Sieroń, L.; Albrecht, A. Electroorganocatalytic Asymmetric Diels–Alder Cycloaddition of Hydroquinones with α,β-Unsaturated Aldehydes. *Chem. Commun.*, **2025**, *61* (36), 6655–6658. https://doi.org/10.1039/D5CC00505A.

[109]   Rios, R.; Sundén, H.; Vesely, J.; Zhao, G.; Dziedzic, P.; Córdova, A. A Simple Organocatalytic Enantioselective Cyclopropanation of α,β-Unsaturated Aldehydes. *Adv. Synth. Catal.*, **2007**, *349* (7), 1028–1032. https://doi.org/10.1002/adsc.200700032.

[110]   Xie, H.; Zu, L.; Li, H.; Wang, J.; Wang, W. Organocatalytic Enantioselective Cascade Michael-Alkylation Reactions: Synthesis of Chiral Cyclopropanes and Investigation of Unexpected Organocatalyzed Stereoselective Ring Opening of Cyclopropanes. *J. Am. Chem. Soc.*, **2007**, *129* (35), 10886–10894. https://doi.org/10.1021/ja073262a.

[111]   Llanes, P.; Rodríguez-Escrich, C.; Sayalero, S.; Pericàs, M. A. Organocatalytic Enantioselective Continuous-Flow Cyclopropanation. *Org. Lett.*, **2016**, *18* (24), 6292–6295. https://doi.org/10.1021/acs.orglett.6b03156.

[112]   Kunzendorf, A.; Xu, G.; Saifuddin, M.; Saravanan, T.; Poelarends, G. J. Biocatalytic Asymmetric Cyclopropanations *via* Enzyme-Bound Iminium Ion Intermediates. *Angew. Chem. Int. Ed.*, **2021**, *60* (45), 24059–24063. https://doi.org/10.1002/anie.202110719.

[113]   Luo, C.; Wang, Z.; Huang, Y. Asymmetric Intramolecular α-Cyclopropanation of Aldehydes Using a Donor/Acceptor Carbene Mimetic. *Nat Commun*, **2015**, *6* (1), 10041. https://doi.org/10.1038/ncomms10041.

[114] Hutchinson, G.; Alamillo-Ferrer, C.; Burés, J. Mechanistically Guided Design of an Efficient and Enantioselective Aminocatalytic α-Chlorination of Aldehydes. *J. Am. Chem. Soc.*, **2021**, *143* (18), 6805–6809. https://doi.org/10.1021/jacs.1c02997.

[115] Silvi, M.; Verrier, C.; Rey, Y. P.; Buzzetti, L.; Melchiorre, P. Visible-Light Excitation of Iminium Ions Enables the Enantioselective Catalytic β-Alkylation of Enals. *Nature Chem*, **2017**, *9* (9), 868–873. https://doi.org/10.1038/nchem.2748.

[116] Luo, C.; Wang, Z.; Huang, Y. Asymmetric Intramolecular α-Cyclopropanation of Aldehydes Using a Donor/Acceptor Carbene Mimetic. *Nat Commun*, **2015**, *6* (1), 10041. https://doi.org/10.1038/ncomms10041.

[117] Novaes, L. F. T.; Ho, J. S. K.; Mao, K.; Villemure, E.; Terrett, J. A.; Lin, S. α,β-Desaturation and Formal β-C(Sp^3)–H Fluorination of *N*-Substituted Amines: A Late-Stage Functionalization Strategy Enabled by Electrochemistry. *J. Am. Chem. Soc.*, **2024**, *146* (33), 22982–22992. https://doi.org/10.1021/jacs.4c02548.

[118] Ma, X.; Tian, H. Photochemistry and Photophysics. Concepts, Research, Applications. By Vincenzo Balzani, Paola Ceroni and Alberto Juris. *Angew. Chem. Int. Ed.*, **2014**, *53* (34), 8817–8817. https://doi.org/10.1002/anie.201405219.

[119] Braslavsky, S. E. Glossary of Terms Used in Photochemistry, 3rd Edition (IUPAC Recommendations 2006). *Pure and Applied Chemistry*, **2007**, *79* (3), 293–465. https://doi.org/10.1351/pac200779030293.

[120] Loudon, R. *The Quantum Theory of Light*, 3rd.; Oxford University Press: Oxford, UK, 2000.

[121] Albini, A.; Dichiarante, V. The 'Belle Époque' of Photochemistry. *Photochem Photobiol Sci*, **2009**, *8* (2), 248–254. https://doi.org/10.1039/b806756b.

[122] Yoon, T. P.; Ischay, M. A.; Du, J. Visible Light Photocatalysis as a Greener Approach to Photochemical Synthesis. *Nature Chem*, **2010**, *2* (7), 527–532. https://doi.org/10.1038/nchem.687.

[123] Buglioni, L.; Raymenants, F.; Slattery, A.; Zondag, S. D. A.; Noël, T. Technological Innovations in Photochemistry for Organic Synthesis: Flow Chemistry, High-Throughput Experimentation, Scale-up, and Photoelectrochemistry. *Chem. Rev.*, **2022**, *122* (2), 2752–2906. https://doi.org/10.1021/acs.chemrev.1c00332.

[124] Huynh, M. H. V.; Meyer, T. J. Proton-Coupled Electron Transfer. *Chem. Rev.*, **2007**, *107* (11), 5004–5064. https://doi.org/10.1021/cr0500030.

[125] Hammes-Schiffer, S.; Stuchebrukhov, A. A. Theory of Coupled Electron and Proton Transfer Reactions. *Chem. Rev.*, **2010**, *110* (12), 6939–6960. https://doi.org/10.1021/cr1001436.

[126] Capaldo, L.; Ravelli, D. Hydrogen Atom Transfer (HAT): A Versatile Strategy for Substrate Activation in Photocatalyzed Organic Synthesis. *Eur. J. Org. Chem.*, **2017**, *2017* (15), 2056–2071. https://doi.org/10.1002/ejoc.201601485.

[127] Chang, L.; Qing An; An, Q.; Lingfei Duan; Kaixuan Feng; Zuo, Z. Alkoxy Radicals See the Light: New Paradigms of Photochemical Synthesis. *Chemical Reviews*, **2021**. https://doi.org/10.1021/acs.chemrev.1c00256.

[128] Capaldo, L.; Ravelli, D.; Fagnoni, M. Direct Photocatalyzed Hydrogen Atom Transfer (HAT) for Aliphatic C–H Bonds Elaboration. *Chem. Rev.*, **2022**, *122* (2), 1875–1924. https://doi.org/10.1021/acs.chemrev.1c00263.

[129] Yayla, H.; Knowles, R. Proton-Coupled Electron Transfer in Organic Synthesis: Novel Homolytic Bond Activations and Catalytic Asymmetric Reactions with Free Radicals. *Synlett*, **2014**, *25* (20), 2819–2826. https://doi.org/10.1055/s-0034-1379304.

[130] Thach, D. Q.; Knowles, R. R. Light-Driven C(Sp³)–C(Sp³) Bond Functionalizations Enabled by the PCET Activation of Alcohol O–H Bonds. *Acc. Chem. Res.*, **2025**, *58* (13), 2061–2071. https://doi.org/10.1021/acs.accounts.5c00246.

[131] Gadde, K.; De Vos, D.; Maes, B. U. W. Basic Concepts and Activation Modes in Visible-Light-Photocatalyzed Organic Synthesis. *Synthesis*, **2023**, *55* (02), 164–192. https://doi.org/10.1055/a-1932-6937.

[132] Cano-Yelo, H.; Deronzier, A. Photo-Oxidation of Some Carbinols by the Ru(II) Polypyridyl Complex-Aryl Diazonium Salt System. *Tetrahedron Letters*, **1984**, *25* (48), 5517–5520. https://doi.org/10.1016/S0040-4039(01)81614-2.

[133] Hedstrand, D. M.; Kruizinga, W. H.; Kellogg, R. M. Light Induced and Dye Accelerated Reductions of Phenacyl Onium Salts by 1,4-Dihydropyridines. *Tetrahedron Letters*, **1978**, *19* (14), 1255–1258. https://doi.org/10.1016/S0040-4039(01)94515-0.

[134] Nicewicz, D. A.; MacMillan, D. W. C. Merging Photoredox Catalysis with Organocatalysis: The Direct Asymmetric Alkylation of Aldehydes. *Science*, **2008**, *322* (5898), 77–80. https://doi.org/10.1126/science.1161976.

[135] Ischay, M. A.; Anzovino, M. E.; Du, J.; Yoon, T. P. Efficient Visible Light Photocatalysis of [2+2] Enone Cycloadditions. *J. Am. Chem. Soc.*, **2008**, *130* (39), 12886–12887. https://doi.org/10.1021/ja805387f.

[136] Narayanam, J. M. R.; Tucker, J. W.; Stephenson, C. R. J. Electron-Transfer Photoredox Catalysis: Development of a Tin-Free Reductive Dehalogenation Reaction. *J. Am. Chem. Soc.*, **2009**, *131* (25), 8756–8757. https://doi.org/10.1021/ja9033582.

[137] Romero, N. A.; Nicewicz, D. A. Organic Photoredox Catalysis. *Chem. Rev.*, **2016**, *116* (17), 10075–10166. https://doi.org/10.1021/acs.chemrev.6b00057.

[138] Prier, C. K.; Rankic, D. A.; MacMillan, D. W. C. Visible Light Photoredox Catalysis with Transition Metal Complexes: Applications in Organic Synthesis. *Chem. Rev.*, **2013**, *113* (7), 5322–5363. https://doi.org/10.1021/cr300503r.

[139] Shaw, M. H.; Twilton, J.; MacMillan, D. W. C. Photoredox Catalysis in Organic Chemistry. *J. Org. Chem.*, **2016**, *81* (16), 6898–6926. https://doi.org/10.1021/acs.joc.6b01449.

[140] Yoon, T. P.; Ischay, M. A.; Du, J. Visible Light Photocatalysis as a Greener Approach to Photochemical Synthesis. *Nature Chem*, **2010**, *2* (7), 527–532. https://doi.org/10.1038/nchem.687.

[141] Ravelli, D.; Dondi, D.; Fagnoni, M.; Albini, A.; Bagno, A. Electronic and EPR Spectra of the Species Involved in [W10O32]4− Photocatalysis. A Relativistic DFT Investigation. *Phys. Chem. Chem. Phys.*, **2013**, *15* (8), 2890. https://doi.org/10.1039/c2cp43950f.

[142] Laudadio, G.; Deng, Y.; Van Der Wal, K.; Ravelli, D.; Nuño, M.; Fagnoni, M.; Guthrie, D.; Sun, Y.; Noël, T. C(Sp³)–H Functionalizations of Light Hydrocarbons Using Decatungstate Photocatalysis in Flow. *Science*, **2020**, *369* (6499), 92–96. https://doi.org/10.1126/science.abb4688.

[143] Ravelli, D.; Fagnoni, M.; Fukuyama, T.; Nishikawa, T.; Ryu, I. Site-Selective C–H Functionalization by Decatungstate Anion Photocatalysis: Synergistic Control by Polar and Steric Effects Expands the Reaction Scope. *ACS Catal.*, **2018**, *8* (1), 701–713. https://doi.org/10.1021/acscatal.7b03354.

[144] Laudadio, G.; Deng, Y.; van der Wal, K.; Ravelli, D.; Nuño, M.; Fagnoni, M.; Guthrie, D.; Sun, Y.; Noël, T. C(Sp³)–H Functionalizations of Light Hydrocarbons Using Decatungstate Photocatalysis in Flow. *Science*, **2020**, *369* (6499), 92–96. https://doi.org/10.1126/science.abb4688.

[145] Schultz, D. M.; Lévesque, F.; DiRocco, D. A.; Reibarkh, M.; Ji, Y.; Joyce, L. A.; Dropinski, J. F.; Sheng, H.; Sherry, B. D.; Davies, I. W. Oxyfunctionalization of the Remote C–H Bonds of Aliphatic Amines by Decatungstate Photocatalysis. *Angew. Chem. Int. Ed.*, **2017**, *56* (48), 15274–15278. https://doi.org/10.1002/anie.201707537.

[146] Laudadio, G.; Govaerts, S.; Wang, Y.; Ravelli, D.; Koolman, H. F.; Fagnoni, M.; Djuric, S. W.; Noël, T. Selective C(Sp^3)–H Aerobic Oxidation Enabled by Decatungstate Photocatalysis in Flow. *Angew. Chem. Int. Ed.*, **2018**, *57* (15), 4078–4082. https://doi.org/10.1002/anie.201800818.

[147] West, J. G.; Huang, D.; Sorensen, E. J. Acceptorless Dehydrogenation of Small Molecules through Cooperative Base Metal Catalysis. *Nat Commun*, **2015**, *6* (1), 10093. https://doi.org/10.1038/ncomms10093.

[148] Halperin, S. D.; Fan, H.; Chang, S.; Martin, R. E.; Britton, R. A Convenient Photocatalytic Fluorination of Unactivated C⬜H Bonds. *Angew. Chem. Int. Ed.*, **2014**, *53* (18), 4690–4693. https://doi.org/10.1002/anie.201400420.

[149] Sarver, P. J.; Bacauanu, V.; Schultz, D. M.; DiRocco, D. A.; Lam, Y.; Sherer, E. C.; MacMillan, D. W. C. The Merger of Decatungstate and Copper Catalysis to Enable Aliphatic C(Sp3)–H Trifluoromethylation. *Nat. Chem.*, **2020**, *12* (5), 459–467. https://doi.org/10.1038/s41557-020-0436-1.

[150] Perry, I. B.; Brewer, T. F.; Sarver, P. J.; Schultz, D. M.; DiRocco, D. A.; MacMillan, D. W. C. Direct Arylation of Strong Aliphatic C–H Bonds. *Nature*, **2018**, *560* (7716), 70–75. https://doi.org/10.1038/s41586-018-0366-x.

[151] Duncan, D. C.; Netzel, T. L.; Hill, C. L. Early-Time Dynamics and Reactivity of Polyoxometalate Excited States. Identification of a Short-Lived LMCT Excited State and a Reactive Long-Lived Charge-Transfer Intermediate Following Picosecond Flash Excitation of [W10O32]4- in Acetonitrile. *Inorg. Chem.*, **1995**, *34* (18), 4640–4646. https://doi.org/10.1021/ic00122a021.

[152] Kothe, T.; Martschke, R.; Fischer, H. Photoreactions of the Decatungstate Anion W10O324− with Organic Substrates in Solution Studied by EPR and Kinetic Absorption Spectroscopy: An Example for the Persistent Radical Effect. *J. Chem. Soc., Perkin Trans. 2*, **1998**, No. 3, 503–508. https://doi.org/10.1039/a708191j.

[153] Waele, V. D.; Poizat, O.; Fagnoni, M.; Bagno, A.; Ravelli, D. Unraveling the Key Features of the Reactive State of Decatungstate Anion in Hydrogen Atom Transfer (HAT) Photocatalysis. *ACS Catal.*, **2016**, *6* (10), 7174–7182. https://doi.org/10.1021/acscatal.6b01984.

[154] Ravelli, D.; Fagnoni, M.; Fukuyama, T.; Nishikawa, T.; Ryu, I. Site-Selective C–H Functionalization by Decatungstate Anion Photocatalysis: Synergistic Control by Polar and Steric Effects Expands the Reaction Scope. *ACS Catal.*, **2018**, *8* (1), 701–713. https://doi.org/10.1021/acscatal.7b03354.

[155] De Waele, V.; Poizat, O.; Fagnoni, M.; Bagno, A.; Ravelli, D. Unraveling the Key Features of the Reactive State of Decatungstate Anion in Hydrogen Atom Transfer (HAT) Photocatalysis. *ACS Catal.*, **2016**, *6* (10). https://doi.org/10.1021/acscatal.6b01984.

[156] Texier, I.; Delaire, J. A.; Giannotti, C. Reactivity of the Charge Transfer Excited State of Sodium Decatungstate at the Nanosecond Time Scale. *Phys. Chem. Chem. Phys.*, **2000**, *2* (6), 1205–2012. https://doi.org/10.1039/a908588b.

[157] Montanaro, S.; Ravelli, D.; Merli, D.; Fagnoni, M.; Albini, A. Decatungstate As Photoredox Catalyst: Benzylation of Electron-Poor Olefins. *Org. Lett.*, **2012**, *14* (16), 4218–4221. https://doi.org/10.1021/ol301900p.

[158] Capaldo, L.; Buzzetti, L.; Merli, D.; Fagnoni, M.; Ravelli, D. Smooth Photocatalyzed Benzylation of Electrophilic Olefins *via* Decarboxylation of Arylacetic Acids. *J. Org. Chem.*, **2016**, *81* (16), 7102–7109. https://doi.org/10.1021/acs.joc.6b00984.

[159] Leone, M.; Arnaldi, D.; Fagnoni, M. Beyond HAT: Harnessing TBADT for Photocatalyzed Giese-Type C(Sp^3)–C(Sp^3) Bond Formation through Reductive Decarboxylation. *Org. Chem. Front.*, **2025**, 10.1039.D5QO00399G. https://doi.org/10.1039/D5QO00399G.

[160] Mattay, J. Charge Transfer and Radical Ions in Photochemistry. *Angew. Chem. Int. Ed.*, **1987**, *26* (9), 825–845. https://doi.org/10.1002/anie.198708251.

[161] Foster, R. Electron Donor-Acceptor Complexes. *J. Phys. Chem.*, **1980**, *84* (17), 2135–2141. https://doi.org/10.1021/j100454a006.

[162] Rosokha, S. V.; Kochi, J. K. Fresh Look at Electron-Transfer Mechanisms *via* the Donor/Acceptor Bindings in the Critical Encounter Complex. *Acc. Chem. Res.*, **2008**, *41* (5), 641–653. https://doi.org/10.1021/ar700256a.

[163] Wortman, A. K.; Stephenson, C. R. J. EDA Photochemistry: Mechanistic Investigations and Future Opportunities. *Chem*, **2023**, *9* (9), 2390–2415. https://doi.org/10.1016/j.chempr.2023.06.013.

[164] Kosower, E. M. The Effect of Solvent on Charge-Transfer Complex Spectra. *J. Am. Chem. Soc.*, **1956**, *78* (21), 5700–5701. https://doi.org/10.1021/ja01602a070.

[165] Tobisu, M.; Furukawa, T.; Chatani, N. Visible Light-Mediated Direct Arylation of Arenes and Heteroarenes Using Diaryliodonium Salts in the Presence and Absence of a Photocatalyst. *Chemistry Letters*, **2013**, *42* (10), 1203–1205. https://doi.org/10.1246/cl.130547.

[166] Arceo, E.; Jurberg, I. D.; Álvarez-Fernández, A.; Melchiorre, P. Photochemical Activity of a Key Donor–Acceptor Complex Can Drive Stereoselective Catalytic α-Alkylation of Aldehydes. *Nature Chem*, **2013**, *5* (9), 750–756. https://doi.org/10.1038/nchem.1727.

[167] Lima, C. G. S.; De M. Lima, T.; Duarte, M.; Jurberg, I. D.; Paixão, M. W. Organic Synthesis Enabled by Light-Irradiation of EDA Complexes: Theoretical Background and Synthetic Applications. *ACS Catal.*, **2016**, *6* (3), 1389–1407. https://doi.org/10.1021/acscatal.5b02386.

[168] Crisenza, G. E. M.; Mazzarella, D.; Melchiorre, P. Synthetic Methods Driven by the Photoactivity of Electron Donor–Acceptor Complexes. *J. Am. Chem. Soc.*, **2020**, *142* (12), 5461–5476. https://doi.org/10.1021/jacs.0c01416.

[169] Tasnim, T.; Ayodele, M. J.; Pitre, S. P. Recent Advances in Employing Catalytic Donors and Acceptors in Electron Donor–Acceptor Complex Photochemistry. *J. Org. Chem.*, **2022**, *87* (16), 10555–10563. https://doi.org/10.1021/acs.joc.2c01013.

[170] Fu, M.-C.; Shang, R.; Zhao, B.; Wang, B.; Fu, Y. Photocatalytic Decarboxylative Alkylations Mediated by Triphenylphosphine and Sodium Iodide. *Science*, **2019**, *363* (6434), 1429–1434. https://doi.org/10.1126/science.aav3200.

[171] De Pedro Beato, E.; Spinnato, D.; Zhou, W.; Melchiorre, P. A General Organocatalytic System for Electron Donor–Acceptor Complex Photoactivation and Its Use in Radical Processes. *J. Am. Chem. Soc.*, **2021**, *143* (31), 12304–12314. https://doi.org/10.1021/jacs.1c05607.

[172] Dewanji, A.; Van Dalsen, L.; Rossi-Ashton, J. A.; Gasson, E.; Crisenza, G. E. M.; Procter, D. J. A General Arene C–H Functionalization Strategy *via* Electron Donor–Acceptor Complex Photoactivation. *Nat. Chem.*, **2023**, *15* (1), 43–52. https://doi.org/10.1038/s41557-022-01092-y.

[173] Zhou, W.; Wu, S.; Melchiorre, P. Tetrachlorophthalimides as Organocatalytic Acceptors for Electron Donor–Acceptor Complex Photoactivation. *J. Am. Chem. Soc.*, **2022**, *144* (20), 8914–8919. https://doi.org/10.1021/jacs.2c03546.

[174] Brandes, D. S.; Lasky, M. R.; Lisboa, A. V. R. D.; Liu, E.-C.; Remy, M. S.; Sanford, M. S. Photoactivation of Electron Donor–Acceptor Complexes for C(Sp[2])–H Amination of Arenes Using an Organocatalytic Acceptor. *Org. Lett.*, **2025**, acs.orglett.5c03040. https://doi.org/10.1021/acs.orglett.5c03040.

[175] Khoury, P. R.; Goddard, J. D.; Tam, W. Ring Strain Energies: Substituted Rings, Norbornanes, Norbornenes and Norbornadienes. *Tetrahedron*, **2004**, *60* (37), 8103–8112. https://doi.org/10.1016/j.tet.2004.06.100.

[176] McDonald, T. R.; Mills, L. R.; West, M. S.; Rousseaux, S. A. L. Selective Carbon–Carbon Bond Cleavage of Cyclopropanols. *Chem. Rev.*, **2021**, *121* (1), 3–79. https://doi.org/10.1021/acs.chemrev.0c00346.

[177] Morcillo, S. P. Radical-Promoted C–C Bond Cleavage: A Deconstructive Approach for Selective Functionalization. *Angew. Chem. Int. Ed.*, **2019**, *58* (40), 14044–14054. https://doi.org/10.1002/anie.201905218.

[178] Chang, L.; An, Q.; Duan, L.; Feng, K.; Zuo, Z. Alkoxy Radicals See the Light: New Paradigms of Photochemical Synthesis. *Chem. Rev.*, **2022**, *122* (2), 2429–2486. https://doi.org/10.1021/acs.chemrev.1c00256.

[179] Blanksby, S. J.; Ellison, G. B. Bond Dissociation Energies of Organic Molecules. *Acc. Chem. Res.*, **2003**, *36* (4), 255–263. https://doi.org/10.1021/ar020230d.

[180] Jia, K.; Zhang, F.; Huang, H.; Chen, Y. Visible-Light-Induced Alkoxyl Radical Generation Enables Selective C(Sp[3])–C(Sp[3]) Bond Cleavage and Functionalizations. *J. Am. Chem. Soc.*, **2016**, *138* (5), 1514–1517. https://doi.org/10.1021/jacs.5b13066.

[181] Wang, D.; Mao, J.; Zhu, C. Visible Light-Promoted Ring-Opening Functionalization of Unstrained Cycloalkanols *via* Inert C–C Bond Scission. *Chem. Sci.*, **2018**, *9* (26), 5805–5809. https://doi.org/10.1039/C8SC01763H.

[182] Huang, L.; Ji, T.; Rueping, M. Remote Nickel-Catalyzed Cross-Coupling Arylation *via* Proton-Coupled Electron Transfer-Enabled C–C Bond Cleavage. *J. Am. Chem. Soc.*, **2020**, *142* (7), 3532–3539. https://doi.org/10.1021/jacs.9b12490.

[183] Laktsevich-Iskryk, M. V.; Varabyeva, N. A.; Kazlova, V. V.; Zhabinskii, V. N.; Khripach, V. A.; Hurski, A. L. Visible-Light-Promoted Catalytic Ring-Opening Isomerization of 1,2-Disubstituted Cyclopropanols to Linear Ketones: Visible-Light-Promoted Catalytic Ring-Opening Isomerization of 1,2-Disubstituted Cyclopropanols to Linear Ketones. *Eur. J. Org. Chem.*, **2020**, *2020* (16), 2431–2434. https://doi.org/10.1002/ejoc.202000094.

[184] Kikuchi, T.; Yamada, K.; Yasui, T.; Yamamoto, Y. Synthesis of Benzo-Fused Cyclic Ketones *via* Metal-Free Ring Expansion of Cyclopropanols Enabled by Proton-Coupled Electron Transfer. *Org. Lett.*, **2021**, *23* (12), 4710–4714. https://doi.org/10.1021/acs.orglett.1c01436.

[185] Laktsevich-Iskryk, M. V.; Krech, A. V.; Zhabinskii, V. N.; Khripach, V. A.; Hurski, A. L. Photocatalytic Stoichiometric Oxidant-Free Synthesis of Linear Unsaturated Ketones from 1,2-Disubstituted Cyclopropanols. *Synthesis*, **2021**, *53* (06), 1077–1086. https://doi.org/10.1055/s-0040-1706088.

[186] Wang, J.; Li, X. Asymmetric β-Arylation of Cyclopropanols Enabled by Photoredox and Nickel Dual Catalysis. *Chem. Sci.*, **2022**, *13* (10), 3020–3026. https://doi.org/10.1039/D1SC07237D.

[187] Zhang, Y.; Niu, Y.; Guo, Y.; Wang, J.; Zhang, Y.; Liu, S.; Shen, X. Photocatalyzed Cascade Reactions of Cyclopropanols and *α* -Trifluoromethyl-Substituted Olefins for the Synthesis of Fused *Gem* -Difluorooxetanes. *Angew. Chem. Int. Ed.*, **2022**, *61* (44), e202212201. https://doi.org/10.1002/anie.202212201.

[188] Zhao, K.; Yamashita, K.; Carpenter, J. E.; Sherwood, T. C.; Ewing, W. R.; Cheng, P. T. W.; Knowles, R. R. Catalytic Ring Expansions of Cyclic Alcohols Enabled by Proton-Coupled Electron Transfer. *J. Am. Chem. Soc.*, **2019**, *141* (22), 8752–8757. https://doi.org/10.1021/jacs.9b03973.

[189] Hu, A.; Chen, Y.; Guo, J.-J.; Yu, N.; An, Q.; Zuo, Z. Cerium-Catalyzed Formal Cycloaddition of Cycloalkanols with Alkenes through Dual Photoexcitation. *J. Am. Chem. Soc.*, **2018**, *140* (42), 13580–13585. https://doi.org/10.1021/jacs.8b08781.

[190] Guo, J.-J.; Hu, A.; Chen, Y.; Sun, J.; Tang, H.; Zuo, Z. Photocatalytic C–C Bond Cleavage and Amination of Cycloalkanols by Cerium(III) Chloride Complex. *Angew. Chem. Int. Ed.*, **2016**, *55* (49), 15319–15322. https://doi.org/10.1002/anie.201609035.

[191] Xue, T.; Zhang, Z.; Zeng, R. Photoinduced Ligand-to-Metal Charge Transfer (LMCT) of Fe Alkoxide Enabled C–C Bond Cleavage and Amination of Unstrained Cyclic Alcohols. *Org. Lett.*, **2022**, *24* (3), 977–982. https://doi.org/10.1021/acs.orglett.1c04365.

[192] Hu, A.; Guo, J.-J.; Pan, H.; Tang, H.; Gao, Z.; Zuo, Z. δ-Selective Functionalization of Alkanols Enabled by Visible-Light-Induced Ligand-to-Metal Charge Transfer. *J. Am. Chem. Soc.*, **2018**, *140* (5), 1612–1616. https://doi.org/10.1021/jacs.7b13131.

[193] Ji, M.; Wu, Z.; Zhu, C. Visible-Light-Induced Consecutive C–C Bond Fragmentation and Formation for the Synthesis of Elusive Unsymmetric 1,8-Dicarbonyl Compounds. *Chem. Commun.*, **2019**, *55* (16), 2368–2371. https://doi.org/10.1039/C9CC00378A.

[194] Bloom, S.; Bume, D. D.; Pitts, C. R.; Lectka, T. Site-Selective Approach to β-Fluorination: Photocatalyzed Ring Opening of Cyclopropanols. *Chem. Eur. J.*, **2015**, *21* (22), 8060–8063. https://doi.org/10.1002/chem.201501081.

[195] Cardinale, L.; Neumeier, M.; Majek, M.; von Wangelin, A. J. Aryl Pyrazoles from Photocatalytic Cycloadditions of Arenediazonium. *Org. Lett.*, **2020**, *22* (18), 7219–7224. https://doi.org/10.1021/acs.orglett.0c02514.

[196] Zhou, Y.; Wu, M.; Liu, Y.; Cheng, C.; Zhu, G. Synthesis of Polysubstituted Pyrroles *via* Silver-Catalyzed Oxidative Radical Addition of Cyclopropanols to Imines. *Org. Lett.*, **2020**, *22* (19), 7542–7546. https://doi.org/10.1021/acs.orglett.0c02735.

[197] Chiba, S.; Cao, Z.; El Bialy, S. A. A.; Narasaka, K. Generation of β-Keto Radicals from Cyclopropanols Catalyzed by $AgNO_3$. *Chem. Lett.*, **2006**, *35* (1), 18–19. https://doi.org/10.1246/cl.2006.18.

[198] Mane, B. B.; Waghmode, S. B. Iron-Catalyzed Ring Opening of Cyclopropanols and Their 1,6-Conjugate Addition to *p* -Quinone Methides. *J. Org. Chem.*, **2021**, *86* (24), 17774–17781. https://doi.org/10.1021/acs.joc.1c02059.

[199] Lou, C.; Wang, X.; Lv, L.; Li, Z. Iron-Catalyzed Ring-Opening Reactions of Cyclopropanols with Alkenes and TBHP: Synthesis of 5-Oxo Peroxides. *Org. Lett.*, **2021**, *23* (19), 7608–7612. https://doi.org/10.1021/acs.orglett.1c02824.

[200] Xing Zhang; Tian-Ming Yang; Lu-Min Hu; Hu, X.-H. Stereoselective Iron-Catalyzed Alkylation of Enamides with Cyclopropanols *via* Oxidative C(Sp^2)–H Functionalization. *Organic Letters*, **2022**. https://doi.org/10.1021/acs.orglett.2c03563.

[201] Zhang, Y.-H.; Zhang, W.-W.; Zhang, Z.-Y.; Zhao, K.; Loh, T.-P. Manganese-Catalyzed Ring-Opening Coupling Reactions of Cyclopropanols with Enones. *Org. Lett.*, **2019**, *21* (13), 5101–5105. https://doi.org/10.1021/acs.orglett.9b01703.

[202] Wang, Y.-F.; Toh, K. K.; Ng, E. P. J.; Chiba, S. Mn(III)-Mediated Formal [3+3]-Annulation of Vinyl Azides and Cyclopropanols: A Divergent Synthesis of Azaheterocycles. *J. Am. Chem. Soc.*, **2011**, *133* (16), 6411–6421. https://doi.org/10.1021/ja200879w.

[203] Sivanandan, S. T.; Bharath Krishna, R.; Baiju, T. V.; Mohan, C. Visible-Light-Mediated Ring-Opening Reactions of Cyclopropanes. *Eur. J. Org. Chem.*, **2021**, *2021* (48), 6781–6805. https://doi.org/10.1002/ejoc.202100986.

[204] Wu, Q.; Liu, W.; Wang, M.; Huang, Y.; Hu, P. Iron-Catalyzed Deconstructive Alkylation through Chlorine Radical Induced C–C Single Bond Cleavage under Visible Light. *Chem. Commun.*, **2022**, *58* (71), 9886–9889. https://doi.org/10.1039/D2CC03896J.

[205] Woźniak, Ł.; Magagnano, G.; Melchiorre, P. Enantioselective Photochemical Organocascade Catalysis. *Angew. Chem. Int. Ed.*, **2018**, *57* (4), 1068–1072. https://doi.org/10.1002/anie.201711397.

[206] Krech, A.; Yakimchyk, V.; Jarg, T.; Kananovich, D.; Ošeka, M. Ring-Opening Coupling Reaction of Cyclopropanols with Electrophilic Alkenes Enabled by Decatungstate as Photoredox Catalyst. *Adv. Synth. Catal.*, **2024**, *366* (1), 91–100. https://doi.org/10.1002/adsc.202300939.

[207] Carli, B.; Salaverri, N.; Martinez-Fernandez, L.; Goicuría, M.; Alemán, J.; Marzo, L. Proton-Coupled Electron Transfer Ring Opening of Cycloalkanols Followed by a Giese Radical Addition Enabled by an Electron Donor–Acceptor Complex. *Org. Lett.*, **2024**, *26* (21), 4542–4547. https://doi.org/10.1021/acs.orglett.4c01443.

[208] Wang, M.; Waser, J. Oxidative Fluorination of Cyclopropylamides through Organic Photoredox Catalysis. *Angew. Chem. Int. Ed.*, **2020**, *59* (38), 16420–16424. https://doi.org/10.1002/anie.202007864.

[209] Guo, L.-N.; Deng, Z.-Q.; Wu, Y.; Hu, J. Transition-Metal Free Alkylarylation of Acrylamides Initiated by Radical C–C Bond Cleavage of the Tertiary Cycloalkanols. *RSC Adv.*, **2016**, *6* (32), 27000–27003. https://doi.org/10.1039/C6RA03431D.

[210] Wan, T.; Capaldo, L.; Laudadio, G.; Nyuchev, A. V.; Rincón, J. A.; García-Losada, P.; Mateos, C.; Frederick, M. O.; Nuño, M.; Noël, T. Decatungstate-Mediated C(Sp^3)–H Heteroarylation *via* Radical-Polar Crossover in Batch and Flow. *Angew. Chem. Int. Ed.*, **2021**, *60* (33), 17893–17897. https://doi.org/10.1002/anie.202104682.

[211] Wang, X.; Yu, M.; Song, H.; Liu, Y.; Wang, Q. Radical Transformation of Aliphatic C–H Bonds to Oxime Ethers *via* Hydrogen Atom Transfer. *Org. Lett.*, **2021**, *23* (21), 8353–8358. https://doi.org/10.1021/acs.orglett.1c03087.

[212] Sambiagio, C.; Noël, T. Flow Photochemistry: Shine Some Light on Those Tubes! *Trends in Chemistry*, **2020**, *2* (2), 92–106. https://doi.org/10.1016/j.trechm.2019.09.003.

[213] Plutschack, M. B.; Pieber, B.; Gilmore, K.; Seeberger, P. H. The Hitchhiker's Guide to Flow Chemistry. *Chem. Rev.*, **2017**, *117* (18), 11796–11893. https://doi.org/10.1021/acs.chemrev.7b00183.

[214] Cao, Y.; Zhang, S.-C.; Zhang, M.; Shen, G.-B.; Zhu, X.-Q. Determination of Thermodynamic Affinities of Various Polar Olefins as Hydride, Hydrogen Atom, and Electron Acceptors in Acetonitrile. *J. Org. Chem.*, **2013**, *78* (14), 7154–7168. https://doi.org/10.1021/jo4010926.

[215] Thordarson, P. Determining Association Constants from Titration Experiments in Supramolecular Chemistry. *Chem. Soc. Rev.*, **2011**, *40* (3), 1305–1323. https://doi.org/10.1039/C0CS00062K.

[216] Cao, Y.; Zhang, S.-C.; Zhang, M.; Shen, G.-B.; Zhu, X.-Q. Determination of Thermodynamic Affinities of Various Polar Olefins as Hydride, Hydrogen Atom, and Electron Acceptors in Acetonitrile. *J. Org. Chem.*, **2013**, *78* (14), 7154–7168. https://doi.org/10.1021/jo4010926.

[217] Lucet, D.; Le Gall, T.; Mioskowski, C. The Chemistry of Vicinal Diamines. *Angew. Chem. Int. Ed.*, **1998**, *37* (19), 2580–2627. https://doi.org/10.1002/(SICI)1521-3773(19981016)37:19%253C2580::AID-ANIE2580%253E3.0.CO;2-L.

[218] Saibabu Kotti, S. R. S.; Timmons, C.; Li, G. Vicinal Diamino Functionalities as Privileged Structural Elements in Biologically Active Compounds and Exploitation of Their Synthetic Chemistry. *Chem. Biol. Drug Des.*, **2006**, *67* (2), 101–114. https://doi.org/10.1111/j.1747-0285.2006.00347.x.

[219] Nakayama, K.; Maruoka, K. Complete Switch of Product Selectivity in Asymmetric Direct Aldol Reaction with Two Different Chiral Organocatalysts from a Common Chiral Source. *J. Am. Chem. Soc.*, **2008**, *130* (52), 17666–17667. https://doi.org/10.1021/ja807807p.

[220] Bennani, Y. L.; Hanessian, S. *Trans* -1,2-Diaminocyclohexane Derivatives as Chiral Reagents, Scaffolds, and Ligands for Catalysis: Applications in Asymmetric Synthesis and Molecular Recognition. *Chem. Rev.*, **1997**, *97* (8), 3161–3196. https://doi.org/10.1021/cr9407577.

[221] Pozhydaiev, V.; Paparesta, A.; Moran, J.; Lebœuf, D. Iron(II)-Catalyzed 1,2-Diamination of Styrenes Installing a Terminal NH_2 Group Alongside Unprotected Amines. *Angew. Chem. Int. Ed.*, **2024**, *63* (45), e202411992. https://doi.org/10.1002/anie.202411992.

[222] Shen, K.; Wang, Q. Copper-Catalyzed Diamination of Unactivated Alkenes with Hydroxylamines. *Chem. Sci.*, **2015**, *6* (7), 4279–4283. https://doi.org/10.1039/C5SC00897B.

[223] Olson, D. E.; Su, J. Y.; Roberts, D. A.; Du Bois, J. Vicinal Diamination of Alkenes under Rh-Catalysis. *J. Am. Chem. Soc.*, **2014**, *136* (39), 13506–13509. https://doi.org/10.1021/ja506532h.

[224] Martínez, C.; Muñiz, K. Palladium-Catalyzed Vicinal Difunctionalization of Internal Alkenes: Diastereoselective Synthesis of Diamines. *Angew. Chem. Int. Ed.*, **2012**, *51* (28), 7031–7034. https://doi.org/10.1002/anie.201201719.

[225] Cardona, F.; Goti, A. Metal-Catalysed 1,2-Diamination Reactions. *Nature Chem*, **2009**, *1* (4), 269–275. https://doi.org/10.1038/nchem.256.

[226] Foubelo, F.; Nájera, C.; Retamosa, M. G.; Sansano, J. M.; Yus, M. Catalytic Asymmetric Synthesis of 1,2-Diamines. *Chem. Soc. Rev.*, **2024**, *53* (15), 7983–8085. https://doi.org/10.1039/D3CS00379E.

[227] Finotti Cordeiro, C.; Lopardi Franco, L.; Teixeira Carvalho, D.; Bonfilio, R. Impurities in Active Pharmaceutical Ingredients and Drug Products: A Critical Review. *Critical Reviews in Analytical Chemistry*, **2024**, 1–21. https://doi.org/10.1080/10408347.2024.2384046.

[228] Muñiz, K.; Martínez, C. Development of Intramolecular Vicinal Diamination of Alkenes: From Palladium to Bromine Catalysis. *J. Org. Chem.*, **2013**, *78* (6), 2168–2174. https://doi.org/10.1021/jo302472w.

[229] Muñiz, K.; Barreiro, L.; Romero, R. M.; Martínez, C. Catalytic Asymmetric Diamination of Styrenes. *J. Am. Chem. Soc.*, **2017**, *139* (12), 4354–4357. https://doi.org/10.1021/jacs.7b01443.

[230] Minakata, S.; Miwa, H.; Yamamoto, K.; Hirayama, A.; Okumura, S. Diastereodivergent Intermolecular 1,2-Diamination of Unactivated Alkenes Enabled by Iodine Catalysis. *J. Am. Chem. Soc.*, **2021**, *143* (11), 4112–4118. https://doi.org/10.1021/jacs.1c00228.

[231] Fu, N.; Sauer, G. S.; Lin, S. A General, Electrocatalytic Approach to the Synthesis of Vicinal Diamines. *Nat Protoc*, **2018**, *13* (8), 1725–1743. https://doi.org/10.1038/s41596-018-0010-0.

[232] Makai, S.; Falk, E.; Morandi, B. Direct Synthesis of Unprotected 2-Azidoamines from Alkenes *via* an Iron-Catalyzed Difunctionalization Reaction. *J. Am. Chem. Soc.*, **2020**, *142* (51), 21548–21555. https://doi.org/10.1021/jacs.0c11025.

[233] Cai, C.-Y.; Shu, X.-M.; Xu, H.-C. Practical and Stereoselective Electrocatalytic 1,2-Diamination of Alkenes. *Nat Commun*, **2019**, *10* (1), 4953. https://doi.org/10.1038/s41467-019-13024-5.

[234] Sekar, G.; Singh, V. K. Efficient Method for Cleavage of Aziridines with Aromatic Amines. *J. Org. Chem.*, **1999**, *64* (7), 2537–2539. https://doi.org/10.1021/jo981869r.

[235] Huang, Y.-Y.; Lv, Z.-C.; Yang, X.; Wang, Z.-L.; Zou, X.-X.; Zhao, Z.-N.; Chen, F. Nucleophilic Ring Opening of Aziridines with Amines under Catalyst- and Solvent-Free Conditions. *Green Chem.*, **2017**, *19* (4), 924–927. https://doi.org/10.1039/C6GC03144G.

[236] Govaerts, S.; Angelini, L.; Hampton, C.; Malet-Sanz, L.; Ruffoni, A.; Leonori, D. Photoinduced Olefin Diamination with Alkylamines. *Angew. Chem. Int. Ed.*, **2020**, *59* (35), 15021–15028. https://doi.org/10.1002/anie.202005652.

[237] Luque, A.; Paternoga, J.; Opatz, T. Strain Release Chemistry of Photogenerated Small-Ring Intermediates. *Chem. Eur. J.*, **2021**, *27* (14), 4500–4516. https://doi.org/10.1002/chem.202004178.

[238] Sweeney, J. B. Aziridines: Epoxides' Ugly Cousins? *Chem. Soc. Rev.*, **2002**, *31* (5), 247–258. https://doi.org/10.1039/B006015L.

[239] Kim, Y.; Ha, H.-J.; Yun, S. Y.; Lee, W. K. The Preparation of Stable Aziridinium Ions and Their Ring-Openings. *Chem. Commun.*, **2008**, No. 36, 4363. https://doi.org/10.1039/b809124b.

[240] Hu, X. E. Nucleophilic Ring Opening of Aziridines. *Tetrahedron*, **2004**, *60* (12), 2701–2743. https://doi.org/10.1016/j.tet.2004.01.042.

[241] Chandrasekhar, M.; Sekar, G.; Singh, V. K. An Efficient Method for Opening Nonactivated Aziridines with TMS Azide: Application in the Synthesis of Chiral 1,2-Diaminocyclohexane. *Tetrahedron Letters*, **2000**, *41* (51), 10079–10083. https://doi.org/10.1016/S0040-4039(00)01793-7.

[242] Trocha, A.; Piotrowska, D. G.; Głowacka, I. E. Synthesis of Enantiomerically Enriched Protected 2-Amino-, 2,3-Diamino- and 2-Amino-3-Hydroxypropylphosphonates. *Molecules*, **2023**, *28* (3), 1466. https://doi.org/10.3390/molecules28031466.

[243] Deng, T.; Mazumdar, W.; Yoshinaga, Y.; Patel, P. B.; Malo, D.; Malo, T.; Wink, D. J.; Driver, T. G. Rh$_2$ (II)-Catalyzed Intermolecular *N* -Aryl Aziridination of Olefins Using Nonactivated N Atom Precursors. *J. Am. Chem. Soc.*, **2021**, *143* (45), 19149–19159. https://doi.org/10.1021/jacs.1c09229.

[244] Marti, A.; Richter, L.; Schneider, C. Iron-Catalyzed Ring-Opening of Meso-Aziridines with Amines. *Synlett*, **2011**, *2011* (17), 2513–2516. https://doi.org/10.1055/s-0030-1260338.

[245] Peruncheralathan, S.; Teller, H.; Schneider, C. Titanium Binolate Catalyzed Aminolysis of *Meso* Aziridines: A Highly Enantioselective and Direct Access to 1,2-Diamines. *Angew. Chem. Int. Ed.*, **2009**, *48* (26), 4849–4852. https://doi.org/10.1002/anie.200901110.

[246] McNally, A.; Haffemayer, B.; Collins, B. S. L.; Gaunt, M. J. Palladium-Catalysed C–H Activation of Aliphatic Amines to Give Strained Nitrogen Heterocycles. *Nature*, **2014**, *510* (7503), 129–133. https://doi.org/10.1038/nature13389.

[247] Anand, R. V.; Pandey, G.; Singh, V. K. Silica Gel Induced Cleavage of Aziridines by Aromatic Amines under Solvent Free Conditions. *Tetrahedron Letters*, **2002**, *43* (22), 3975–3976. https://doi.org/10.1016/S0040-4039(02)00727-X.

[248] Lee, B. K.; Kim, M. S.; Hahm, H. S.; Kim, D. S.; Lee, W. K.; Ha, H.-J. An Efficient Synthesis of Chiral Terminal 1,2-Diamines Using an Enantiomerically Pure [1-(1'R)-Methylbenzyl]Aziridine-2-Yl]Methanol. *Tetrahedron*, **2006**, *62* (35), 8393–8397. https://doi.org/10.1016/j.tet.2006.06.024.

[249] Kim, Y.; Ha, H.-J.; Han, K.; Ko, S. W.; Yun, H.; Yoon, H. J.; Kim, M. S.; Lee, W. K. Preparation of 2,3-Diaminopropionate from Ring Opening of Aziridine-2-Carboxylate. *Tetrahedron Letters*, **2005**, *46* (25), 4407–4409. https://doi.org/10.1016/j.tetlet.2005.04.039.

[250] Trinchera, P.; Musio, B.; Degennaro, L.; Moliterni, A.; Falcicchio, A.; Luisi, R. One-Pot Preparation of Piperazines by Regioselective Ring-Opening of Non-Activated Arylaziridines. *Org. Biomol. Chem.*, **2012**, *10* (10), 1962. https://doi.org/10.1039/c2ob07099e.

[251] Jas, G.; Kirschning, A. Continuous Flow Techniques in Organic Synthesis. *Chem. Eur. J.*, **2003**, *9* (23), 5708–5723. https://doi.org/10.1002/chem.200305212.

[252] Capaldo, L.; Wen, Z.; Noël, T. A Field Guide to Flow Chemistry for Synthetic Organic Chemists. *Chem. Sci.*, **2023**, *14* (16), 4230–4247. https://doi.org/10.1039/D3SC00992K.

[253] Britton, J.; Jamison, T. F. The Assembly and Use of Continuous Flow Systems for Chemical Synthesis. *Nat Protoc*, **2017**, *12* (11), 2423–2446. https://doi.org/10.1038/nprot.2017.102.

[254] Hartman, R. L.; McMullen, J. P.; Jensen, K. F. Deciding Whether To Go with the Flow: Evaluating the Merits of Flow Reactors for Synthesis. *Angew. Chem. Int. Ed.*, **2011**, *50* (33), 7502–7519. https://doi.org/10.1002/anie.201004637.

[255] Movsisyan, M.; Delbeke, E. I. P.; Berton, J. K. E. T.; Battilocchio, C.; Ley, S. V.; Stevens, C. V. Taming Hazardous Chemistry by Continuous Flow Technology. *Chem. Soc. Rev.*, **2016**, *45* (18), 4892–4928. https://doi.org/10.1039/C5CS00902B.

[256] Plutschack, M. B.; Pieber, B.; Gilmore, K.; Seeberger, P. H. The Hitchhiker's Guide to Flow Chemistry. *Chem. Rev.*, **2017**, *117* (18), 11796–11893. https://doi.org/10.1021/acs.chemrev.7b00183.

[257] Kirschning, A.; Monenschein, H.; Wittenberg, R. Functionalized Polymers-Emerging Versatile Tools for Solution-Phase Chemistry and Automated Parallel Synthesis. *Angew. Chem. Int. Ed.*, **2001**, *40* (4), 650–679. https://doi.org/10.1002/1521-3773(20010216)40:4%253C650::AID-ANIE6500%253E3.0.CO;2-C.

[258] Coley, C. W.; Thomas, D. A.; Lummiss, J. A. M.; Jaworski, J. N.; Breen, C. P.; Schultz, V.; Hart, T.; Fishman, J. S.; Rogers, L.; Gao, H.; et al. A Robotic Platform for Flow Synthesis of Organic Compounds Informed by AI Planning. *Science*, **2019**, *365* (6453), eaax1566. https://doi.org/10.1126/science.aax1566.

[259] Hardwick, T.; Ahmed, N. Digitising Chemical Synthesis in Automated and Robotic Flow. *Chem. Sci.*, **2020**, *11* (44), 11973–11988. https://doi.org/10.1039/D0SC04250A.

[260] Slattery, A.; Wen, Z.; Tenblad, P.; Sanjosé-Orduna, J.; Pintossi, D.; Den Hartog, T.; Noël, T. Automated Self-Optimization, Intensification, and Scale-up of Photocatalysis in Flow. *Science*, **2024**, *383* (6681), eadj1817. https://doi.org/10.1126/science.adj1817.

[261] Elsherbini, M.; Wirth, T. Electroorganic Synthesis under Flow Conditions. *Acc. Chem. Res.*, **2019**, *52* (12), 3287–3296. https://doi.org/10.1021/acs.accounts.9b00497.

[262] Noël, T.; Cao, Y.; Laudadio, G. The Fundamentals Behind the Use of Flow Reactors in Electrochemistry. *Acc. Chem. Res.*, **2019**, *52* (10), 2858–2869. https://doi.org/10.1021/acs.accounts.9b00412.

[263] Tucker, J. W.; Zhang, Y.; Jamison, T. F.; Stephenson, C. R. J. Visible-Light Photoredox Catalysis in Flow. *Angew. Chem. Int. Ed.*, **2012**, *51* (17), 4144–4147. https://doi.org/10.1002/anie.201200961.

[264] Su, Y.; Straathof, N. J. W.; Hessel, V.; Noël, T. Photochemical Transformations Accelerated in Continuous-Flow Reactors: Basic Concepts and Applications. *Chem. Eur. J.*, **2014**, *20* (34), 10562–10589. https://doi.org/10.1002/chem.201400283.

[265] Sambiagio, C.; Noël, T. Flow Photochemistry: Shine Some Light on Those Tubes! *Trends in Chemistry*, **2020**, *2* (2), 92–106. https://doi.org/10.1016/j.trechm.2019.09.003.

[266] Crawford, R.; Baumann, M. Continuous Flow Technology Enabling Photochemistry. *Adv. Synth. Catal.*, **2025**, *367* (9), e202500133. https://doi.org/10.1002/adsc.202500133.

[267] Porta, R.; Benaglia, M.; Puglisi, A. Flow Chemistry: Recent Developments in the Synthesis of Pharmaceutical Products. *Org. Process Res. Dev.*, **2016**, *20* (1), 2–25. https://doi.org/10.1021/acs.oprd.5b00325.

[268] Gutmann, B.; Cantillo, D.; Kappe, C. O. Continuous-Flow Technology—A Tool for the Safe Manufacturing of Active Pharmaceutical Ingredients. *Angew. Chem. Int. Ed.*, **2015**, *54* (23), 6688–6728. https://doi.org/10.1002/anie.201409318.

[269] Britton, J.; Raston, C. L. Multi-Step Continuous-Flow Synthesis. *Chem. Soc. Rev.*, **2017**, *46* (5), 1250–1271. https://doi.org/10.1039/C6CS00830E.

[270] Guidi, M.; Seeberger, P. H.; Gilmore, K. How to Approach Flow Chemistry. *Chem. Soc. Rev.*, **2020**, *49* (24), 8910–8932. https://doi.org/10.1039/C9CS00832B.

[271] Jiao, J.; Nie, W.; Yu, T.; Yang, F.; Zhang, Q.; Aihemaiti, F.; Yang, T.; Liu, X.; Wang, J.; Li, P. Multi-Step Continuous-Flow Organic Synthesis: Opportunities and Challenges. *Chem. Eur. J.*, **2021**, *27* (15), 4817–4838. https://doi.org/10.1002/chem.202004477.

[272] Oseka, M.; Laudadio, G.; Van Leest, N. P.; Dyga, M.; Bartolomeu, A. D. A.; Gooßen, L. J.; De Bruin, B.; De Oliveira, K. T.; Noël, T. Electrochemical Aziridination of Internal Alkenes with Primary Amines. *Chem*, **2021**, *7* (1), 255–266. https://doi.org/10.1016/j.chempr.2020.12.002.

[273] Laktsevich-Iskryk, M.; Krech, A.; Fokin, M.; Kimm, M.; Jarg, T.; Noël, T.; Ošeka, M. Telescoped Synthesis of Vicinal Diamines *via* Ring-Opening of Electrochemically Generated Aziridines in Flow. *J. Flow Chem.*, **2024**, *14* (1), 139–147. https://doi.org/10.1007/s41981-023-00296-8.

[274] Colomer, I.; Chamberlain, A. E. R.; Haughey, M. B.; Donohoe, T. J. Hexafluoroisopropanol as a Highly Versatile Solvent. *Nat Rev Chem*, **2017**, *1* (11), 0088. https://doi.org/10.1038/s41570-017-0088.

[275] Pozhydaiev, V.; Power, M.; Gandon, V.; Moran, J.; Lebœuf, D. Exploiting Hexafluoroisopropanol (HFIP) in Lewis and Brønsted Acid-Catalyzed Reactions. *Chem. Commun.*, **2020**, *56* (78), 11548–11564. https://doi.org/10.1039/D0CC05194B.

[276] Li, G.-X.; Qu, J. Friedel–Crafts Alkylation of Arenes with Epoxides Promoted by Fluorinated Alcohols or Water. *Chem. Commun.*, **2010**, *46* (15), 2653. https://doi.org/10.1039/b926684d.

[277] Laudadio, G.; De Smet, W.; Struik, L.; Cao, Y.; Noël, T. Design and Application of a Modular and Scalable Electrochemical Flow Microreactor. *J. Flow Chem.*, **2018**, *8* (3–4), 157–165. https://doi.org/10.1007/s41981-018-0024-3.

[278] Kanzian, T.; Nigst, T. A.; Maier, A.; Pichl, S.; Mayr, H. Nucleophilic Reactivities of Primary and Secondary Amines in Acetonitrile. *Eur. J. Org. Chem.*, **2009**, *2009* (36), 6379–6385. https://doi.org/10.1002/ejoc.200900925.

Acknowledgements

First of all, I would like to express my deepest gratitude to my supervisor, Prof. Maksim Oševka, for giving me the opportunity to be part of his research group. I cannot express how honored I am to be your student. The time you dedicated for teaching me and sharing everything you know about working in the lab, writing papers, and approaching problems was enormous. I am definitely a better scientist now, and I believe a better person too. Thank you for your support, encouragement, understanding, trust, and respect. I am exceptionally lucky to work with you.

I am also deeply grateful to my colleague and co-author, Margo, who has always been kind and helpful no matter the circumstances. Your professionalism, deep knowledge, and passion for chemistry are incredibly inspiring, as well as your creativity and photography. Additional thanks for reading the final version of this thesis. I am happy that Nora and Misha joined our lab and brought so much laughter and joy there. You are not only students but also friends now. Thank you both Tanya and Tanya, for your warmth and friendship.

I am thankful to Dr. Mariliis Kimm for your calm and joyful spirit and your ability to solve problems quickly at any level. I am also grateful to Dr. Kristin Erkman for your kindness, our talks, and your valuable help. To all the members of my group and the organic chemistry groups: thank you for being supportive and kind colleagues. I have always been impressed by Prof. Tõnis Karger and Prof. Riina Aav, who are constant inspirations and always attentive to newcomers. I am also thankful to Dr. Dzmitry Kananovich for his enthusiasm, support, and occasional supervision. Without the analytical expertise and help, my work wouldn't be possible. I am grateful to Tatsiana Jarg and Marina Kudrjašova for that.

I am thankful to Dr. Aleksandra Murre and Dr. Mikk Kaasik for reviewing my thesis.

I thank Erasmus for funding my stay at ICIQ and Prof. Marcos G. Suero for hosting me in his research group. I met so many wonderful people in sunny Tarragona! Guillaume, thank you for being the incredible person you are, I hope we will climb many more mountains together. Alisa, your laughter and kindness made my time in Tarragona unforgettable. Alessio, thank you for sharing with me your love for the cinema and disappointment with that-must-not-be-named. I also want to thank Leonardo, Francesco, Josep, Paula, Martina and Pablo. I am honored to know you and hope to meet you again.

I want to thank my parents, Volha and Viktar, my brother Artsiom, and my grandmother Yana. Even from afar I feel your love and care. I am grateful to my partner, Sasha, for his enormous support at all times. You mean the world to me.

These four years in Estonia have been long, and the path of a PhD student is often filled with challenges and failures. Without all the wonderful people I met here outside the lab, this journey would have been impossible. Thank you, Volia, Stiven, Nik, and Anna-Maria. Thank you to my previous lab colleagues and always friends, Volia and Masha, who always inspire me to live life to the fullest.

Abstract

Enabling Technologies for the Construction and Ring-Opening of Three-Membered Cycles

Enabling technologies such as electrochemistry, photochemistry, and flow chemistry unlock new possibilities for discovering novel reactions and conducting organic transformations more sustainably and efficiently. Therefore, the primary objective of this study was to apply these enabling technologies to the construction and ring-opening of three-membered rings to obtain valuable products.

This thesis is divided into three chapters according to three original publications it is based on. The first chapter introduces organic electrochemistry and, importantly, describes the state of the art in asymmetric electro-organocatalysis. The results and discussion section of this chapter presents the development of a reaction that merges electrochemistry with iminium ion organocatalysis for highly enantioselective cyclopropanation. Compared to previous methods, the developed transformation eliminates the need for pre-synthesized halogenated reagents and uses electrons to drive the reaction. The robustness of the method was verified through a substrate scope featuring various cyclopropanes obtained in moderate to good yields, and the mechanism was elucidated with the support of control experiments and electroanalytical techniques.

The second chapter focuses on photochemistry and photoredox catalysis in organic synthesis. The results and discussion section introduces a photocatalytic methodology for generating β-ketoalkyl radicals from tertiary cyclopropanols and their subsequent reaction with electron-deficient alkenes under ultraviolet irradiation. Using tetrabutylammonium decatungstate (TBADT) as a photoredox catalyst enabled the fast and efficient access to distantly functionalized ketones. The formation of electron donor-acceptor (EDA) complexes between electron-rich aromatic cyclopropanols and electron-deficient olefins is also described, which led to the development of new reaction pathways for cyclopropanol ring-opening. A photochemical flow setup was employed for the scale-up of this reaction.

The third chapter presents methods for synthesizing valuable diamines and provides a detailed introduction to flow chemistry. The results and discussion section describes the effective use of continuous flow chemistry for the electrochemical synthesis of aziridines and their subsequent ring-opening in a single telescoped process. This approach enables the synthesis of vicinal diamines in a streamlined and efficient manner directly from simple starting materials, alkenes and primary amines, without the isolation of unstable aziridine intermediates.

In summary, this thesis demonstrates the successful application of enabling technologies, such as electrochemistry, photochemistry, and flow chemistry, to both the construction and ring-opening of three-membered rings, offering sustainable routes to the synthesis of valuable organic compounds.

Lühikokkuvõte

Sünteesitehnoloogiad kolmeliikmeliste tsüklite saamiseks ja avamiseks

Erinevate sünteesitehnoloogiate nagu elektrokeemia, fotokeemia ja voolukeemia kasutamine aitab kaasa uute reaktsioonide avastamisele ja võimaldab orgaanilisi muundumisi läbi viia jätkusuutlikumal ja efektiivsemal viisil. Seetõttu on käesoleva uurimistöö peamine eesmärk rakendada erinevaid sünteesitehnoloogiaid kolmeliiklemiste tsüklite saamiseks ja avamiseks, et saada kasulikke keemilisi ühendeid.

Doktoritöö koosneb kolmest peatükist, mille aluseks on vastavad teaduspublikatsioonid. Esimene peatükk tutvustab orgaanilist elektrokeemiat ja keskendub kaasaegsele asümmeetrilisele elekto-organokatalüüsile. Tulemuste ja arutelu osa kirjeldab reaktsiooni arendamist, mis ühendab elektrokeemia imiinium-ioon organokatalüüsiga kõrge enantioselektiivsusega tsüklopropaneerimiseks. Võrreldes varasemate meetoditega võimaldab arendatud muundumine vältida eelnevalt sünteesitud halogeenitud reagentide kasutamist ning elektrone kasutatakse redoksagendina reaktsiooni käivitamiseks. Reaktsiooni ulatuse uurimise käigus sünteesiti erinevad tsüklopropaanid keskmiste kuni kõrgete saagistega ning reaktsiooni mehhanismi seletati toetudes kontrolleksperimentidele ja elektrianalüütiliste meetoditele.

Teine peatükk keskendub fotokeemiale ja fotoredokskatalüüsile orgaanilises sünteesis. Tulemuste ja arutelu osa tutvustab fotokatalüütilist meetodit β-ketoalküül radikaalide genereerimiseks tertsiaarsetest tsüklopropanoolidest ja nende reageerimist elektronvaesete alkeenidega ultraviolettkiirguse toimel. Tetrabutüülammooniumvolframaadi kasutamine fotoredokskatalüsaatorina võimaldas kiiret ja efektiivset ligipääsu β-funktsialiseeritud ketoonidele. Lisaks kirjeldati elektron-doonor-aktseptor kompleksi moodustumist elektronrikaste aromaatse tsüklopropanoolide ja elektronvaeste olefiinide vahel, mis viis uute reaktsiooniradade arendamiseni tsüklopropanooli avamisel. Reaksiooni skaleerimiseks viidi fotokatalüüs läbi pidevas voolus.

Kolmandas peatükis kirjeldatakse meetodeid väärtuslike diamiinide sünteesiks ja tutvustatakse voolukeemiat. Tulemuste ja arutelu osa kirjeldab pideva voolu keemia efektiivset kasutamist asiridiinide elektrokeemilises sünteesis ja nende avamist samas teleskoopprotsessis. See lähenemine võimaldab sünteesida vitsiniaalseid diamiine efektiivselt lihtsatest lähteainetest nagu alkeenid ja primaarsed amiinid ilma ebastabiiliseid asiridiini vaheühendeid eraldamata.

Kokkuvõtvalt kirjeldab käesolev doktoritöö erinevate sünteesitehnoloogiate nagu elektrokeemia, fotokeemia ja voolukeemia edukat rakendamist nii kolmeliikmeliste tsüklite saamiseks kui ka avamises pakkudes jätkusuutlikke sünteesiradasid väärtuslike orgaaniliste ühendite sünteesiks.

Appendix 1

ChemComm

Chemical Communications

rsc.li/chemcomm

ROYAL SOCIETY
OF **CHEMISTRY**

COMMUNICATION
Maksim Ošeka *et al.*
Asymmetric cyclopropanation *via* an electro-organocatalytic cascade

60 YEARS
ANNIVERSARY

ChemComm

Check for updates

Asymmetric cyclopropanation *via* an electro-organocatalytic cascade†

Anastasiya Krech, [ID] ‡ Marharyta Laktsevich-Iskryk, [ID] ‡ Nora Deil, [ID] Mihhail Fokin, [ID] Mariliis Kimm [ID] and Maksim Ošeka [ID] *

We report an iminium ion-promoted, asymmetric synthesis of cyclopropanes *via* an electrocatalytic, iodine-mediated ring closure. The mild, controlled electrochemical generation of electrophilic iodine species in catalytic quantities prevents organocatalyst deactivation, while also eliminating the need for halogenating reagents, thus simplifying traditional synthetic approaches.
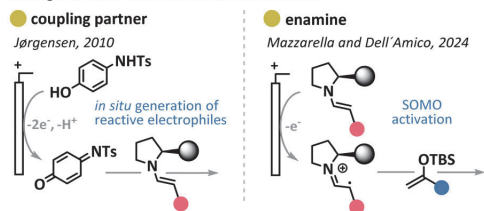
Over the past two decades, amino-organocatalysis has been extensively employed in the development of asymmetric reactions, exploiting both polar and radical pathways, while combining organocatalysis with metal- and photocatalysis has enabled unconventional transformations.[1] Electrochemistry, in turn, offers a greener approach to synthesizing simple molecules and performing late-stage functionalization of complex targets.[2] Thus, merging aminocatalysis with electrochemistry presents a highly attractive strategy that could unlock novel enantioselective reactivities in a more sustainable manner.[3] However, electrochemical aminocatalysis has been demonstrated feasible only *via* asymmetric enamine-mediated pathways, which can be categorized into two main strategies (Scheme 1a). The first involves the *in situ* electrochemical generation of electrophilic partners, which subsequently react with enamines,[4] while the second is based on the single-electron oxidation of the enamine intermediate, leading to the formation of a radical cation.[5] A major limitation of such transformations stems from the oxidative degradation of chiral organocatalysts or their intermediates under electrochemical conditions. To address this, Mazzarella and Dell'Amico recently employed redox shuttles for a milder, indirect single-electron transfer (SET) oxidation of the enamine intermediate, thereby protecting the catalyst from oxidative damage.[5c] In another approach, the Hao Xu group designed a bifunctional, diarylprolinol-based chiral electrocatalyst, which acts both as a

redox mediator for substrate electrooxidation and a promoter for asymmetric induction through the enamine formation.[4f]

Despite these advances, electrochemical aminocatalysis involving the formation of an iminium ion remains underexplored to the best of our knowledge. Inspired by the concept of constructing cyclopropane rings electrochemically,[6] particularly *via* halogen-mediated reactions,[6c–i] we sought to develop an asymmetric cyclopropanation under electrochemical conditions to demonstrate the proof-of-principle that electrochemistry is compatible with iminium ion organocatalysis. Considering our group's expertise in Michael-initiated ring closure (MIRC) reactions[7] and electrochemical transformations,[8] we selected an established protocol for asymmetric cyclopropanation *via* iminium ion catalysis that previously utilized a cascade process
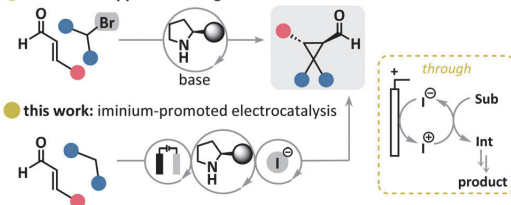

Scheme 1 (a) Asymmetric organocatalytic electrochemical strategies. (b) Asymmetric cyclopropanation *via* MIRC.

Department of Chemistry and Biotechnology, Tallinn University of Technology, Akadeemia tee 15, Tallinn 12618, Estonia. E-mail: maksim.oseka@taltech.ee

† Electronic supplementary information (ESI) available. See DOI: https://doi.org/10.1039/d4cc05092d

‡ These authors contributed equally.

involving α,β-unsaturated aldehydes and halogenated Michael donors as a benchmark reaction (Scheme 1b).[9] Importantly, streamlining this protocol to employ simple malonates, while performing the ring-closure cascade using electrocatalytically generated electrophilic halogen species, would improve atom economy for the overall process by eliminating the additional step for the synthesis of halogenated Michael donors that involves stoichiometric amounts of electrophilic halogen sources.

We initiated our investigation using cinnamic aldehyde **1a** and dimethyl malonate **2a** as model substrates, with organocatalyst **I** (20 mol%) in a simple undivided cell setup, featuring a graphite (G) anode and a stainless-steel (SS) cathode, under galvanostatic conditions (Table 1). Following the work of the Nikishin group,[10] preliminary experiments were conducted in ethanol with catalytic amounts of tetraethylammonium iodide as a halogen source and acid additives (see Table S1 in ESI†). The reproducibility of the reaction improved significantly when ethanol was replaced by dichloromethane as the solvent, with hexafluoroisopropanol (HFIP) and water as additives, and tetra-butylammonium perchlorate as the electrolyte. HFIP serves as a protons source for the cathodic reaction and was found to stabilize iminium ions,[11] while water most likely plays a role in the formation and hydrolysis of the iminium ion. The optimal reaction time for our transformation was determined to be 5 hours (Table 1, entry 1). Upon completion of the reaction, we observed the intermediate **4a** (up to 32%) in some instances, which results from the nucleophilic addition of malonate **2a** to the iminium

ion, along with the byproduct **5a** (7–24% yield). The formation of **5a** has previously been reported in the aminocatalyzed synthesis of **3a**, arising from a base-induced retro-Michael reaction of the cyclopropane adduct.[9b] Prolonging the reaction time to 16 hours led to further conversion of the product **3a** into **5a** (Table 1, entry 2). Lowering the amount of tetraethylammonium iodide or substituting it with other halogen sources reduced the yield (entries 3–6). To address the partial catalyst decomposition caused by oxidation,[5c,12] we explored the use of presumably more stable aminocatalysts **II–VI**.[13] Unfortunately, none of these catalysts improved the yield of the desired product and all showed some degree of decomposition, as confirmed by GC-MS and NMR analyses of the crude reaction mixtures (Table 1, entry 7). Substituting the cathode material with graphite or platinum significantly suppressed cyclopropane **3a** formation (Table 1, entry 8), and using acetonitrile as the solvent also lowered the yield (entry 9). Without a halogen source, the reaction yielded only the Michael adduct **4a** with excellent enantioselectivity (96% ee, Table 1, entry 10), while no reaction occurred in the absence of the organocatalyst (entry 11). Lastly, a control experiment confirmed that electricity is essential for cyclopropane ring formation (entry 12).

With the optimal conditions established, we investigated the substrate scope for the cascade electro-organocatalytic cyclopropanation (Scheme 2). Aromatic α,β-unsaturated aldehydes (**1**) reacted efficiently with malonate (**2a**) under the optimized conditions, yielding the corresponding cyclopropanes (**3a–j**) with excellent stereoselectivity (94–98% ee and >20:1 d.r. in all cases). Notably, cyclopropanes **3b–3g**, containing electron-deficient substituents in the aromatic ring, were isolated in moderate to good yields. Potentially sensitive to electrochemical conditions nitro- or methoxy- groups were tolerated in the reaction (**3f**, **3g**, **3i**). However, in the case of 4-methoxycinnamaldehyde, rapid formation of the byproduct **5i** was observed at room temperature (Scheme 4a). To suppress the side product formation, the reaction was performed at 0 °C, which improved the yield of cyclopropane **3i**, with 24 hours identified as the optimal reaction time. Similarly, cyclopropane **3j**, bearing an electron-donating alkyl group, was obtained at a lower temperature. We then explored different nucleophilic reaction partners. Dibenzyl malonate reacted smoothly, yielding product **3k** with results comparable to those obtained with dimethyl malonate. When 1,3-ketoester was used as the nucleophile, cyclopropane **3l** was obtained in only 1.5 hours, though with moderate yield and diastereoselectivity. Furthermore, we were pleased to obtain biologically relevant spirooxindoles **3m** and **3n** with good diastereoselectivity.[14]

Based on our observations and previous studies, we propose a plausible mechanism, as depicted in Scheme 3. First, in the organocatalytic cycle, condensation of the chiral aminocatalyst **I** with cinnamic aldehyde **1a** occurs forming an iminium ion (**i**). Upon Michael addition of malonate **2a** to the iminium ion (**i**), an enamine (**ii**) is generated, which may hydrolyze to intermediate **4a**. Electrooxidation of iodide occurs at the anode, forming electrophilic iodine species, which are captured by the enamine (**ii**).[15] The iodinated iminium ion (**iii**) then undergoes intramolecular alkylation, releasing iodide anion back into the electrocatalytic cycle and forming an iminium ion (**iv**).

**Table 1** Reaction condition optimization

#	Deviation from reaction conditions	Yield,[a] %			ee 3a,[b] %
		3a[c]	4a	5a	
1	None	59	—	12	96
2	1.0 mA, 16 h	48	—	24	96
3	nBu₄NI instead of Et₄NI	47	4	7	97
4	I₂ instead of Et₄NI	29	—	—	94
5	nBu₄NBr instead of Et₄NI	6	21	—	nd
6	0.1 equiv. of Et₄NI	39	14	7	98
7	II–VI as organocatalyst	38–46	—	Traces	70–92
8	Pt or G as cathode	9	29–32	—	nd
9	CH₃CN instead of CH₂Cl₂	30	9	—	94
10	No halogen source	—	33	—	
11	No organocatalyst	—	—	—	
12	No electricity	—	49	—	

[a] Yields were determined by ¹H NMR analysis of the crude reaction mixture using trimethoxybenzene as an internal standard. [b] Enantiomeric excess of **3a** was determined by chiral HPLC analysis. [c] Diastereomeric ratio of **3a** was determined by ¹H NMR analysis of the crude reaction mixture and was for all entries >20:1. n.d.: not determined.
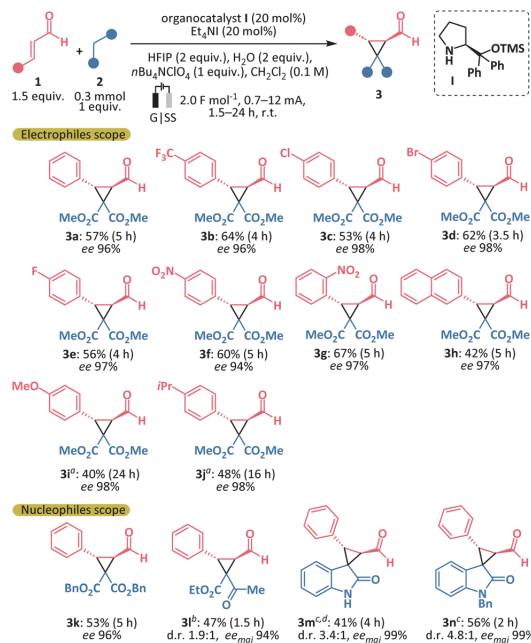
Scheme 2 Substrate scope of the electro-organocatalytic cyclopropa-nation. Yields and enantiomeric excess refer to isolated products. [a] The reaction was performed at 0 °C. [b] Yield and d.r. were determined by ^1H NMR analysis of the crude reaction mixture using trimethoxybenzene as an internal standard. The yield of the isolated major diastereomer is 30%. [c] Yields, d.r. and ee of products **3m** and **3n** correspond to the isolated products after *in situ* reduction to the corresponding alcohols with sodium borohydride. [d] The reaction was performed at −10 °C.
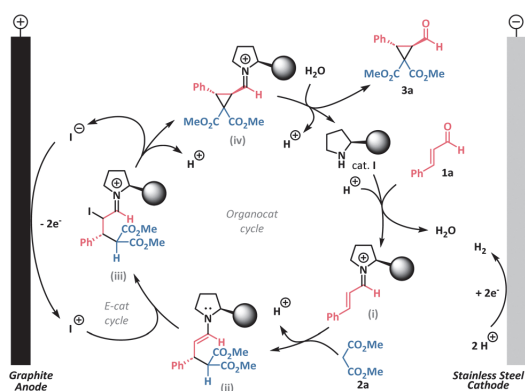

Scheme 3 Proposed mechanism.

Subsequent hydrolysis of the iminium ion (**iv**) yields the desired product **3a** and regenerates the organocatalyst **I**. Under certain conditions, the intermediate (**iv**) can undergo a retro-Michael reaction, leading to the formation of the byproduct **5a**.

Meanwhile, the evolution of hydrogen occurs at the cathode as the counter half-reaction. Thus, the reaction mechanism involves two catalytic cycles, and balancing their rates is crucial for efficient product formation. The electrochemical cycle is controlled by current density, while the organocatalytic cycle can be influenced by temperature (see kinetic studies in Fig. S4 in ESI†).

To better understand the reaction mechanism, we first measured the oxidation potentials of the main reaction components using cyclic voltammetry (Scheme 4b). Iodide exhibits two distinct oxidation peaks at potentials of +0.19 V and +0.38 V, with the first oxidation occurring at the lowest potential in the system. However, the enamine (**II**), formed from the intermediate **4a** and organocatalyst **I**, shows an oxidation peak at +0.27 V, which is lower than iodine's second oxidation peak, suggesting that it may undergo SET oxidation under the reaction conditions. The other reaction components have higher oxidation potentials than iodide and are unlikely to undergo anodic oxidation. Nevertheless, decomposition of the free catalyst through reaction with electrophilic iodine species *via* Grob-type fragmentation is also possible.[6d,11a]

We then conducted several control experiments. In the reaction with stoichiometric amounts of molecular iodine or N-iodosuccinimide under the standard conditions, but without applying electricity, no conversion of the starting materials was detected, and organocatalyst **I** began to decompose. This suggests that controlled electrocatalytic generation of electrophilic iodine likely protects the catalyst from Grob-type fragmenta-tion. Next, we attempted to form the cyclopropane ring under our electrochemical conditions using the pre-synthesized inter-mediate **4a**.[16] After the addition of 2.0 F mol^{-1} over 5 hours,
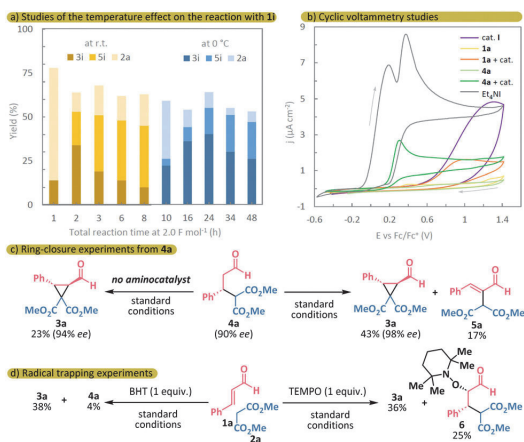
Scheme 4 (a) Temperature effect studies. Separate reactions with 2.0 F mol^{-1}. (b) Cyclic voltammetry measurements. Voltammograms recorded in 0.1 M nBu$_4$NPF$_6$ CH$_3$CN solution with Ag/Ag$^+$ reference electrode and realigned with respect to Fc/Fc$^+$ couple. Arrows indicate the direction of the potential scan. (c) Electrochemical ring closure of pre-synthesized intermediate **4a**. (d) Experiments with TEMPO and BHT as presumed radical scavengers.

43% of the desired product **3a** was formed, along with 17% of the byproduct **5a** (Scheme 4c). Interestingly, after 1 hour of reaction, the intermediate **4a** partially fragmented back to cinnamic aldehyde **1a** and dimethyl malonate **2a** (40% NMR yield). This demonstrates the reversibility of the Michael addition step and highlights the complex kinetics of the overall process (see Fig. S5 in ESI†). In the absence of the organocatalyst, the product **3a** was formed less efficiently, with a yield of 23%, and no formation of **1a** or **2a** was observed.

To determine whether the reaction mechanism has a polar or radical nature, we conducted control experiments with radical scavengers (Scheme 4d). The reaction with 2,2,6,6-tetramethyl-piperidine-1-oxyl (TEMPO) under our electrochemical conditions resulted in only minor suppression of the product **3a** formation (36% NMR yield), and a TEMPO-adduct **6** was observed (25% NMR yield) (see Scheme S2 in ESI† for the alternative radical pathway).[61] However, electrochemical experiments using TEMPO as a radical trap can produce ambiguous results, as TEMPO can be oxidized to its N-oxoammonium salt under electrochemical conditions and react with the enamine (**ii**) in a polar manner.[17] We then switched to dibutylhydroxytoluene (BHT) as a more reliable radical scavenger in electrochemistry and still observed the formation of cyclopropane **3a** (38% NMR yield), with only 4% of **4a** detected in the crude NMR, indicating that no quenching of the potential enamine radical cation occurred. These results, combined with the earlier experiment demonstrating ring closure in the absence of the aminocatalyst directly from the intermediate **4a**, suggest a predominantly polar mechanistic pathway in the electrochemical catalytic cycle.

In conclusion, we demonstrated the successful integration of electrochemistry with iminium ion organocatalysis to achieve highly enantioselective cyclopropanation. This streamlined process enhances atom economy by eliminating the need for pre-synthesized halogenated Michael donors. Mechanistic studies, supported by cyclic voltammetry and control experiments, suggest a predominantly polar pathway in the electrochemical catalytic cycle, driven by anodic iodide oxidation.

Data availability

The data supporting this article are included as part of the ESI.†

Conflicts of interest

There are no conflicts to declare.

Notes and references

1 Selected reviews on asymmetric organocatalysis with metal- and photocatalysis, see: (a) D.-F. Chen, Z.-Y. Han, X.-L. Zhou and L.-Z. Gong, *Acc. Chem. Res.*, 2014, **47**, 2365–2377; (b) Q. Zhou, *Angew. Chem., Int. Ed.*, 2016, **55**, 5352–5353; (c) M. Silvi and P. Melchiorre, *Nature*, 2018, **554**, 41–49; (d) D. A. Nagib, *Chem. Rev.*, 2022, **122**, 15989–15992; (e) T. Bortolato, S. Cuadros, G. Simionato and L. Dell'Amico, *Chem. Commun.*, 2022, **58**, 1263–1283.

2 (a) Y. Wang, S. Dana, H. Long, Y. Xu, Y. Li, N. Kaplaneris and L. Ackermann, *Chem. Rev.*, 2023, **123**, 11269–11335; (b) L. F. T. Novaes, J. S. K. Ho, K. Mao, E. Villemure, J. A. Terrett and S. Lin, *J. Am. Chem. Soc.*, 2024, **146**, 22982–22992; (c) B. P. Smith, N. J. Truax, A. S. Pollatos, M. Meanwell, P. Bedekar, A. F. Garrido-Castro and P. S. Baran, *Angew. Chem., Int. Ed.*, 2024, **63**, e202401107.

3 For recent reviews on asymmetric electrochemistry, see: (a) K. A. Ogawa and A. J. Boydston, *Chem. Lett.*, 2015, **44**, 10–16; (b) C. Margarita and H. Lundberg, *Catalysts*, 2020, **10**, 982; (c) J. Rein, S. B. Zacate, K. Mao and S. Lin, *Chem. Soc. Rev.*, 2023, **52**, 8106–8125; (d) D. Mazzarella, *J. Flow Chem.*, 2024, **14**, 357–366.

4 (a) K. L. Jensen, P. T. Franke, L. T. Nielsen, K. Daasbjerg and K. A. Jørgensen, *Angew. Chem., Int. Ed.*, 2010, **49**, 129–133; (b) N. Fu, L. Li, Q. Yang and S. Luo, *Org. Lett.*, 2017, **19**, 2122–2125; (c) L. Li, Y. Li, N. Fu, L. Zhang and S. Luo, *Angew. Chem., Int. Ed.*, 2020, **59**, 14347–14351; (d) F.-Y. Lu, Y.-J. Chen, Y. Chen, X. Ding, Z. Guan and Y.-H. He, *Chem. Commun.*, 2020, **56**, 623–626; (e) Z.-H. Wang, P.-S. Gao, X. Wang, J.-Q. Gao, X.-T. Xu, Z. He, C. Ma and T.-S. Mei, *J. Am. Chem. Soc.*, 2021, **143**, 15599–15605; (f) J.-Y. He, C. Zhu, W.-X. Duan, L.-X. Kong, N.-N. Wang, Y.-Z. Wang, Z.-Y. Fan, X.-Y. Qiao and H. Xu, *Angew. Chem., Int. Ed.*, 2024, e202401355.

5 (a) X. Ho, S. Mho, H. Kang and H. Jang, *Eur. J. Org. Chem.*, 2010, 4436–444s1; (b) N. Bui, X. Ho, S. Mho and H. Jang, *Eur. J. Org. Chem.*, 2009, 5309–5312; (c) D. Mazzarella, C. Qi, M. Vanzella, A. Sartorel, G. Pelosi and L. Dell'Amico, *Angew. Chem., Int. Ed.*, 2024, **63**, e202401361.

6 (a) X. Han, N. Zhang, Q. Li, Y. Zhang and S. Das, *Chem. Sci.*, 2024, **15**, 13576–13604; (b) L.-H. Jie and H.-C. Xu, *J. Electrochem.*, 2024, **30**, 2313001For the reviews and examples of halogen-mediated transformations, see: (c) B. V. Lyalin and V. A. Petrosyan, *Russ. J. Electrochem.*, 2013, **49**, 497–529; (d) C. Luo, Z. Wang and Y. Huang, *Nat. Commun.*, 2015, **6**, 10041; (e) M. N. Elinson, E. O. Dorofeeva, A. N. Vereshchagin and G. I. Nikishin, *Russ. Chem. Rev.*, 2015, **84**, 485–497; (f) K. Liu, C. Song and A. Lei, *Org. Biomol. Chem.*, 2018, **16**, 2375–2387; (g) H.-T. Tang, J.-S. Jia and Y.-M. Pan, *Org. Biomol. Chem.*, 2020, **18**, 5315–5333; (h) Z. Wang, M. Gausmann, J.-H. Dickoff and M. Christmann, *Green Chem.*, 2024, **26**, 2546–2551; (i) P. Zhou, W. Li, J. Lan and T. Zhu, *Nat. Commun.*, 2022, **13**, 3827.

7 (a) A. Noole, M. Ošeka, T. Pehk, M. Öeren, I. Järving, M. R. J. Elsegood, A. V. Malkov, M. Lopp and T. Kanger, *Adv. Synth. Catal.*, 2013, **355**, 829–835; (b) M. Ošeka, A. Noole, S. Žari, M. Öeren, I. Järving, M. Lopp and T. Kanger, *Eur. J. Org. Chem.*, 2014, 3599–3606.

8 (a) M. Ošeka, G. Laudadio, N. P. Van Leest, M. Dyga, A. D. A. Bartolomeu, L. J. Gooßen, B. De Bruin, K. T. De Oliveira and T. Noël, *Chem*, 2021, **7**, 255–266; (b) A. Kooli, L. Wesenberg, M. Beslać, A. Krech, M. Lopp, T. Noël and M. Ošeka, *Eur. J. Org. Chem.*, 2022, e202200011; (c) M. Laktsevich-Iskryk, A. Krech, M. Fokin, M. Kimm, T. Jarg, T. Noël and M. Ošeka, *J. Flow Chem.*, 2024, **14**, 139–147.

9 Previous reports on the reaction: (a) R. Rios, H. Sundén, J. Vesely, G. Zhao, P. Dziedzic and A. Córdova, *Adv. Synth. Catal.*, 2007, **349**, 1028–1032; (b) H. Xie, L. Li, H. Li, J. Wang and W. Wang, *J. Am. Chem. Soc.*, 2007, **129**, 10886–10894; (c) I. Ibrahem, G. Zhao, R. Rios, J. Vesely, H. Sundén, P. Dziedzic and A. Córdova, *Chem. Eur. J.*, 2008, **14**, 7867–7879; (d) P. Llanes, C. Rodríguez-Escrich, S. Sayalero and M. A. Pericàs, *Org. Lett.*, 2016, **18**, 6292–6295; (e) A. Kunzendorf, G. Xu, M. Saifuddin, T. Saravanan and G. J. Poelarends, *Angew. Chem., Int. Ed.*, 2021, **60**, 24059–24063.

10 M. N. Elinson, S. K. Feducovich, A. N. Vereshchagin, S. V. Gorbunov, P. A. Belyakov and G. I. Nikishin, *Tetrahedron Lett.*, 2006, **47**, 9129–9133.

11 (a) G. Hutchinson, C. Alamillo-Ferrer and J. Burés, *J. Am. Chem. Soc.*, 2021, **143**, 6805–6809; (b) N. Zeidan, S. Bicic, R. J. Mayer, D. Lebœuf and J. Moran, *Chem. Sci.*, 2022, **13**, 8436–8443.

12 M. Silvi, C. Verrier, Y. P. Rey, L. Buzzetti and P. Melchiorre, *Nat. Chem.*, 2017, **9**, 868–873.

13 (a) M. H. Haindl, M. B. Schmid, K. Zeitler and R. M. Gschwind, *RSC Adv.*, 2012, **2**, 5941; (b) X. Companyó and J. Burés, *J. Am. Chem. Soc.*, 2017, **139**, 8432–8435.

14 L.-M. Zhou, R.-Y. Qu and G.-F. Yang, *Expert Opin. Drug Discovery*, 2020, **15**, 603–625.

15 T. Kano, M. Ueda and K. Maruoka, *J. Am. Chem. Soc.*, 2008, **130**, 3728–3729.

16 S. Brandau, A. Landa, J. Franzén, M. Marigo and K. A. Jørgensen, *Angew. Chem., Int. Ed.*, 2006, **45**, 4305–4309.

17 M. Schämann and H. J. Schäfer, *Electrochim. Acta*, 2005, **50**, 4956–4972.

Appendix 2

RESEARCH ARTICLE

doi.org/10.1002/adsc.202300939

Advanced
Synthesis &
Catalysis

Check for updates

Ring-Opening Coupling Reaction of Cyclopropanols with Electrophilic Alkenes Enabled by Decatungstate as Photoredox Catalyst

Anastasiya Krech,[a] Viktoryia Yakimchyk,[a] Tatsiana Jarg,[a] Dzmitry Kananovich,[a,*] and Maksim Ošeka[a,*]

[a] Department of Chemistry and Biotechnology, Tallinn University of Technology, Akadeemia tee 15, 12618 Tallinn, Estonia
E-mail: dzmitry.kananovich@taltech.ee; maksim.oseka@taltech.ee

Supporting information for this article is available on the WWW under https://doi.org/10.1002/adsc.202300939

Abstract: We introduce a methodology for the photocatalytic generation of β-ketoalkyl radicals from tertiary cyclopropanols, utilizing tetrabutylammonium decatungstate (TBADT) as a photoredox catalyst. The application is demonstrated by the synthesis of distantly functionalized ketones via the redox-neutral addition of the cyclopropanol-derived β-ketoalkyl radicals to the double bond of electrophilic olefins. The transformation occurs under ambient temperature conditions and is suitable for coupling a wide range of cyclopropanol and alkene substrates. This was demonstrated by the preparation of 33 ketone products with 35–92% yield. The method's preparative robustness has been validated through upscaled preparations conducted under continuous flow conditions. Mechanistic investigations support the role of TBADT as a photoredox catalyst, which facilitates the single electron oxidation of cyclopropanols, followed by the electron transfer from the reduced form of decatungstate to the electrophilic double bond of alkene. Moreover, we found that electron-rich aromatic cyclopropanols and electron-deficient olefins form photoactive electron donor-acceptor (EDA) complexes. This property allows the reaction to proceed under UV light irradiation via the photoinduced charge transfer in the absence of the photocatalyst.
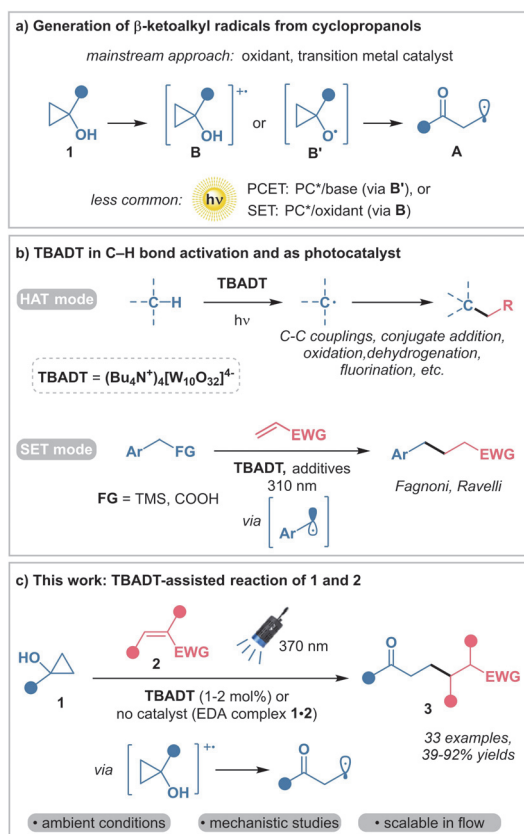
Keywords: photochemistry; single electron transfer; cyclopropanols; TBADT; flow chemistry; electron donor-acceptor complex

Introduction

Cyclopropanols have emerged as useful building blocks in organic synthesis due to their facile preparation and distinct reactivity driven by ring-strain release.[1–3] Specifically, cyclopropanols can serve as a source of β-ketoalkyl radicals, which have been employed for assembling new carbon-carbon bonds, such as in radical addition to alkenes. The generation of β-ketoalkyl radicals **A** from cyclopropanols **1** may proceed through the β-fragmentation of two distinct transient species: radical cation **B** and alkoxy radical **B'** (Scheme 1, a). The direct single electron oxidation of cyclopropanol **1** leads to the formation of radical cation **B**, whereas cyclopropoxy radical **B'** is produced upon the homolytic cleavage of the O–H bond. The latter process is challenging due to the relatively strong O–H bond (typical BDE values 103–105 kcal mol^{-1}).[4]

The traditional methods for the generation of radicals **A** with the subsequent addition to double bonds of olefins require strong oxidative conditions provided by stoichiometric oxidants[5] and/or transition metal derivatives (Ag(I),[6–8] Fe(III),[9–11] Mn(III)[12–14]) and elevated temperatures.[5,6,10,11,14]

Currently, photoredox catalysis offers a number of bypassing strategies that allow the generation of ketoalkyl radicals from cyclopropanols[15,16] and even unstrained cycloalkanols under mild conditions.[17] This process can readily occur through proton-coupled electron transfer (PCET),[17–24] photoinduced ligand-to-metal charge transfer,[25–29] or by photocatalytic single electron transfer (SET) oxidation, which typically requires stoichiometric oxidants.[15,30,31] There are some reported examples of photocatalytic ring-opening coupling reactions of cyclopropanols with electrophilic alkenes. The group of Yamamoto used PCET strategy

Scheme 1. a) Generation of β-ketoalkyl radicals from cyclopropanols. b) Previous applications of TBADT photocatalysis. c) Outline of this work.

easily abstract H-atoms (hydrogen atom transfer, HAT) from C–H bonds with bond dissociation energies of up to 100 kcal mol⁻¹ upon photoexcitation with UV light (310–400 nm).[38] This keynote property has resulted in the emergence of several facile C–H activation methodologies, such as the works of Fagnoni,[39–44] MacMillan,[45,46] Noël,[39,40,47] and Melchiorre groups,[48] to name a few. On the contrary, even though the decatungstate anion is a strong one-electron oxidant in its photoexcited state ($E_{1/2}$ *$[W_{10}O_{32}]^{4-}$/$[W_{10}O_{32}]^{5-}$ = + 2.4 V vs SCE), the applications of decatungstate as a photoredox catalyst remain largely underdeveloped.[37] To the best of our knowledge, such transformations have been limited to SET oxidation of aromatic hydrocarbons[49] and to a few synthetic applications reported by Fagnoni and Ravelli, who developed benzylation of electrophilic alkenes via TBADT-photocatalyzed generation of resonance-stabilized benzylic radicals by oxidation of benzylsilanes and arylacetic acids.[50,51] In view of our expertise in the cyclopropanol chemistry,[18,52–54] we envisioned that SET oxidation of tertiary cyclopropanols **1** by the photoexcited decatungstate should be a feasible process (E_p of cyclopropanols = + 1.06−+1.54 V vs SCE)[30] and therefore suitable for generation of β-ketoalkyl radicals **A**. Similarly to the previous works,[50,51] we expected that the produced radicals **A** could be readily intercepted by electron-deficient alkenes **2** to furnish a new C–C bond in the respective adducts **3**.

Here, we present a photocatalytic methodology that enables redox-neutral addition of cyclopropanol-derived β-ketoalkyl radicals **A** to electrophilic olefins (Scheme 1, c). The methodology utilizes TBADT as a photoredox catalyst, features a broad substrate scope of synthesized ketone products **3** (33 examples), and operates under ambient temperature conditions. Notably, no competitive HAT processes have been observed and sensitive C–H bonds remained intact. Mechanistic studies have validated the role of photoexcited decatungstate as a SET oxidant. Moreover, we have revealed the existence of photoactive electron donor-acceptor (EDA) complexes between some electron-rich aromatic cyclopropanols **1** and electron-deficient alkenes **2**. The EDA complexes can produce the corresponding adducts **3** upon photoexcitation without the assistance of the photoredox catalyst.

Results and Discussion

Optimization studies were performed on the model cross-coupling reaction of *p*-methoxyphenyl cyclopropanol **1a** with electrophilic benzylidene malononitrile **2a** under ultraviolet light (370 nm) irradiation (Table 1; see also Table S1 in the Supporting Information for additional data). The experiments were carried out in a 3D printed reactor designed by the Noël group[55] and equipped with a Kessil lamp (43 W at 100% light

for the intramolecular reaction of cyclopropanols and electron-deficient alkenes leading to the ring expansion.[22] Hu and co-workers developed chlorine radical-induced reaction of alcohols, including cyclopropanols, and alkenes catalyzed by iron salts under blue LED irradiation.[32] The Melchiorre group reported enantioselective photochemical cascade reaction of cyclopropanols and α,β-unsaturated aldehydes, which combined the excited-state and ground-state reactivity of chiral organocatalytic intermediates.[33] However, the photocatalytic approaches are still limited in number and necessitate further development, especially towards employing accessible photocatalysts and expanding the diversity of transformations.
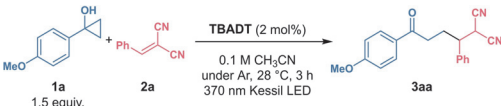
In this regard, tetrabutylammonium decatungstate (TBADT) represents a versatile and inexpensive photocatalyst that has been extensively studied over the past decade (Scheme 1, b).[34–37] The mainstream use of the decatungstate photocatalysis relies on its property to

Table 1. Optimization of the reaction conditions.[a]

Entry	Deviations	Yield, %[b]
1	none	84
2	CH$_2$Cl$_2$ as solvent, 1 mol% TBADT, 1 h	90
3	CH$_3$CN/H$_2$O 10:1 as solvent, 1 h	88
4	no light	n.r.[c]
5	without photocatalyst	25
6	10 mol% benzophenone instead of TBADT	44

[a] Reaction conditions: alkene **2a** (0.2 mmol), cyclopropanol **1a** (1.5 equiv.), TBADT (2 mol%), CH$_3$CN (0.1 M), 43 W 370 nm Kessil LED, under Ar, 28 °C, 3 h.

[b] Yields were determined by ^{1}H NMR analysis of the crude reaction mixture against triphenylmethane as an internal standard.

[c] n.r. = no reaction.

intensity). Previously reported conditions[44,49] (2 mol% TBADT in acetonitrile solution) were employed in the initial experiment (entry 1) which delivered ketone **3aa** in 84% yield after 3 h of irradiation. However, slightly improved 88–90% yields and shorter reaction time (1 h) were achieved at lower catalyst loading (1 mol%) when acetonitrile was replaced with dichloromethane or acetonitrile/water mixture (entry 2 and 3). Interestingly, the efficacy of the reaction was enhanced by dichloromethane, despite the suboptimal solubility of TBADT in this solvent. To confirm the photochemical nature of the process, a control experiment without light was carried out and no reaction occurred (entry 4). Moreover, the reaction was sensitive to the light intensity, as the conversion decreased when the lamp was used at lower power output (see Table S1 in the Supporting Information). Surprisingly, **3aa** was obtained in 25% yield even in the absence of the photocatalyst (entry 5) indicating a plausible slower reaction via an EDA complex of **1a** and **2a** (see discussion below). However, TBADT was crucial to facilitate the reaction efficiently. Benzophenone (10 mol%) as an alternative photocatalyst afforded **3aa** in only 44% yield (entry 6).[56]

With the optimal reaction conditions established (CH$_2$Cl$_2$ as a solvent, 1 mol% TBADT), we explored the scope of different cyclopropanols in their photo-catalytic reactions with benzylidene malononitrile **2a** (Scheme 2, a). Cyclopropanols with electron-rich aromatic substituents afforded β-functionalized ketones in 56–87% yields (compounds **3aa**–**3ia**). Among them, cyclopropanols **1b** and **1c** with MeO-substituents in *meta*- and *ortho*-positions gave the respective products **3ba** and **3ca** in lower 61% and 56% yields

compared to *para*-methoxyphenyl cyclopropanol (**3aa**, 87% yield), which could be caused by steric factors or somewhat different electronic properties. For the reactions yielding *m*-MeO-substituted **3ba** and 2-naphthyl derivative **3da**, acetonitrile/water mixture was more beneficial reaction media compared to CH$_2$Cl$_2$, in which lower yields were obtained (e.g., 71% vs 59% for **3da**). Notably, pyrrolyl and thiophen-yl substituents tolerated the reaction conditions and the corresponding products **3ha** and **3ia** were obtained in 57% and 88% yields, respectively. The reaction with cyclopropanol **1j**, bearing an electron-withdrawing *p*-trifluoromethyl group, afforded the product **3ja** in moderate 54% yield. However, less electron-deficient *p*-chlorophenyl cyclopropanol **1k** produced the corresponding adduct **3ka** in excellent 92% yield. By contrast to aryl-substituted cyclopropanols **1a**–**k**, alkyl and alkenyl cyclopropanols **1l**–**p** and were less reactive and afforded the respective products **3la**–**3pa** in low to moderate yields (40–61%) after significantly longer reaction time (20–48 h; Scheme 2, b). Noteworthy, some of the products derived from alkyl cyclopropanols with benzylidene malononitrile (**3la**, **3ma**, **3qa**) were isolated along with minor (ca. 10% yield) by-products. Based on the literature precedents and the comparison of NMR spectra,[57,58] we concluded that the by-products are cyclopentanol derivatives resulted from a reversible intramolecular aldol cyclization. In the reactions of alkenyl cyclopropanols, **3na** was produced from 1-cyclohexenyl cyclopropanol **1n** in low 41% yield. Styryl cyclopropanol **1o** behaved similarly resulting in the formation of **3oa** in 42% yield as an 8:1 mixture of *E/Z* isomers. *N*-Boc-protected cyclopropanol **1p** was a competent substrate that produced **3pa** in 40% yield, while its *N*-benzyl analogue **1r** was incompatible and resulted in a complex mixture in which no respective coupling product was detected. Additionally, we found that oxidants such as *N*-fluorobenzenesulfonimide (NFSI) or potassium persulfate as substoichiometric additives (0.2–0.5 equiv.) can improve yields, accelerate, or even trigger the reaction of otherwise unreactive cyclo-propanols. For instance, compound **3la** was obtained in 63% yield after 3 h with NFSI additive (0.5 equiv.) while the standard conditions delivered only 53% yield after 20 h. Similarly, *n*-amylcyclopropanol **1q** was converted into the corresponding ketone product **3qa**. Besides highly electrophilic alkene **2a**, 2-phenylethyl cyclopropanol **1l** was also able to react with dimethyl fumarate **2f** and diethyl benzylidenemalonate **2k**, affording the respective products **3lf** and **3lk** in 58% and 40% yields, while only traces of the products were formed without NFSI additive.
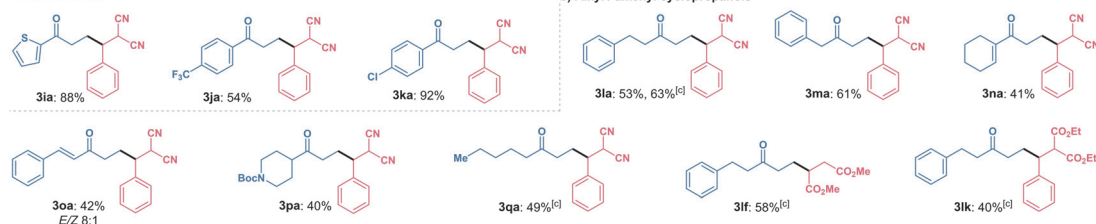
Next, we turned our attention to outline the scope of the amenable alkene substrates (Scheme 2, c). Various benzylidene malononitriles with electron-donating and -withdrawing substituents in the phenyl
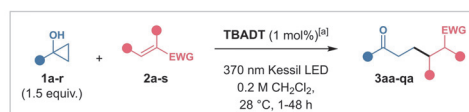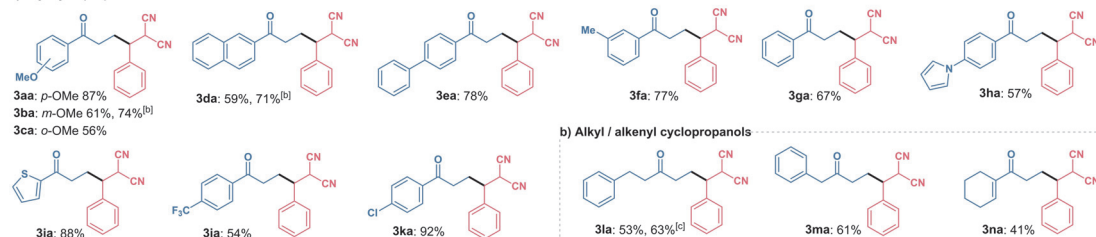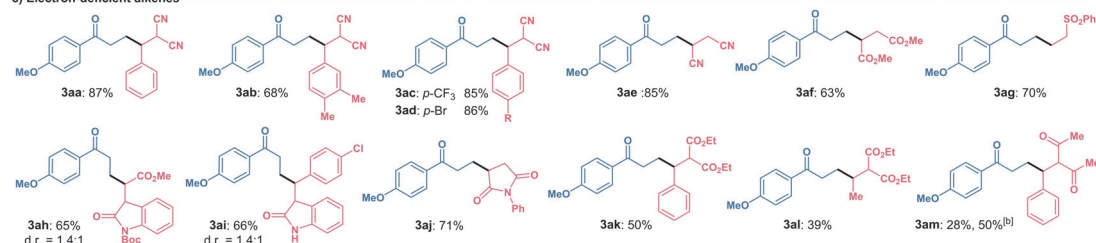
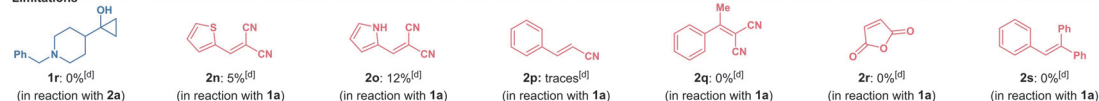**Scheme 2.** Scope of the TBADT-photocatalyzed reaction of cyclopropanols with electron-deficient alkenes. [a] General procedure A: alkene **2** (0.2 mmol), cyclopropanol **1** (1.5 equiv.), TBADT (1 mol%), CH$_2$Cl$_2$ (0.2 M), 43 W 370 nm Kessil LED, under argon, 28 °C, 1–48 h. Yields correspond to isolated products. [b] General procedure B: alkene **2** (0.2 mmol), cyclopropanol **1** (1.5 equiv.), TBADT (2 mol%), CH$_3$CN/H$_2$O (9:1, 0.2 M substrate **2 a**), 43 W 370 nm Kessil LED, under argon, 28 °C, 3–24 h. Yields correspond to isolated products. [c] General procedure C: alkene **2** (0.2 mmol), cyclopropanol **1** (3 equiv.), TBADT (1 mol%), NFSI (0.5 equiv.), CH$_2$Cl$_2$ (0.2 M), 43 W 370 nm Kessil LED, under argon, 28 °C, 3–24 h. Yields correspond to isolated products. [d] Yield determined by ^{1}H NMR analysis of the crude reaction mixture against triphenylmethane as an internal standard.

moiety provided the respective products in 68–86% yields (compounds **3 ab**, **3 ac** and **3 ad**). However, complex reaction mixtures and negligible (5–12%) yields of the respective adducts **3** were observed in the reactions with heteroarylidene malononitriles **2 n** and **2 o**, as well as with a substrate with a single nitrile group **2 p**. In addition, no product was found in the reaction of cyclopropanol **1 a** with methyl-substituted benzylidene malononitrile **2 q**, which was unreactive under the standard conditions and in the presence of NFSI, probably due to steric hindrance caused by the methyl group. Fumaronitrile **2 e**, dimethyl fumarate **2 f** and vinyl phenyl sulfone **2 g** were alkylated efficiently furnishing the respective products **3 ae-ag** in 63–85% yields. Notably, the products synthesized from alkylidene oxindoles were isolated in good yields (**3 ah** and **3 ai**, 65% and 66% yield, respectively). Compounds containing an oxindole moiety in their structure have demonstrated a wide range of biological activities.[59–61] Phenylmaleimide **2 j** was converted into the corresponding ketone **3 aj** in good 71% yield. However, similar maleic anhydride **2 r** was unreactive and only decomposition products of cyclopropanol **1 a** were observed. Malonate and 1,3-diketone derivatives underwent the desired transformation more sluggish than the rest of the substrates, nevertheless, compounds **3 ak**, **3 al** and **3 am** were isolated in acceptable 39–50% yields. The reaction with less electron-deficient triphe-

nylethylene **2s** failed to deliver the corresponding adduct. The evident influence of the electrophilic properties of the alkene indicated that it was not an insignificant bystander in the reaction, merely intercepting the cyclopropanol-derived β-ketoalkyl radical. Instead, it plays a crucial role in the reaction mechanism (see discussion below).

The batch reactions of cyclopropanols **1a** and **1l** with benzylidene malononitrile **2a** have been upscaled when translated into a continuous-flow process (Scheme 3, a). Flow chemistry is especially advantageous for performing photochemical transformations, since it ensures more efficient light irradiation, consistency of results, and scalability among other benefits.[62,63] Recently, TBADT recycling strategy by nanofiltration was developed by the group of Noël, allowing to use TBADT-photocatalyzed reactions at industrial scale.[64] After a brief optimization (see Tables S4 and S5 in the Supporting Information), we were able to prepare compounds **3aa** and **3la** in good 74–75% yields and gram amounts with 20–30 min of residence time. Owing to the limited solubility of TBADT in dichloromethane, acetonitrile was employed as a solvent under continuous-flow conditions.

To demonstrate the synthetic utility of the obtained products containing multiple activated sites with prominent and diverse reactivity, compound **3la** was converted into a variety of derivatives (Scheme 3, b). First, we engaged compound **3la** into an intramolecular aldol condensation reaction by treatment with trimethylsilyl triflate (TMSOTf) and triethylamine. The process afforded TMS-protected cyclopentanol **4a** in excellent 95% yield. Similarly, in the analogous reaction of **3aa**, TMS-protected cyclopentanol was obtained with 96% yield, indicating that such cyclizations can also be performed with other comparable products **3**. Besides the cyclization reaction, the rich chemistry of malononitrile and carbonyl moieties in **3la** also allowed its facile conversion into methyl ester **4b** (85% yield) by oxidation with molecular oxygen,[65] synthesis of amide **4c** in 65% yield by Cu-catalyzed hydrolysis of the nitrile group,[66] and featured alcohol **4d** by reduction with NaBH₄.

The investigation of the substrate scope revealed that the electrophilic properties of alkenes are crucial for the reaction. Moreover, benzylidene malononitrile **2a**, which is a quite strong electron acceptor and an one-electron oxidant,[67] could react with electron-rich aryl cyclopropanol **1a** even without the catalytic assistance of TBADT, though the reaction is slower (Table 1, entry 1 vs 5). This observation can be explained by the formation of a photoactive electron donor-acceptor complex between the substrates (a plausible reaction pathway is depicted in Scheme 5 below). EDA is a molecular aggregate in the ground state, formed by the association of an electron-rich substrate with an electron-accepting molecule.[68,69]
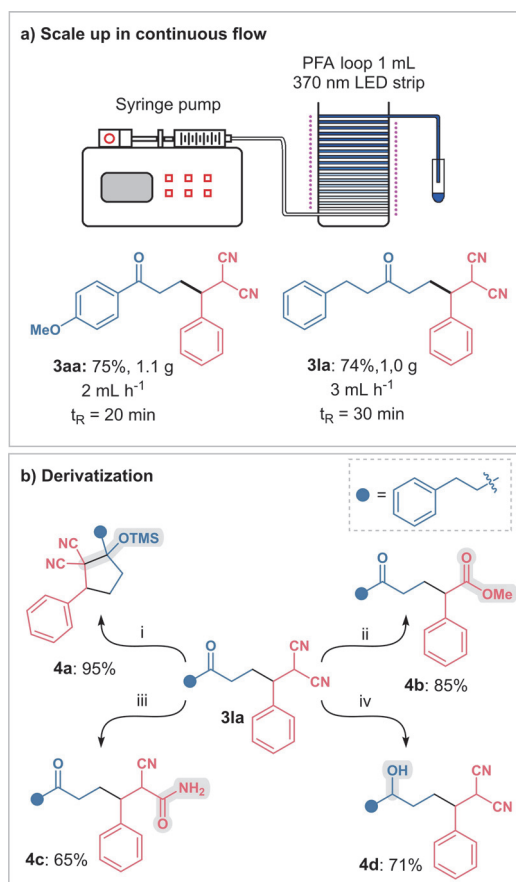
Scheme 3. a) Translation to continuous-flow conditions and scale up. Reaction conditions for **3aa**: alkene **2a** (4.5 mmol), cyclopropanol **1a** (1.2 equiv.), TBADT (2 mol%), CH₃CN (0.1 M), 370 nm LED strip, under Ar, r.t., $t_R = 20$ min, flow rate = 2 mL min⁻¹. Reaction conditions for **3la**: alkene **2a** (4.5 mmol), cyclopropanol **1l** (3 equiv.), TBADT (2 mol%), NFSI (0.5 equiv.), CH₃CN (0.1 M), 370 nm LED strip, under Ar, r.t., $t_R = 30$ min, flow rate = 3 mL min⁻¹. Yields correspond to isolated products. b) Derivatization of **3la**: i) TMSOTf, Et₃N, CH₂Cl₂; ii) O₂, MeOH, Cs₂CO₃, CH₃CN; iii) Cu(OAc)₂, AcOH; iv) NaBH₄, MeOH. Yields correspond to isolated products.

Light excitation results in an intramolecular single electron transfer event that occurs within the solvent cage, leading to the formation of the radical cation **B** and the radical anion **C**. The radical cation **B** undergoes fast cyclopropane ring opening into the β-ketoalkyl radical **A**, which in turn reacts with the **C** producing the coupling products **3**. In the reaction with benzylidene malononitrile **2a**, cyclopropanol **1a** produced **3aa** in 25% yield after 3 h of UV light irradiation in acetonitrile. A significantly higher yield

of 77% was achieved after 24 h of irradiation (see Scheme S1 in the Supporting Information). Phenyl cyclopropanol **1g**, possessing a less electron-donating aryl moiety, reacted with **2a** noticeably slower, resulting in only 13% yield of **3ga** after 3 h. Similarly, the reaction of **1a** with less electron-deficient dimethyl fumarate **2f** also occurred with the reduced rate, yielding **3af** in only 16% yield after 19 h. These results stay in line with intermediacy of EDA complexes in this reaction, which are stronger for more electron-deficient alkenes and for cyclopropanols with more electron-rich aryl moieties.

To confirm the formation of an EDA complex between **1a** and **2a**, a UV-Vis spectroscopic study has been conducted (Figure 1, a). As commonly observed for weakly associated EDA complexes, a UV absorption band for a mixture of **2a** and **1a** (blue line in Figure 1, a) experienced a bathochromic shift with respect to the individual substrate **1a** (gray line in Figure 1, a).[68] The excessive absorption in the range of ca. 370–400 nm can be more clearly visualized by subtracting the spectrum of **1a** from the spectrum of the mixture (yellow line). To obtain additional evidence for the complex formation and to evaluate the association constant, a ^{1}H NMR titration experiment was performed (Figure 1, b). Clear and gradual changes in the chemical shifts of the two diagnostic protons H_a and H_b of **2a** were observed, shifting towards the high-field region of the ^{1}H NMR spectrum upon the addition of **1a** (ranging from 1 to 95 equivalents). Fitting the experimental titration curve (see Figure S8 in the Supporting Information) yielded the value of the association constant $K_a = 0.16$ M^{-1}.[70] These results suggest that the EDA interaction is relatively weak, even between electron-rich cyclopropanol **1a** and highly electron-deficient olefin **2a**.

Next, several mechanistic experiments have been performed to provide an insight into the reaction mechanism (Scheme 4). First, we confirmed the role of β-ketoalkyl radical **A** as the key intermediate by performing the reaction in the presence of TEMPO (2,2,6,6-tetramethyl piperidine-*N*-oxyl) as a radical scavenger (Scheme 4, a). TEMPO interrupted the formation of **3aa** as the TEMPO-trapped adduct **5** was formed instead (83% ^{1}H NMR yield). In addition, the reaction with disubstituted cyclopropanol **1s** smoothly afforded **3sa** (75% yield, Scheme 4, b), indicating that the ring opening occurred exclusively at the most substituted C$_1$–C$_2$ bond of the cyclopropane ring and therefore proceeded via a more stable secondary alkyl radical.

Then, deuterium labelling experiments were performed to trace the origin of the δ-hydrogen in **3aa**. We found that deuterium was not transferred from solvent (acetonitrile-*d$_3$*) to the product by HAT (Scheme 4, c). However, the reaction of **2a** with deuterium-labeled cyclopropanol **1a-*d*** (87% D) in dry

a) **UV-Vis studies**
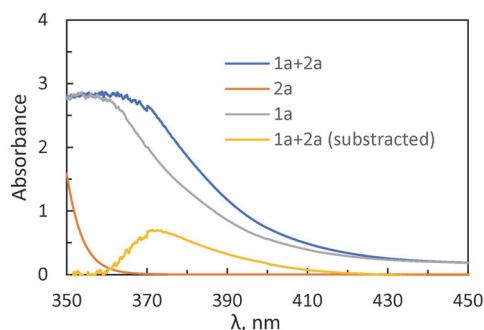
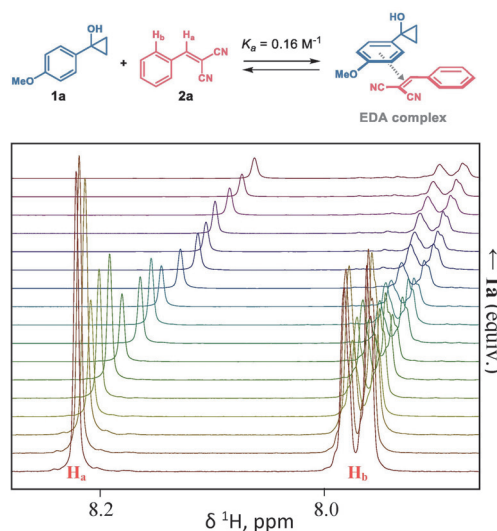b) **^{1}H NMR titration**

Figure 1. Spectroscopic studies to confirm generation of an EDA complex. a) UV-Vis studies: experimental UV-Vis spectra of cyclopropanol **1a** (1.5 M, gray line), alkene **2a** (0.01 M, orange line), and their mixture (150:1 ratio, 0.01 M for **2a**, blue line) in methanol. The yellow line is the result of subtraction of a spectrum of pure **1a** (gray line) from the mixture of **1a** and **2a** (blue line). b) ^{1}H NMR titration experiment in CD$_3$OD.

dichloromethane resulted in **3aa-*d*** with 69% D incorporation at the δ-position, indicating that the OH-group of **1a** is the source of the δ-hydrogen (Scheme 4, d). Notably, the reaction of **1a-*d*** was much slower than that of **1a**, resulting in only 44% yield after 20 h of irradiation. The remarkable difference in the reaction rates along with lower deuterium incorporation in the product **3aa-*d*** (69% D), in comparison to the content of deuterium in the starting material **1a-*d*** (87% D), were a likely consequence of a primary kinetic isotope effect. This indicates that oxidation of
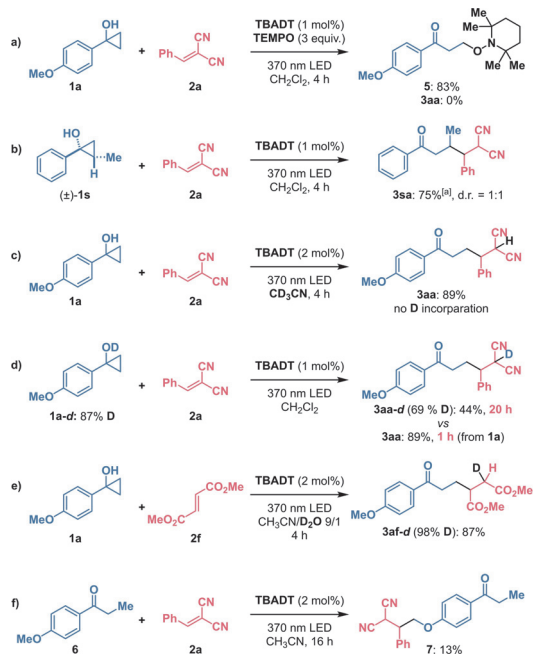
Scheme 4. Control experiments for mechanistic investigation. Yields determined by ^1H NMR analysis of the crude reaction mixture against triphenylmethane as an internal standard. [a] Yield of isolated product is given.
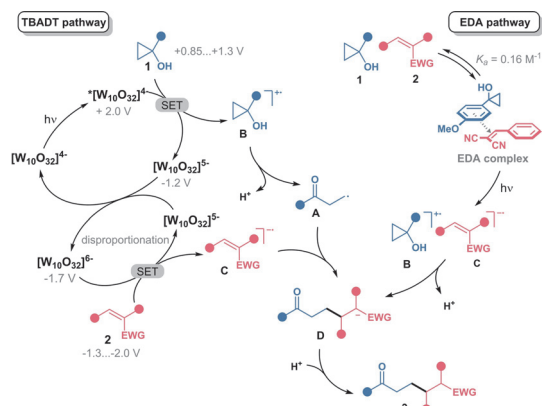
Scheme 5. Proposed mechanism. The numbers in gray color represent measured redox potentials for the species involved (see Figure 2).

1a followed by the breakage of the O–H bond is the rate-limiting step of the whole process. In another experiment performed with fumarate **2f**, we noticed an efficient transfer of deuterium to product **3af-d** (98%

D incorporation) from heavy water, that served as a co-solvent (Scheme 4, e). Finally, by performing the reaction with ketone **6** instead of **1a**, we confirmed that competitive HAT processes catalyzed by TBADT do not play a significant role and occur slowly under the standard reaction conditions (Scheme 4, f). The relatively weak C–H bond in the methoxy group of **6** was cleaved and produced the respective product **7** in low 13% yield after 16 h. Furthermore, TBADT did not provoke any notable C–H activation side processes at the sensitive benzylic sites during the investigation of the substrate scope (for example, in the synthesis of compounds **3la** and **3ma**).

Based on these observations, as well as the literature precedents,[50,51] we suggest a plausible mechanism of the reaction (Scheme 5). Photoexcitation of TBADT followed by intersystem crossing produces the triplet excited state $*[W_{10}O_{32}]^{4-}$. The photoexcited W(VI) species oxidizes cyclopropanol **1** via SET as a plausible rate-limiting step, resulting in cation radical **B**, that deprotonates and rapidly produces β-keto alkyl radical **A**. We believe that generation of cyclopropoxy radical **B′** via a homolytic cleavage of O–H bond is less likely in view of high BDE of the O–H bond in alcohols. Disproportionation of the reduced W(V) species $[W_{10}O_{32}]^{5-}$ regenerates the initial photocatalyst $[W_{10}O_{32}]^{4-}$ and also produces W(IV) species $[W_{10}O_{32}]^{6-}$, which is a stronger reductant than initially produced $[W_{10}O_{32}]^{5-}$.[46] The reduced forms of the photocatalyst turn the reaction mixture deep blue,[37,46,71] which was also observed in our experiments. Considering the remarkable influence of alkenes as well as the results of deuterium labeling experiments, we believe that electron-deficient alkenes **2** act as one-electron oxidants to produce radical anion **C**, which recombines with β-ketoalkyl radical **A** to form anionic intermediate **D**. Upon protonation of **D**, the product **3** is finally formed. We do not completely exclude an alternative mechanism, which involves a Giese-type radical addition of the nucleophilic radical **A** to electrophilic alkene, followed by SET from $[W_{10}O_{32}]^{5-}$ or $[W_{10}O_{32}]^{6-}$ to reduce the initially formed radical adduct (see Scheme S2 in the Supporting Information). A non-catalytic reaction via photoin-duced charge transfer in the respective EDA complexes features a complementary mechanistic pathway, that might occur in the case of electron-rich cyclopropanols and highly electron-deficient olefins.

The proposed mechanism aligns with the reductive and oxidative properties of the involved species, as confirmed through the measurements of their respective redox potentials. The electroanalytical character-istics of TBADT have been extensively studied previously and provide information on the electro-chemical potentials for single electron oxidation and reduction of active catalytic species in acetonitrile and other solvents, but the values vary in the presence of

water and are pH-dependent.[35–37] Examination of the reaction scope (Scheme 2) showed that the yields of the products and the reaction rates depend on the nature of reacting cyclopropanols and alkenes. Such behavior correlates with the values of the respective oxidation and reduction potentials, as summarized in Figure 2. For example, 2-phenylethyl cyclopropanol **1l** is the most resistant to oxidation ($E_p = +1.3$ V) among the three cyclopropanols tested, which agrees with its slow reaction rate (20 h) delivering **3la** in a moderate 53% yield. This contrasts to the fast and high yielding reaction of electron-rich **1a**, which is the strongest reductant ($E_p = +0.84$ V). The reactions of the least susceptible for SET oxidation aliphatic cyclopropanols are accelerated or even initiated by the addition of an external oxidant (NFSI, $K_2S_2O_8$). The role of the additive remains unclear, as only substoichiometric loadings (20–50 mol%) are required and the reaction does not yield the products **3** without TBADT (see Table S3 in the Supporting Information). We believe that NFSI could act either as a radical initiator that induces homolytic (rather than via SET oxidation) cleavage of the O–H bond in **1** or could recover the reduced forms of TBADT catalyst as was reported previously.[72–77] An analogous correlation between reactivity and single-electron oxidative properties has also been observed for alkenes: stronger oxidants, as revealed by comparison of the respective E_p values (Figure 2), are more favorable substrates in their reaction with **1a**. The clear dependence on the electronic properties of alkenes offers further support for the intermediacy of the radical anion **C**. It was noted that the reduction potentials measured for the radicals formed in the Giese reaction showed these are much stronger one-electron oxidants (−0.3 to −0.1 V vs Fc$^+$/Fc)[67] and the reaction rate in this case should be less dependent on starting alkene.

Conclusion

In conclusion, we have developed the decatungstate-photocatalyzed methodology for the redox-neutral alkylation of electron-deficient alkenes by β-ketoalkyl radicals derived from tertiary cyclopropanols. Aryl-substituted cyclopropanols and electron-poor alkenes are favorable substrates in this protocol, which has been adjusted to involve less reactive alkyl cyclopropanols by the addition of NFSI as a substoichiometric additive. The developed protocols were scaled up by translating them into a continuous flow regime, allowing the preparation of distantly functionalized ketones in gram quantities. Mechanistic studies confirm the role of TBADT as a photoredox catalyst that facilitates the single electron transfer between the reactants. The formation of EDA complexes between electron-donating aryl cyclopropanols and electron-accepting alkenes has been disclosed. The EDA complexes can transform into the same distantly functionalized ketone products by means of photo-induced charge transfer, although the reaction is slower than the TBADT-catalyzed process.

Experimental Section

General Procedure A

In an oven-dried 10 mL Schlenk tube equipped with a stirring bar, alkene **2** (0.2 mmol), cyclopropanol **1** (0.3 mmol, 1.5 equiv.), and tetrabutylammonium decatungstate (6.6 mg, 0.002 mmol, 1 mol%), were dissolved in dichloromethane (1 mL). The tube was capped, and the reaction mixture was degassed three times via three cycles of freeze-pump-thaw and then back-filled with argon gas. The Schlenk tube was then placed in the reactor and irradiated for 1–48 h at ambient temperature. After the completion of the reaction, the solvents were removed by evaporation and the residue was purified by flash column chromatography on silica gel.

General Procedure B

In an oven-dried 10 mL Schlenk tube equipped with a stirring bar, alkene **2** (0.2 mmol), cyclopropanol **1** (0.3 mmol, 1.5 equiv.), and tetrabutylammonium decatungstate (13.2 mg, 0.004 mmol, 2 mol%), were dissolved in 1 mL of 9:1 mixture of CH$_3$CN/H$_2$O. The tube was capped, and the reaction mixture was degassed three times via three cycles of freeze-pump-thaw and then back-filled with argon gas. The Schlenk tube was then placed in the reactor and irradiated for 3–24 h at ambient temperature. After the completion of the reaction, the solvents were removed by evaporation and the residue was purified by flash column chromatography on silica gel.

General Procedure C

In an oven-dried 10 mL Schlenk tube equipped with a stirring bar, alkene **2** (0.2 mmol), cyclopropanol **1** (0.6 mmol, 3 equiv.), tetrabutylammonium decatungstate (6.6 mg, 0.002 mmol,
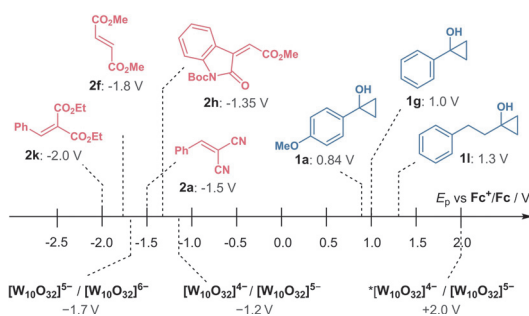

Figure 2. Relative scale of the peak potentials measured for the selected alkenes and cyclopropanols in CH$_3$CN (see Figure S9 in the Supporting Information). $E_{1/2}$ [W$_{10}$O$_{32}$]$^{5-}$/[W$_{10}$O$_{32}$]$^{6-}$ and [W$_{10}$O$_{32}$]$^{4-}$/[W$_{10}$O$_{32}$]$^{5-}$ has been measured under the same conditions, $E_{1/2}$ *[W$_{10}$O$_{32}$]$^{4-}$/[W$_{10}$O$_{32}$]$^{5-}$ are reported by Ravelli et al.[37] and realigned with respect to Fc$^+$/Fc couple.

1 mol%), and NFSI (0.1 mmol, 0.5 equiv.) were dissolved dichloromethane (1 mL). The tube was capped, and the reaction mixture was degassed three times via three cycles of freeze-pump-thaw and then back-filled with argon gas. The Schlenk tube was then placed in the reactor and irradiated for 3–24 h at ambient temperature. After the completion of the reaction, the solvents were removed by evaporation and the residue was purified by flash column chromatography on silica gel.

Acknowledgements

References

[1] O. G. Kulinkovich, *Chem. Rev.* **2003**, *103*, 2597–2632.

[2] T. R. McDonald, L. R. Mills, M. S. West, S. A. L. Rousseaux, *Chem. Rev.* **2021**, *121*, 3–79.

[3] S. P. Morcillo, *Angew. Chem. Int. Ed.* **2019**, *58*, 14044–14054.

[4] L. Chang, Q. An, L. Duan, K. Feng, Z. Zuo, *Chem. Rev.* **2022**, *122*, 2429–2486.

[5] L.-N. Guo, Z.-Q. Deng, Y. Wu, J. Hu, *RSC Adv.* **2016**, *6*, 27000–27003.

[6] S. Chiba, Z. Cao, S. A. A. El Bialy, K. Narasaka, *Chem. Lett.* **2006**, *35*, 18–19.

[7] J. Sheng, J. Liu, L. Chen, L. Zhang, L. Zheng, X. Wei, *Org. Chem. Front.* **2019**, *6*, 1471–1475.

[8] Y. Zhou, M. Wu, Y. Liu, C. Cheng, G. Zhu, *Org. Lett.* **2020**, *22*, 7542–7546.

[9] B. B. Mane, S. B. Waghmode, *J. Org. Chem.* **2021**, *86*, 17774–17781.

[10] C. Lou, X. Wang, L. Lv, Z. Li, *Org. Lett.* **2021**, *23*, 7608–7612.

[11] X. Zhang, T.-M. Yang, L.-M. Hu, X.-H. Hu, *Org. Lett.* **2022**, *24*, 8677–8682.

[12] N. Iwasawa, S. Hayakawa, M. Funahashi, K. Isobe, K. Narasaka, *Bull. Chem. Soc. Jpn.* **1993**, *66*, 819–827.

[13] Y.-F. Wang, K. K. Toh, E. P. J. Ng, S. Chiba, *J. Am. Chem. Soc.* **2011**, *133*, 6411–6421.

[14] Y.-H. Zhang, W.-W. Zhang, Z.-Y. Zhang, K. Zhao, T.-P. Loh, *Org. Lett.* **2019**, *21*, 5101–5105.

[15] S. Bloom, D. D. Bume, C. R. Pitts, T. Lectka, *Chem. Eur. J.* **2015**, *21*, 8060–8063.

[16] K. Jia, F. Zhang, H. Huang, Y. Chen, *J. Am. Chem. Soc.* **2016**, *138*, 1514–1517.

[17] H. G. Yayla, H. Wang, K. T. Tarantino, H. S. Orbe, R. R. Knowles, *J. Am. Chem. Soc.* **2016**, *138*, 10794–10797.

[18] M. V. Laktsevich-Iskryk, A. V. Krech, V. N. Zhabinskii, V. A. Khripach, A. L. Hurski, *Synthesis* **2021**, *53*, 1077–1086.

[19] D. Wang, J. Mao, C. Zhu, *Chem. Sci.* **2018**, *9*, 5805–5809.

[20] L. Huang, T. Ji, M. Rueping, *J. Am. Chem. Soc.* **2020**, *142*, 3532–3539.

[21] M. V. Laktsevich-Iskryk, N. A. Varabyeva, V. V. Kazlova, V. N. Zhabinskii, V. A. Khripach, A. L. Hurski, *Eur. J. Org. Chem.* **2020**, 2431–2434.

[22] T. Kikuchi, K. Yamada, T. Yasui, Y. Yamamoto, *Org. Lett.* **2021**, *23*, 4710–4714.

[23] Y. Zhang, Y. Niu, Y. Guo, J. Wang, Y. Zhang, S. Liu, X. Shen, *Angew. Chem. Int. Ed.* **2022**, *61*, e202212201.

[24] J. Wang, X. Li, *Chem. Sci.* **2022**, *13*, 3020–3026.

[25] K. Zhao, K. Yamashita, J. E. Carpenter, T. C. Sherwood, W. R. Ewing, P. T. W. Cheng, R. R. Knowles, *J. Am. Chem. Soc.* **2019**, *141*, 8752–8757.

[26] A. Hu, Y. Chen, J.-J. Guo, N. Yu, Q. An, Z. Zuo, *J. Am. Chem. Soc.* **2018**, *140*, 13580–13585.

[27] J.-J. Guo, A. Hu, Y. Chen, J. Sun, H. Tang, Z. Zuo, *Angew. Chem. Int. Ed.* **2016**, *55*, 15319–15322.

[28] T. Xue, Z. Zhang, R. Zeng, *Org. Lett.* **2022**, *24*, 977–982.

[29] A. Hu, J.-J. Guo, H. Pan, H. Tang, Z. Gao, Z. Zuo, *J. Am. Chem. Soc.* **2018**, *140*, 1612–1616.

[30] L. Cardinale, M. Neumeier, M. Majek, A. J. von Wangelin, *Org. Lett.* **2020**, *22*, 7219–7224.

[31] M. Ji, Z. Wu, C. Zhu, *Chem. Commun.* **2019**, *55*, 2368–2371.

[32] Q. Wu, W. Liu, M. Wang, Y. Huang, P. Hu, *Chem. Commun.* **2022**, *58*, 9886–9889.

[33] Ł. Woźniak, G. Magagnano, P. Melchiorre, *Angew. Chem. Int. Ed.* **2018**, *57*, 1068–1072.

[34] T. Yamase, N. Takabayashi, M. Kaji, *J. Chem. Soc. Dalton Trans.* **1984**, 793–799.

[35] R. F. Renneke, M. Pasquali, C. L. Hill, *J. Am. Chem. Soc.* **1990**, *112*, 6585–6594.

[36] D. Ravelli, D. Dondi, M. Fagnoni, A. Albini, A. Bagno, *Phys. Chem. Chem. Phys.* **2013**, *15*, 2890.

[37] V. De Waele, O. Poizat, M. Fagnoni, A. Bagno, D. Ravelli, *ACS Catal.* **2016**, *6*, 7174–7182.

[38] L. Capaldo, D. Ravelli, M. Fagnoni, *Chem. Rev.* **2022**, *122*, 1875–1924.

[39] G. Laudadio, Y. Deng, K. Van Der Wal, D. Ravelli, M. Nuño, M. Fagnoni, D. Guthrie, Y. Sun, T. Noël, *Science* **2020**, *369*, 92–96.

[40] G. Laudadio, S. Govaerts, Y. Wang, D. Ravelli, H. F. Koolman, M. Fagnoni, S. W. Djuric, T. Noël, *Angew. Chem. Int. Ed.* **2018**, *57*, 4078–4082.

[41] I. Ryu, A. Tani, T. Fukuyama, D. Ravelli, M. Fagnoni, A. Albini, *Angew. Chem. Int. Ed.* **2011**, *50*, 1869–1872.

[42] D. Ravelli, S. Protti, M. Fagnoni, *Acc. Chem. Res.* **2016**, *49*, 2232–2242.

[43] M. Okada, T. Fukuyama, K. Yamada, I. Ryu, D. Ravelli, M. Fagnoni, *Chem. Sci.* **2014**, *5*, 2893–2898.

[44] S. Esposti, D. Dondi, M. Fagnoni, A. Albini, *Angew. Chem. Int. Ed.* **2007**, *46*, 2531–2534.

[45] I. B. Perry, T. F. Brewer, P. J. Sarver, D. M. Schultz, D. A. DiRocco, D. W. C. MacMillan, *Nature* **2018**, *560*, 70–75.

[46] P. J. Sarver, N. B. Bissonnette, D. W. C. MacMillan, *J. Am. Chem. Soc.* **2021**, *143*, 9737–9743.

[47] D. Mazzarella, A. Pulcinella, L. Bovy, R. Broersma, T. Noël, *Angew. Chem. Int. Ed.* **2021**, *60*, 21277–21282.

[48] J. Murphy, D. Bastida, S. Paria, M. Fagnoni, P. Melchiorre, *Nature* **2016**, *532*, 218–222.

[49] I. Texier, J. A. Delaire, C. Giannotti, *Phys. Chem. Chem. Phys.* **2000**, *2*, 1205–1212.

[50] S. Montanaro, D. Ravelli, D. Merli, M. Fagnoni, A. Albini, *Org. Lett.* **2012**, *14*, 4218–4221.

[51] L. Capaldo, L. Buzzetti, D. Merli, M. Fagnoni, D. Ravelli, *J. Org. Chem.* **2016**, *81*, 7102–7109.

[52] D. G. Kananovich, Y. A. Konik, D. M. Zubrytski, I. Järving, M. Lopp, *Chem. Commun.* **2015**, *51*, 8349–8352.

[53] G. Z. Elek, V. Borovkov, M. Lopp, D. G. Kananovich, *Org. Lett.* **2017**, *19*, 3544–3547.

[54] M. Iskryk, M. Barysevich, M. Ošeka, J. Adamson, D. Kananovich, *Synthesis* **2019**, *51*, 1935–1948.

[55] T. Wan, L. Capaldo, D. Ravelli, W. Vitullo, F. J. De Zwart, B. De Bruin, T. Noël, *J. Am. Chem. Soc.* **2023**, *145*, 991–999.

[56] M. Wang, J. Waser, *Angew. Chem. Int. Ed.* **2020**, *59*, 16420–16424.

[57] M. Schlegel, S. Qian, D. A. Nicewicz, *ACS Catal.* **2022**, *12*, 10499–10505.

[58] Y. C. Kang, S. M. Treacy, T. Rovis, *Synlett* **2021**, 1767–1771.

[59] S. Peddibhotla, *Curr. Bioact. Compd.* **2009**, *5*, 20–38.

[60] X. Hu, Q. Bian, Z.-L. Wang, L.-J. Guo, Y.-Z. Xu, G. Wang, D.-Z. Xu, *J. Org. Chem.* **2022**, *87*, 66–75.

[61] A. Bort, S. Quesada, Á. Ramos-Torres, M. Gargantilla, E. M. Priego, S. Raynal, F. Lepifre, J. M. Gasalla, N. Rodriguez-Henche, A. Castro, I. Díaz-Laviada, *Sci. Rep.* **2018**, *8*, 4370.

[62] C. Sambiagio, T. Noël, *Trends Chem.* **2020**, *2*, 92–106.

[63] T. H. Rehm, *Chem. Eur. J.* **2020**, *26*, 16952–16974.

[64] Z. Wen, D. Pintossi, M. Nuño, T. Noël, *Nat. Commun.* **2022**, *13*, 6147.

[65] S. Förster, O. Tverskoy, G. Helmchen, *Synlett* **2008**, 2803–2806.

[66] X. Xin, D. Xiang, J. Yang, Q. Zhang, F. Zhou, D. Dong, *J. Org. Chem.* **2013**, *78*, 11956–11961.

[67] Y. Cao, S.-C. Zhang, M. Zhang, G.-B. Shen, X.-Q. Zhu, *J. Org. Chem.* **2013**, *78*, 7154–7168.

[68] G. E. M. Crisenza, D. Mazzarella, P. Melchiorre, *J. Am. Chem. Soc.* **2020**, *142*, 5461–5476.

[69] B. Saxena, R. I. Patel, A. Sharma, *Adv. Synth. Catal.* **2023**, *365*, 1538–1564.

[70] P. Thordarson, *Chem. Soc. Rev.* **2011**, *40*, 1305–1323.

[71] A. Chemseddine, C. Sanchez, J. Livage, J. P. Launay, M. Fournier, *Inorg. Chem.* **1984**, *23*, 2609–2613.

[72] M. C. Quattrini, S. Fujii, K. Yamada, T. Fukuyama, D. Ravelli, M. Fagnoni, I. Ryu, *Chem. Commun.* **2017**, *53*, 2335–2338.

[73] X. Wang, M. Yu, H. Song, Y. Liu, Q. Wang, *Org. Lett.* **2021**, *23*, 8353–8358.

[74] L. Capaldo, L. L. Quadri, D. Merli, D. Ravelli, *Chem. Commun.* **2021**, *57*, 4424–4427.

[75] T. Wan, L. Capaldo, G. Laudadio, A. V. Nyuchev, J. A. Rincón, P. García-Losada, C. Mateos, M. O. Frederick, M. Nuño, T. Noël, *Angew. Chem. Int. Ed.* **2021**, *60*, 17893–17897.

[76] P. Xie, C. Xue, J. Luo, S. Shi, D. Du, *Green Chem.* **2021**, *23*, 5936–5943.

[77] J. Zhang, A. Studer, *Nat. Commun.* **2022**, *13*, 3886.

[78] A. Krech, V. Yakimchyk, T. Jarg, D. Kananovich, M. Ošeka, *ChemRxiv.* **2023**, doi: 10.26434/chemrxiv-2023-2llln.

Appendix 3

COMMUNICATIONS

Telescoped synthesis of vicinal diamines via ring-opening of electrochemically generated aziridines in flow

Marharyta Laktsevich-Iskryk[1] · Anastasiya Krech[1] · Mihhail Fokin[1] · Mariliis Kimm[1] · Tatsiana Jarg[1] · Timothy Noël[2] · Maksim Ošeka[1]

Abstract

A vicinal diamine motif can be found in numerous natural compounds and pharmaceuticals, making it an important synthetic target. Herein, we report a telescoped synthesis of vicinal diamines under continuous flow conditions. This approach involves the electrochemical aziridination of alkenes with primary amines, followed by the strain-release driven ring-opening using various nitrogen nucleophiles. The efficacy of the developed method was demonstrated through the synthesis of diverse symmetrically and non-symmetrically substituted vicinal diamines, as well as vicinal amino azides, which can be further hydrogenated to diamines in flow. Additionally, *O*-centered nucleophiles were employed for the ring-opening of aziridines in our telescoped synthesis, yielding vicinal amino ethers and alcohol. This process offers a streamlined and efficient pathway for the direct synthesis of valuable products from readily available starting materials, bypassing the isolation of unstable aziridine intermediates.

Keywords Flow chemistry · Telescoped synthesis · Electrochemical synthesis · Ring-opening · Aziridines · Vicinal diamines

Introduction

Vicinal diamines are compounds of profound importance, playing pivotal roles across the fields of chemistry, biology, and industry (Fig. 1). This structural motif is present in multiple natural compounds and pharmaceuticals, each exhibiting diverse bioactivities [1] such as anti-viral, anti-cancer, antihypertensive, and more. The chelating properties of 1,2-diamines determine their extensive application in various industrial processes, including the removal of heavy metal ions from wastewater [2]. They also serve as sensors [3] in analytical chemistry and find utility in organic synthesis as ligands in transition-metal catalysis [4–6].

Several synthetic routes to vicinal diamines have been explored [7, 8], with strain-release driven ring-opening of aziridines by nitrogen-centered nucleophiles emerging particularly advantageous. This approach offers high yields, control over stereoselectivity due to the three-membered ring structure, and utilizes readily available starting materials [9]. The reactivity of aziridines toward nucleophilic ring-opening depends on a substituent attached to the nitrogen atom of the aziridine core, dividing them into two categories: activated aziridines, featuring an electron-withdrawing group, and non-activated aziridines, substituted with an electron-donating group (Fig. 2a). Electron-withdrawing groups, such as *N*-carbonyl or *N*-sulfonyl groups, stabilize the negative charge on the nitrogen atom formed during ring-opening, enabling the reaction to proceed without the need for a promoter [10]. On the contrary, *N*-alkyl or unsubstituted aziridines require activation prior to a nucleophilic attack [11]. This activation can be achieved through quaternarization [12, 13], protonation by strong Brønsted acids [14] like HCl, H_2SO_4, TfOH, or complexation with Lewis acids. However, certain acidic promoters might be incompatible with amines as nucleophiles due to their high basicity [14]. Several researches have evidence that non-activated aziridines can

✉ Maksim Ošeka
maksim.oseka@taltech.ee

1 Department of Chemistry and Biotechnology, Tallinn University of Technology, Akadeemia tee 15, 12618 Tallinn, Estonia

2 Van't Hoff Institute for Molecular Sciences (HIMS), University of Amsterdam, Science Park 904, Amsterdam 1098 XH, The Netherlands

Fig. 1 Pharmaceuticals and ligands containing vicinal diamines

Pharmaceuticals

Oseltamivir
anti-viral agent

S046001
calcium channel blocker

Oxalylplatin
anti-cancer agent

Bepridil
treatment of angina

Ligands

Grubbs catalyst

Noyori catalyst

salen ligands
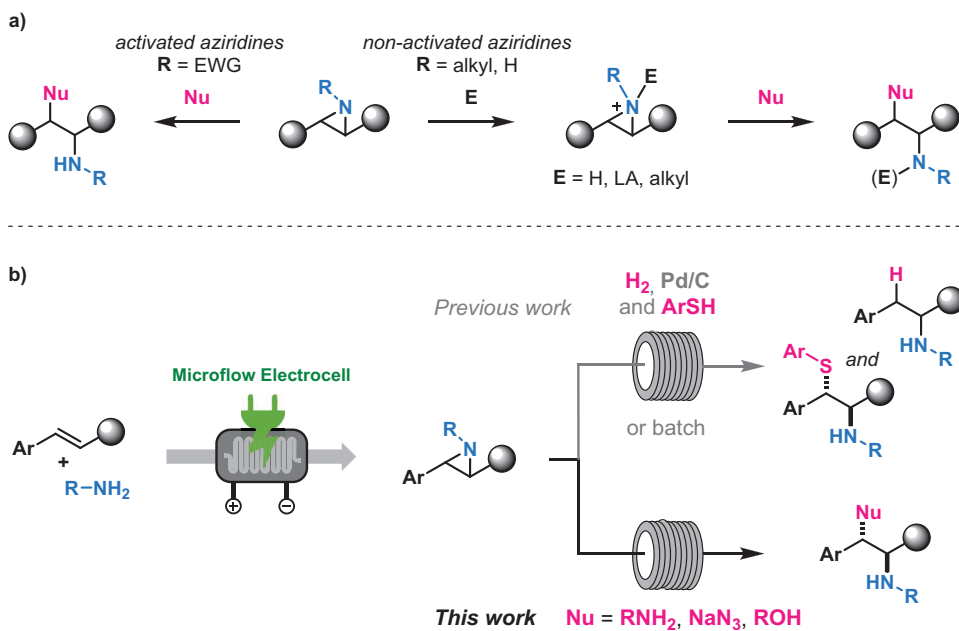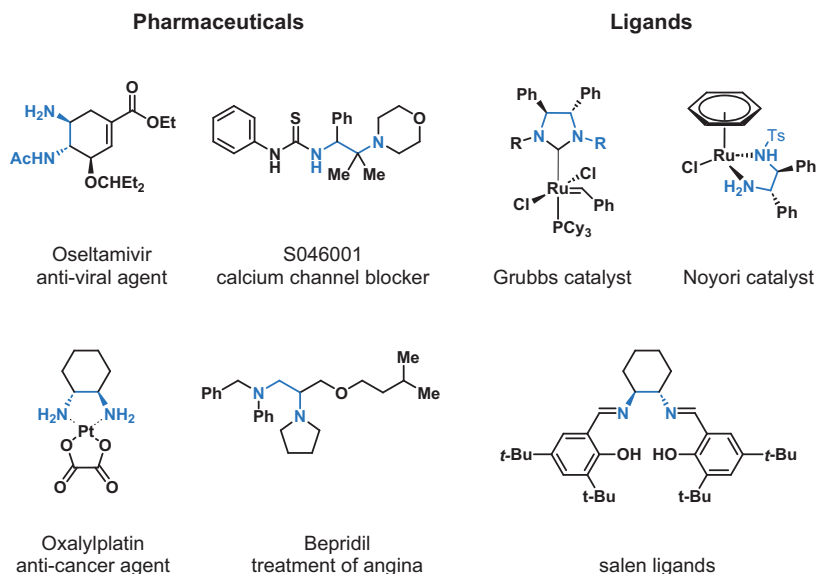
Fig. 2 a) General strategies for aziridine ring-opening. **b**) Electrochemical aziridine synthesis and nucleophilic ring-opening sequence

undergo ring-opening by amines utilizing LiNTf$_2$ [15], PBu$_3$ [16], LiClO$_4$ [17], B(C$_6$F$_5$)$_3$ [18], yet extended reaction times are often required for optimal results.

Conventional methods for the synthesis of non-activated aziridines often need purification of sensitive products

before initiating a nucleophilic ring-opening reaction, making these approaches time consuming and wasteful. Due to the inherent instability of aziridines, their low reactivity toward amine nucleophiles, and the potential toxicity arising from their alkylating properties [19], the prospect of a

telescopic process for synthesizing vicinal diamines directly from simple starting materials in a continuous flow setup is highly appealing [20]. In the previous study, we have introduced the electrochemical synthesis of non-activated aziridines directly from styrene-type alkenes and primary amines in a flow microreactor (Fig. 2b) [21, 22]. This strategy significantly reduced the time that unstable aziridines were exposed to electrochemical conditions compared to the batch process, preventing their decomposition, and minimizing the formation of byproducts [23–25]. The resulting aziridines directly underwent Pd-catalyzed hydrogenation in flow, as well as nucleophilic ring-opening with thiophenol without the need for prior isolation. In this work, we extend this methodology by demonstrating a telescoped process, where electrochemically synthesized non-activated aziridines were efficiently opened by various nitrogen nucleophiles in a continuous flow system.

Results and discussion

During the investigation of the electrochemical aziridination in continuous flow, we noticed the formation of vicinal diamines in the crude mixture. This occurred when the crude mixture collected from the electrochemical microreactor was left at room temperature for an extended period. This observation can be explained by the nucleophilic ring-opening of aziridines with an excess of unreacted amine, which was employed to maximize the yield of the electrochemical transformation. The excess of hexafluoroisopropanol (HFIP) was also necessary for the efficient hydrogen reduction at the counter electrode and stabilization of intermediate radical

species during the aziridine synthesis. Consistent with literature findings, HFIP, as a weak organic acid, could activate the formed aziridine and facilitate the nucleophilic ring-opening [26]. To our satisfaction, when the crude reaction mixture containing model aziridine derived from anethole and cyclohexylamine was heated at 60 °C, complete conversion of the starting material into diamine **1** was achieved overnight under batch conditions. Based on these results, we decided to render the telescoped process in flow by merging nucleophilic ring-opening reactions with electrochemical aziridine synthesis (Fig. 3). To achieve this objective, a flow setup was constructed, comprising a syringe pump connected to the in-house-built electrochemical microreactor [27], a degassing vessel, and an HPLC pump linked to a custom-made coil reactor submerged in an oil bath. A back pressure regulator was attached to the outlet of the coil reactor, allowing the ring-opening reaction to be conducted at elevated temperatures while preventing solvent and amine boiling. Directly connecting the electrochemical reactor to the coil reactor was not feasible due to the operational limitations of the electrochemical reactor, which cannot be operated at pressures above 2 bars. Additionally, the hydrogen gas formed during the electrochemical step needed to be eliminated from the reaction mixture before passing it to the HPLC pump. Therefore, the presence of the degassing vessel was necessary for these purposes.

While reaction conditions for the electrochemical synthesis of aziridines had been established previously, a brief optimization of the ring-opening step was conducted. This optimization involved varying the temperature of the oil bath and residence time by adjusting the volume of the coil reactor. The designed setup ensured complete conversion
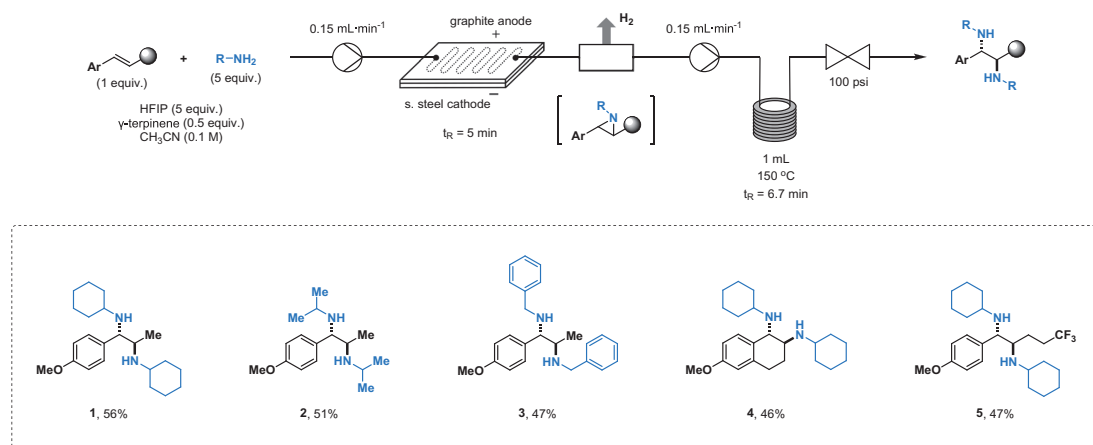

Fig. 3 Telescoped synthesis of symmetrically substituted vicinal diamines. Reaction Conditions: alkene (1 mmol), amine (5 mmol), HFIP (5 mmol), γ-terpinene (0.5 mmol), CH_3CN (10 mL), graphite anode/stainless steel cathode, 2.3–3.1 mA cm^{-2}, collection time 66.6 min. The yields correspond to isolated products

of the model aziridine within a residence time of 6.7 min at 150 °C, yielding desired diamine **1** in 56%. The ring-opening step proceeded stereoselectively via S_N2 mechanism providing diamines exclusively as *anti*-isomers [28]. Isopropyl and benzyl amine were also competent and corresponding vicinal diamines **2** and **3** were isolated in good yields. Additionally, the elongation of the alkyl chain and the presence of an additional cycle in alkene did not influence the rate or selectivity of the nucleophilic opening reaction, as bicyclic diamine **4** and diamine **5** with a terminal trifluoromethyl group were obtained with similar yields. It is worth mentioning that *N*-isopropyl-substituted aziridine exhibited lower reactivity under the test batch conditions, requiring 48 h for full conversion. This highlights the advantage of the flow process, where the same conversion is achieved within a few minutes. Unfortunately, some aziridines were incompatible with the nucleophilic ring-opening reaction, even at elevated temperatures and longer residence times. For example, in the reaction involving stilbene-derived aziridine, only traces of the diaminated product were detected, whereas aziridines derived from trisubstituted alkenes did not yield any

desirable product and were prone to unproductive decomposition at high temperatures.

Next, we turned our attention to the synthesis of non-symmetrically substituted 1,2-diamines (Fig. 4). This was achieved by addition of external amine, distinct from the one used during the aziridine synthesis. A 20-fold excess of external amine was found to be optimal to almost suppress the formation of diamine **1**, as further increase did not result in any significant yield improvement of targeted diamines. In the flow system, external amines were injected from the second syringe as an acetonitrile solution into the degassing flask, and the flow rate of the HPLC pump was doubled to keep the productivity of the telescoped process at the same level as previously (see Fig. S2 in SI). Despite the shortened ring-opening reaction time, aziridine was fully consumed, and diamines **6–9**, derived from external primary amines, were obtained in 40–51% yields. Even though the formation of small amounts of diamine **1** was observed in these experiments, we were able to isolate the desired products **6–9** as individual compounds using reverse phase chromatography. Moreover, the formation of diamine **1** was completely suppressed, when secondary amines as stronger nucleophiles
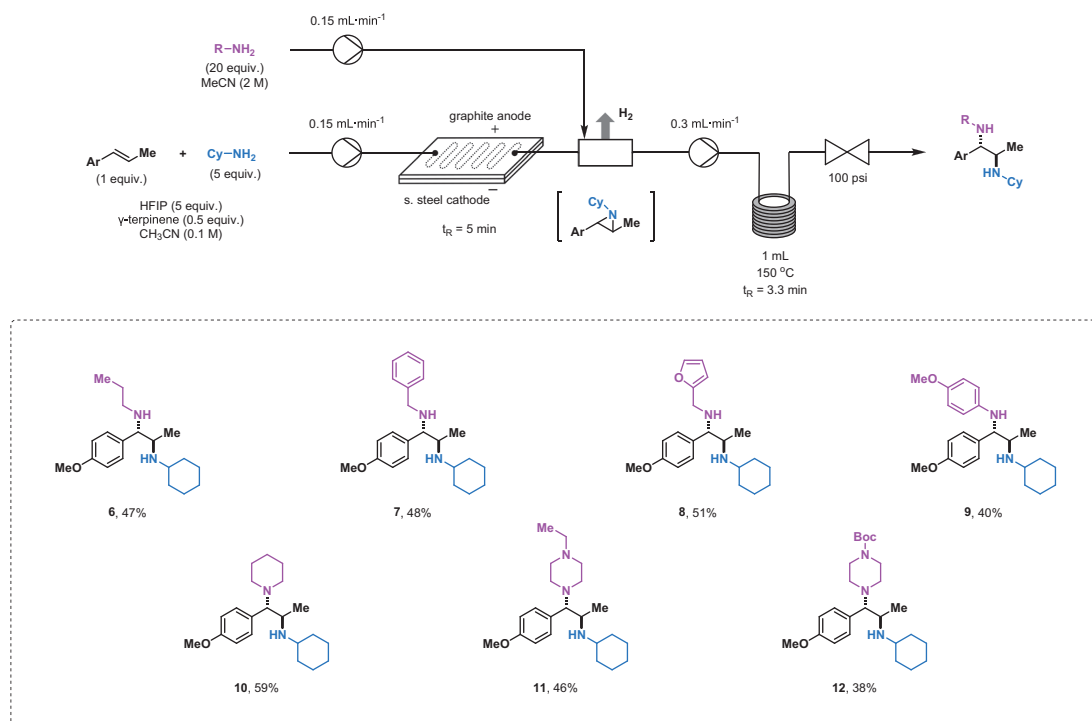

Fig. 4 Telescoped synthesis of non-symmetrically substituted vicinal diamines. Reaction Conditions: anethole (1 mmol), cyclohexyl amine (5 mmol), HFIP (5 mmol), γ-terpinene (0.5 mmol), CH₃CN (10 mL), graphite anode/stainless steel cathode, 3.1 mA cm⁻², external amine (20 mmol in 10 mL of CH₃CN), collection time 66.6 min. The yields correspond to isolated products

were used for the ring-opening reaction (products **10**–**12**) [29]. However, the additional amino groups in the structures of compounds **11** and **12** made their purification more tedious, which resulted in a considerable reduction of isolated yields.

An alternative method for generating a 1,2-diamine moiety involves reduction of vicinal amino azide compounds, which can be obtained through nucleophilic ring-opening of aziridines by azides [30, 31]. It is important to emphasize that azides are potentially explosive compounds that are sensitive to elevated temperatures, light, and shock, and therefore should be handled with extra caution [32]. Nevertheless, when a reaction involving azides is conducted in a continuous flow setup, the risks are considerably reduced, since only small amounts of hazardous chemicals are exposed simultaneously to reaction conditions in the active zone of a reactor [33, 34]. In our study, sodium azide was selected as a widely used and cost-effective reagent for the synthesis of vicinal amino azides through the ring-opening azidation of aziridines in flow (Fig. 5a). A solution of sodium azide in an isopropanol/water mixture was prepared to ensure homogeneity

of the reaction mixture and was injected to the coil reactor through a Y-mixer by a syringe pump. This modification of the reaction setup was necessary because some phase separation occurred, causing the HPLC pump to malfunction, when we attempted to add the azide solution directly to the degassing vessel as done previously. As anticipated, the nucleophilic ring-opening by sodium azide was highly efficient, even at lower temperatures, completely preventing the competing formation of symmetrically substituted diamines [35]. The enhanced nucleophilicity and small size of the azide anion, in comparison to amine, enabled us to synthesize five different amino azides **13**–**17** with yields up to 71%, even in the instances involving sterically hindered aziridines. To demonstrate the usefulness of the developed method, the derivatization of azidated products was conducted (Fig. 5b). First, we transformed amino azide **15** into vicinal diamine **18** by palladium-catalyzed hydrogenation in continuous flow, employing H-Cube® equipment. The flow setup facilitates hydrogenation through efficient mass-transfer between gaseous and liquid phases, while minimizing the risks associated with handling of combustible hydrogen gas, as the active
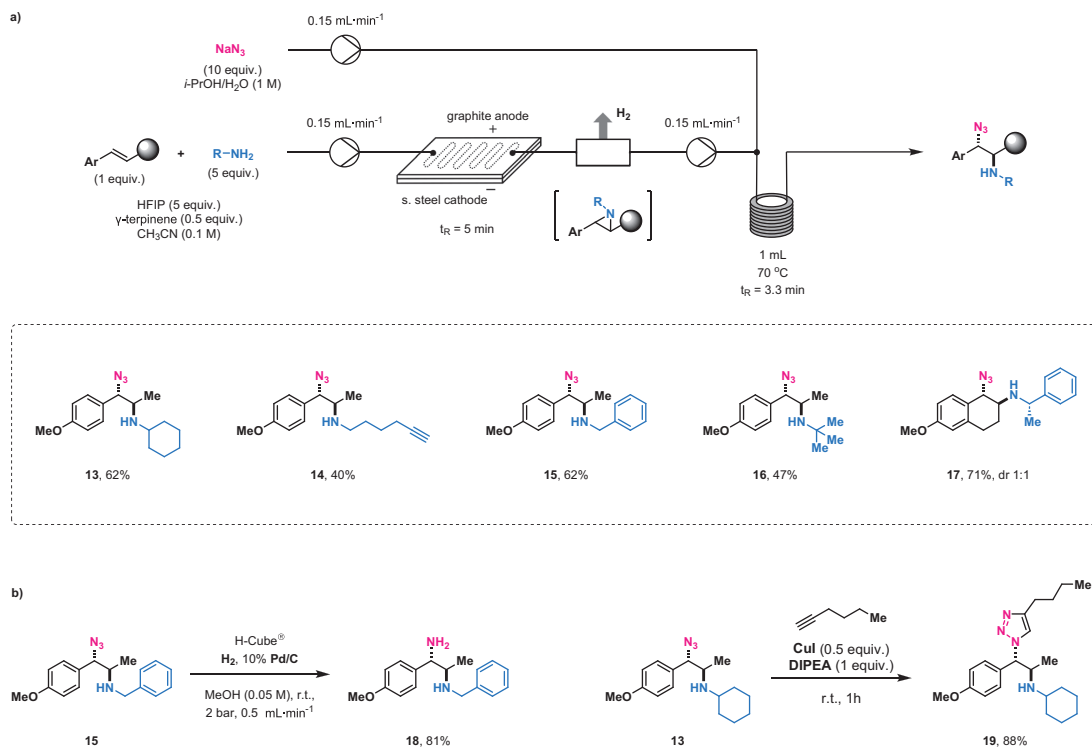

Fig. 5 a) Telescoped synthesis of vicinal amino azides. Reaction Conditions: alkene (1 mmol), amine (5 mmol), HFIP (5 mmol), γ-terpinene (0.5 mmol), CH₃CN (10 mL), graphite anode/stainless steel cathode, 1.9–3.3 mA cm⁻², sodium azide (10 mmol in 10 mL of *i*-PrOH/H₂O 1:1), collection time 66.6 min. The yields correspond to isolated products. **b**) Derivatization of amino azides

catalyst remains unexposed to oxygen [36]. Despite the presence of two *N*-benzylic groups in compound **15**, which could potentially undergo hydrogenation, the reaction was chemoselective, and only the azido group was reduced to the amino group. Lastly, amino azide **13** proved to be a compatible substrate for the intermolecular click reaction with hexyne, yielding the corresponding triazole **19** in high yield.

Besides amines and sodium azide, we explored the potential of *O*-centered nucleophiles to participate in the ring-opening reaction (Fig. 6). When methanol without additives was used as a nucleophile, the mixture containing symmetrically substituted diamine **1** and corresponding amino ether **20** was obtained. However, the exclusive formation of desired amino ether **20** was achieved by adding a 1 M solution of hydrochloric acid (10 equiv.) in alcohol to the degassing flask. The acidic environment led to the protonation of unreacted cyclohexylamine, hindering its nucleophilicity and ensuring the targeted outcome. Although the isolated yields of amino ethers **20** and **21** remained consistent compared to the previous results, a significant drop in diastereoselectivity was observed. We believe that nucleophilic ring-opening of the aziridinium ion proceeds through S_N1 mechanism under strong acidic conditions, involving the formation of the stabilized benzylic carbocation. Thus, the nucleophilic attack by alcohols can happen from the both sides of the planar carbocation, leading to the formation of a mixture of *anti-* and *syn*-isomers [37]. In addition, we successfully obtained amino alcohol **22** by the slightly modified procedure, employing water as a nucleophile. Surprisingly,

the ring-opening reaction with water showed high stereoselectivity, yielding the product as a single diastereomer.

Conclusions

In summary, we have developed a telescoped protocol for synthesizing vicinal diamines from internal alkenes and primary amines. This method involves the electrochemical synthesis of non-activated aziridines in a flow microreactor, followed by the ring-opening reaction with *N*-nucleophiles in a self-assembled flow setup. The continuous flow system ensured efficient mass and heat transfer, and allowed us to use superheated solvents, resulting in considerably reduced reaction times compared to traditional batch conditions. We obtained symmetrically substituted vicinal diamines using an excess of amines employed for aziridine synthesis. Alternatively, non-symmetrically substituted vicinal diamines were synthesized by adding an excess of external amine after the aziridination step. Nucleophilic ring-opening of aziridines with sodium azide yielded various amino azides, which can be transformed into vicinal diamine and corresponding triazole. Crucially, our continuous flow conditions substantially reduced the risks associated with handling hazardous azides compared to batch operations. Additionally, the introduction of hydrochloric acid suppressed the nucleophilicity of amines and enabled aziridine-opening with water and alcohols, broadening the scope of our protocol to vicinal amino alcohol and ethers.
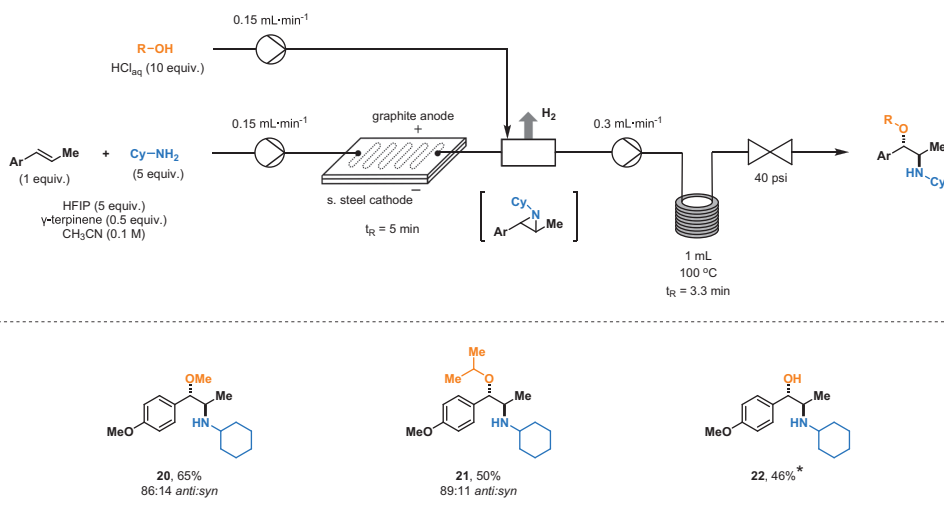

Fig. 6 Telescoped synthesis of vicinal amino ethers and alcohol. Reaction Conditions: anethole (1 mmol), cyclohexyl amine (5 mmol), HFIP (5 mmol), γ-terpinene (0.5 mmol), CH$_3$CN (10 mL), graphite anode/stainless steel cathode, 3.1 mA cm^{-2}, HCl$_{aq}$ (10 mmol in 10 mL of alcohol or *in 10 mL of H$_2$O/THF 1:1), collection time 66.6 min. The yields correspond to isolated products

Declarations

Conflict of interest Timothy Noël, a co-author of this article, is the Editor-in-Chief of Journal of Flow Chemistry.

References

1. Michalson ET, Szmuszkovicz J (1989) Medicinal agents incorporating the 1,2-diamine functionality. In: Jucker E (ed) Progress in Drug Research. Birkhäuser Basel, Basel, pp 135–149
2. Zhang K, Dai Z, Zhang W, Gao Q, Dai Y, Xia F, Zhang X (2021) EDTA-based adsorbents for the removal of metal ions in wastewater. Coord Chem Rev 434:213809
3. Ye Q, Ren S, Huang H, Duan G, Liu K, Liu J-B (2020) Fluorescent and colorimetric sensors based on the oxidation of *o*-phenylenediamine. ACS Omega 5:20698–20706
4. Deshpande SH, Shende VS, Shingote SK, Chakravarty D, Puranik VG, Chaudhari RV, Kelkar AA (2015) Rhodium complex with unsymmetrical vicinal diamine ligand: excellent catalyst for asymmetric transfer hydrogenation of ketones. RSC Adv 5:51722–51729
5. Janssen-Müller D, Schlepphorst C, Glorius F (2017) Privileged chiral N-heterocyclic carbene ligands for asymmetric transition-metal catalysis. Chem Soc Rev 46:4845–4854
6. Shaw S, White JD (2019) Asymmetric catalysis using chiral salen-metal complexes: recent advances. Chem Rev 119:9381–9426
7. Saibabu Kotti SRS, Timmons C, Li G (2006) Vicinal diamino functionalities as privileged structural elements in biologically active compounds and exploitation of their synthetic chemistry. Chem Biol Drug Des 67:101–114
8. Lucet D, Le Gall T, Mioskowski C (1998) The chemistry of vicinal diamines. Angew Chem Int Ed 37:2580–2627
9. Dequina HJ, Jones CL, Schomaker JM (2023) Recent updates and future perspectives in aziridine synthesis and reactivity. Chem 9:1658–1701
10. Jung J-H, Ha H-J (2015) New perspective on the synthesis of Aziridine. Bull Korean Chem Soc 36:1741–1742
11. Stanković S, D'hooghe M, Catak S, Eum H, Waroquier M, Van Speybroeck V, De Kimpe N, Ha H-J (2012) Regioselectivity in the ring opening of non-activated aziridines. Chem Soc Rev 41:643–665
12. Choi J, Yu T, Ha H-J (2021) Alkylative aziridine ring-opening reactions. Molecules 26:1703
13. Govaerts S, Angelini L, Hampton C, Malet-Sanz L, Ruffoni A, Leonori D (2020) Photoinduced olefin diamination with Alkylamines. Angew Chem 132:15131–15138
14. Katagiri T, Takahashi M, Fujiwara Y, Ihara H, Uneyama K (1999) General syntheses of optically active α-trifluoromethylated amines via ring-opening reactions of *N*-Benzyl-2-trifluoromethylaziridine. J Org Chem 64:7323–7329
15 Cossy J, Bellosta V, Alauze V (2002) Desmurs J-R (2002) Lithium bistrifluoromethanesulfonimidate-mediated regioselective ring opening of aziridines by amines. Synthesis 15:2211–2214
16. Hou X-L, Fan R-H, Dai L-X (2002) Tributylphosphine: a remarkable promoting reagent for the ring-opening reaction of aziridines. J Org Chem 67:5295–5300
17. De Parrodi CA, Vázquez V, Quintero L, Juaristi E (2001) Preparation of *TRANS* -1,2-Diaminocyclohexane derivatives by lithium perchlorate catalyzed ring opening of aziridines. Synth Commun 31:3295–3302
18. Watson IDG, Yudin AK (2003) Ring-opening reactions of nonactivated aziridines catalyzed by Tris(pentafluorophenyl)borane. J Org Chem 68:5160–5167
19 Dembitsky VM, Terent'ev AO, Levitsky DO (2013) Aziridine Alkaloids: Origin, Chemistry and activity. In: Ramawat KG, Mérillon J-M (eds) Natural Products. Springer, Berlin Heidelberg, Berlin, Heidelberg, pp 977–1006
20. Guidi M, Seeberger PH, Gilmore K (2020) How to approach flow chemistry. Chem Soc Rev 49:8910–8932
21. Ošeka M, Laudadio G, Van Leest NP, Dyga M, Bartolomeu ADA, Gooßen LJ, De Bruin B, De Oliveira KT, Noël T (2021) Electrochemical aziridination of internal alkenes with primary amines. Chem 7:255–266
22. Noël T, Cao Y, Laudadio G (2019) The fundamentals behind the use of flow reactors in electrochemistry. Acc Chem Res 52:2858–2869
23 Costa E, Silva R, Vega C, Regnier M, Capaldo L, Wesenberg L, Lowe G, Thiago De Oliveira K, Noël T (2023) Electrosynthesis of aryliminophosphoranes in continuous flow. Adv Synth Catal. https://doi.org/10.1002/adsc.202300635
24. Bajada MA, Sanjosé-Orduna J, Di Liberto G, Tosoni S, Pacchioni G, Noël T, Vilé G (2022) Interfacing single-atom catalysis with continuous-flow organic electrosynthesis. Chem Soc Rev 51:3898–3925
25. Kooli A, Wesenberg L, Beslać M, Krech A, Lopp M, Noël T, Ošeka M (2022) Electrochemical hydroxylation of electron-rich arenes in continuous flow. Eur J Org Chem 2022:e202200011
26. Dover TL, McDonald FE (2021) Fluorinated alcohols: powerful promoters for ring-opening reactions of epoxides with carbon nucleophiles. ARKIVOC 2021:85–114
27. Laudadio G, De Smet W, Struik L, Cao Y, Noël T (2018) Design and application of a modular and scalable electrochemical flow microreactor. J Flow Chem 8:157–165
28. Hu XE (2004) Nucleophilic ring opening of aziridines. Tetrahedron 60:2701–2743
29. Kanzian T, Nigst TA, Maier A, Pichl S, Mayr H (2009) Nucleophilic reactivities of primary and secondary amines in acetonitrile. Eur J Org Chem 2009:6379–6385
30. Makai S, Falk E, Morandi B (2020) Direct synthesis of unprotected 2-Azidoamines from Alkenes via an Iron-Catalyzed Difunctionalization Reaction. J Am Chem Soc 142:21548–21555
31. Chandrasekhar M, Sekar G, Singh VK (2000) An efficient method for opening nonactivated aziridines with TMS azide: application in the synthesis of chiral 1,2-diaminocyclohexane. Tetrahedron Lett 41:10079–10083
32. Treitler DS, Leung S (2022) How dangerous is too dangerous? a perspective on azide chemistry. J Org Chem 87:11293–11295
33. Pandey AM, Mondal S, Gnanaprakasam B (2022) Continuous-flow direct azidation of alcohols and peroxides for the synthesis of quinoxalinone, benzooxazinone, and triazole derivatives. J Org Chem 87:9926–9939
34. Capaldo L, Wen Z, Noël T (2023) A field guide to flow chemistry for synthetic organic chemists. Chem Sci 14:4230–4247
35. Brotzel F, Chu YC, Mayr H (2007) Nucleophilicities of Primary and Secondary Amines in Water. J Org Chem 72:3679–3688
36. Jones RV, Godorhazy L, Varga N, Szalay D, Urge L, Darvas F (2006) Continuous-flow high pressure hydrogenation reactor

for optimization and high-throughput synthesis. J Comb Chem 8:110–116

37 D'hooghe M, Mollet K, Dekeukeleire S, De Kimpe N (2010) Stereoselective synthesis of trans- and cis-2-aryl-3-(hydroxymethyl)aziridines through transformation of 4-aryl-3-chloro-β-lactams and study of their ring opening. Org Biomol Chem 8:607–615

Publisher's Note Springer Nature remains neutral with regard to jurisdictional claims in published maps and institutional affiliations.

Marharyta Laktse-vich-Iskryk received a bachelor's degree in pharmaceutical chemistry from the Belarusian State University in 2016. As an undergraduate, she became a member of the Laboratory of Steroidal Chemistry at the Institute of Bioorganic Chemistry of the National Academy of Sciences of Belarus, conducting research on metal and photoredox catalysis. Marharyta successfully defended her master's thesis in 2017 under the supervision of Dr. Alaksiej Hurski. Later, she joined the Dr. Dzmitry Kananovich group as a visiting researcher, where she worked on enantioselective synthesis of cyclopropanols. In 2023, Marharyta started PhD studies at Tallinn University of Technology under the supervision of Prof. Maksim Ošeka with a focus on enantioselective electrochemical synthesis.

Anastasiya Krech graduated from Belarusian State University in 2019 and received her M.Sc. in chemistry in 2020 from the Graduate School of the National Academy of Sciences of Belarus. During her bachelor's and master's studies, she worked at the Institute of Bioorganic Chemistry at the National Academy of Sciences of Belarus. She initially worked in Dr. Vladimir Zhabinskii's group, conducting the synthesis of new pharmacologically important steroids. Later, she joined Dr. Alaksiej Hurski's group, where she focused on the reactions of cyclopropanols. In 2021, she moved to Estonia for her PhD studies and joined Dr. Maksim Ošeka's group at Tallinn University of Technology. She is currently working on the development of photochemical reactions of cyclopropanols and asymmetric electrochemical reactions.

Mihhail Fokin graduated with cum laude from Maardu Gümnaasium, where he demonstrated a strong interest in chemistry and even worked as a teacher after graduation. He currently studies applied chemistry and gene technology at Tallinn University of Technology and conducts research on flow electrochemistry as an undergraduate student in the Ošeka group.

Mariliis Kimm received her bachelor's, master's, and doctoral degrees in chemistry and biotechnology from Tallinn University of Technology, Estonia. She became a member of Professor Tõnis Kanger's research group in 2013, where she focused on developing new asymmetric organocatalyzed reactions. As a visiting PhD student, Mariliis further enriched her research experience by joining Professor Jan H. Maarseveen's research group at the University of Amsterdam, Netherlands. During her time there, she engaged in synthesizing mechanically chiral [2]rotaxanes. Mariliis defended her thesis in 2021. She currently works as a researcher at the Ošeka group, focusing on the development of electrochemical reactions in continuous flow.

Tatsiana Jarg graduated from Belarusian State University in 2014 and started working at the Institute of Bioorganic Chemistry at the National Academy of Sciences of Belarus. As a pharmaceutical chemist, she focused on quality control and development of analytical methods for anti-tumor drugs and active pharmaceutical ingredients. In 2018, based on the carried out R&D work she received her M.Sc. in Chemistry from Belarusian State Technological University. In 2019 she started her PhD studies at Tallinn University of Technology, where she joined supramolecular chemistry group under supervision of Prof. Riina Aav. She is currently working on LC and MS analysis of novel macrocyclic receptors and their host-guest binding, and is additionally involved into projects related to organic synthesis, mechanochemistry, green synthesis of pharmaceuticals and food waste valorization.

Timothy Noël is a Full Professor and Chair of Flow Chemistry at the University of Amsterdam, where he focuses on the delicate synergy between synthetic organic chemistry and technology. He has received several awards for his research in flow chemistry, including the DECHEMA prize (2017), the Hoogewerff Jongerenprijs (2019), the IUPAC-ThalesNano prize (2020), the KNCV Gold Medal (2021), the ACS Sustainable Chemistry & Engineering Lectureship Award (2022), and the ChemSocRev Pioneering Investigator Lectureship (2023). In addition, he serves as Editor-in-Chief of the Journal of Flow Chemistry, as president of the Flow Chemistry Society and is co-organizer of #RSCPoster.

Maksim Ošeka studied biotechnology and applied chemistry in Tallinn University of Technology, Estonia. He joined the Professor Tõnis Kanger research group first as an undergraduate student in 2009 and then successfully completed his PhD in 2017. Maksim's research in the group was mainly focused on the development of new asymmetric organocatalyzed reactions and mechanistic studies. As part of his master's studies, Maksim undertook an Erasmus placement at Oslo University, Norway, working with Prof. Lise-Lotte Gundersen and as a visiting PhD student he joined the Melchiorre group at ICIQ, Spain, where he participated in the development of a novel photocatalytic enantioselective alkylation reaction. After obtaining his doctoral degree, he conducted research with Dr. Dzmitry Kananovich and then moved to the Netherlands to pursue postdoctoral studies. During the two-year postdoc under Professor Timothy Noël at Eindhoven University of Technology, Maksim worked on the development of novel electrochemical methods in continuous flow. In 2021, Maksim returned to Tallinn University of Technology to start his independent career and was later promoted to Assistant Professor. The Ošeka group's research at TalTech is focused on synergizing organic synthesis areas including photochemistry, electrochemistry, asymmetric organocatalysis, and flow chemistry.

Curriculum vitae

Personal data

Name:	Anastasiya Krech
Date of birth:	06.07.1997
Place of birth:	Akciabrski, Belarus
Citizenship:	Belarusian

Contact data

E-mail:	anastasiya.krech@gmail.com

Education

2021–2025	Tallinn University of Technology, PhD
2019–2020	Graduate School of the National Academy of Sciences of Belarus, MSc
2014–2019	Belarusian State University, BSc

Language competence

Belarusian	Native
Russian	Native
English	Fluent

Professional employment

2021–2025	Tallinn University of Technology, Department of Chemistry and Biotechnology, early stage researcher
2018–2019	The Institute of Bioorganic Chemistry of the National Academy of Sciences of Belarus, junior research fellow
2018–2019	Competentum LLC, Chemistry engineer

Honours and awards

2025	Best oral presentation award, XLIX "A. Corbella" International Summer School on Organic Synthesis, Gargnano, Italy
2025	Erasmus scholarship, research stay, Institute of Chemical Research of Catalonia (ICIQ), Tarragona, Spain
2023	Best Poster Prize at the Paul Walden 13th Symposium on Organic Chemistry, Riga, Latvia
2017	Erasmus scholarship for exchange studies, Jagellonian University, Krakow, Poland

Supervised theses

2024–2025	Nora Deil, BSc thesis, Tallinn University of Technology, Department of Chemistry and Biotechnology
2023–2024	Rasmus Käsper, BSc thesis, Tallinn University of Technology, Department of Chemistry and Biotechnology

Author's publications

1. Palomo, E., Krech, A., Hsueh, Y. J., Li, Z., Suero, M. G. Rh-catalyzed Enantioselective Aryl C–H Bond Cyclopropylation. *J. Am. Chem. Soc.* **2025**, *147* (16), 13120–13125. https://doi.org/10.1021/jacs.5c02331.

2. Krech, A.; Laktsevich-Iskryk, M.; Deil, N.; Fokin, M.; Kimm, M.; Ošeka, M. Asymmetric Cyclopropanation *via* an Electro-Organocatalytic Cascade. *Chem. Commun.*, **2024**, *60* (95), 14026–14029. https://doi.org/10.1039/D4CC05092D.

3. Laktsevich-Iskryk, M.; Krech, A.; Fokin, M.; Kimm, M.; Jarg, T.; Noël, T.; Ošeka, M. Telescoped Synthesis of Vicinal Diamines *via* Ring-Opening of Electrochemically Generated Aziridines in Flow. *J. Flow Chem.*, **2024**, *14* (1), 139–147. https://doi.org/10.1007/s41981-023-00296-8.

4. Krech, A.; Yakimchyk, V.; Jarg, T.; Kananovich, D.; Ošeka, M. Ring-Opening Coupling Reaction of Cyclopropanols with Electrophilic Alkenes Enabled by Decatungstate as Photoredox Catalyst. *Adv. Synth. Catal.*, **2024**, *366* (1), 91–100. https://doi.org/10.1002/adsc.202300939.

5. Leushukou, A. A., Krech, A. V., Hurski, A. L. Visible-Light-Promoted Nickel-Catalyzed Cross-Coupling of Alkyltitanium Alkoxides with Aryl and Alkenyl Halides. *Org. Lett.* **2022**, *24* (34), 6277–6281. https://doi.org/10.1021/acs.orglett.2c02428.

6. Kooli, A., Wesenberg, L., Beslać, M., Krech, A., Lopp, M., Noël, T., Ošeka, M. Electrochemical Hydroxylation of Electron-Rich Arenes in Continuous Flow. *Eur. J. Org. Chem*. **2022**, e202200011. https://doi.org/10.1002/ejoc.202200011.

7. Laktsevich-Iskryk, M. V., Krech, A. V., Zhabinskii, V. N., Khripach, V. A., Hurski, A. L. Photocatalytic Stoichiometric Oxidant-Free Synthesis of Linear Unsaturated Ketones from 1,2-Disubstituted Cyclopropanols. *Synthesis* **2021**, *53* (6), 1077–1086. https://doi.org/10.1055/s-0040-1706088.

8. Barysevich, M. V., Laktsevich-Iskryk, M. V., Krech, A. V., Zhabinskii, V. N., Khripach, V. A., Hurski, A. L. Palladium-Catalyzed 2-(Neopentylsulfinyl)aniline Directed C–H Acetoxylation and Alkenylation of Arylacetamides. *Eur. J. Org. Chem*. **2020**, *2020* (8), 937-943. https://doi.org/10.1002/ejoc.201901646.

Elulookirjeldus

Isikuandmed

Nimi:	Anastasiya Krech
Sünniaeg:	06.07.1997
Sünnikoht:	Akciabrski, Valgevene
Kodakondsus:	Valgevene

Kontaktandmed

E-post:	anastasiya.krech@gmail.com

Hariduskäik

2021–2025	Tallinna Tehnikaülikool, Keemia ja biotehnoloogia instituut, PhD
2019–2020	Valgevene Teaduste Akadeemia Teadurite Koolitusinstituut, MSc
2014–2019	Valgevene Riiklik Ülikool, keemia, BSc

Keelteoskus

Valgevene keel	emakeel
Vene keel	emakeel
Inglise keel	kõrgtase

Teenistuskäik

2021–2025	Tallinna Tehnikaülikool, Keemia ja biotehnoloogia instituut, doktorant-nooremteadur
2018–2019	Valgevene Teaduste Akadeemia Bioorgaanilise Keemia Instituut, nooremteadur
2018–2019	Competentum LLC, keemiainsener

Teaduspreemiad ja tunnustused

2025	Parima suulise ettekande auhind, XLIX "A. Corbella" rahvusvaheline suvekool orgaanilises sünteesis, Gargnano, Itaalia
2025	Erasmuse stipendium, teadustööpraktika, Kataloonia Keemiauuringute Instituut (ICIQ), Tarragona, Hispaania
2023	Parima postri auhind Paul Waldeni 13. orgaanilise keemia sümpoosiumil, Riia, Läti
2017	Erasmuse stipendium vahetusõpinguteks, Jagellooni Ülikool, Kraków, Poola

Juhendatud lõputööd

2024–2025	Nora Deil, bakalaureusetöö, Tallinna Tehnikaülikool, Keemia ja biotehnoloogia instituut
2023–2024	Rasmus Käsper, bakalaureusetöö, Tallinna Tehnikaülikool, Keemia ja biotehnoloogia instituut